Springer Theses
Recognizing Outstanding Ph.D. Research

Naohiro Terasaka

Applications of Aminoacylation Ribozymes That Recognize the 3'-end of tRNA

Springer

Springer Theses

Recognizing Outstanding Ph.D. Research

Aims and Scope

The series "Springer Theses" brings together a selection of the very best Ph.D. theses from around the world and across the physical sciences. Nominated and endorsed by two recognized specialists, each published volume has been selected for its scientific excellence and the high impact of its contents for the pertinent field of research. For greater accessibility to non-specialists, the published versions include an extended introduction, as well as a foreword by the student's supervisor explaining the special relevance of the work for the field. As a whole, the series will provide a valuable resource both for newcomers to the research fields described, and for other scientists seeking detailed background information on special questions. Finally, it provides an accredited documentation of the valuable contributions made by today's younger generation of scientists.

Theses are accepted into the series by invited nomination only and must fulfill all of the following criteria

- They must be written in good English.
- The topic should fall within the confines of Chemistry, Physics, Earth Sciences, Engineering and related interdisciplinary fields such as Materials, Nanoscience, Chemical Engineering, Complex Systems and Biophysics.
- The work reported in the thesis must represent a significant scientific advance.
- If the thesis includes previously published material, permission to reproduce this must be gained from the respective copyright holder.
- They must have been examined and passed during the 12 months prior to nomination.
- Each thesis should include a foreword by the supervisor outlining the significance of its content.
- The theses should have a clearly defined structure including an introduction accessible to scientists not expert in that particular field.

More information about this series at http://www.springer.com/series/8790

Naohiro Terasaka

Applications of Aminoacylation Ribozymes That Recognize the 3′-end of tRNA

Doctoral Thesis accepted by
the University of Tokyo, Tokyo, Japan

Springer

Author
Dr. Naohiro Terasaka
ETH Zurich
Zurich
Switzerland

Supervisor
Prof. Hiroaki Suga
The University of Tokyo
Tokyo
Japan

ISSN 2190-5053 ISSN 2190-5061 (electronic)
Springer Theses
ISBN 978-4-431-56515-4 ISBN 978-4-431-56517-8 (eBook)
DOI 10.1007/978-4-431-56517-8

Library of Congress Control Number: 2017932420

Printed on acid-free paper

This Springer imprint is published by Springer Nature
The registered company is Springer Japan KK
The registered company address is: Chiyoda First Bldg. East, 3-8-1 Nishi-Kanda, Chiyoda-ku, Tokyo 101-0065, Japan

Supervisor's Foreword

I am delighted to introduce Dr. Naohiro Terasaka, who received his Doctor of Science degree from the University of Tokyo in 2015. He is truly the most amazing student whom I have ever had in terms of his independence and ability in planning and conducting research.

In Dr. Terasaka's Springer Thesis, he has described his two major research programs that are quite different from each other. One of the programs involves engineering of a reconstituted translation system, where a new pair of ribosome–tRNAs acting orthogonally to the wild-type ribosome–tRNAs was invented. Using this new pair and wild-type pair, he has demonstrated the expression of two different peptides catalyzed by the respective ribosome–tRNA pairs from a single kind of mRNA. I believe that this work has made a strong impact on a growing area of chemical and synthetic biology, as published in *Nature Chemical Biology*, co-authored with Dr. Gosuke Hayashi and other members of my research group.

The other program involves a new technique developed in my research team, referred to as tRid (tRNA-Rid). The tRid was originally developed for facilitating isolation of small RNA fractions with lengths of 50–100 nucleotides, which are generally inaccessible in cellular RNA molecules because they overlap with mass numbers of tRNAs. Dr. Terasaka has applied this technique to the discovery of cellular RNA aptamers from small RNA transcripts isolated by the tRid. He was able to identify a human precursor microRNA, known as hsa-pre-miR-125a, capable of binding to folic acid. We referred to this technology as smaRt-SELEX (small RNA transcriptomic SELEX). This work was published in *RNA*, co-authored with Dr. Kazuki Futai and other members of my research group.

These works involve not only Dr. Terasaka's talent in conducting research but also his patient and steady efforts. I have no doubt that, without him these research programs could not have been realized and completed. Clearly, his achievements were recognized in various conferences, and he received several awards, such as the Best Presenter Award in the 15th annual meeting of the RNA Society of Japan (2013); the Sidney Altman Endowment Travel Award at the 25th tRNA conference (2014); and the Research Incentive Award from the Graduate School of Science,

the University of Tokyo (2015). He is currently working in ETH Zurich as a Human Frontier Science Program fellow under the supervision of Prof. Donald Hilvert and expanding his knowledge to protein science. I am delighted to see his further growth during his postdoctoral work.

On behalf of the Department of Chemistry, Graduate School of Science, the University of Tokyo, I would like to congratulate Dr. Terasaka on the Springer Theses Award. Personally, I sincerely wish him continued success in his career development with the hope that he will contribute to progress in science and technology in academics, industry, and society.

Tokyo, Japan
December 2016

Prof. Hiroaki Suga

Parts of this thesis have been published in the following journal articles

Terasaka N, Futai K, Katoh T, Suga H (2016) A human micro RNA precursor binding to folic acid discovered by small RNA transcriptomic SELEX. RNA. doi:10.1261/rna.057737.116

Terasaka N, Suga H (2014) Flexizymes-facilitated genetic code reprogramming leading to the discovery of drug-like peptides. Chem Lett 43 (1):11-19. doi:10.1246/Cl.130910

Terasaka N, Hayashi G, Katoh T, Suga H (2014) An orthogonal ribosome-tRNA pair via engineering of the peptidyl transferase center. Nat Chem Biol 10 (7): 555-557. doi:10.1038/nchembio.1549

Acknowledgements

I would like to express my sincere gratitude to Prof. Hiroaki Suga for his kind guidance, valuable suggestions, and encouragement throughout this work. I am deeply grateful to Prof. Naokazu Kano, Prof. Takayuki Katoh, Prof. Yuki Goto, and Prof. Toby Passioura for their helpful advice and discussion. I am greatly indebted to Dr. Kazuki Futai and Dr. Gosuke Hayashi for teaching me about experimental matters and discussing the research with me. I also thank all members of the laboratory.

I thank the Japan Society for the Promotion of Science (JSPS) for a grant and financial support.

Finally, I would like to thank my parents and brother for invaluable assistance and encouraging words.

Contents

Chapter 1
General Introduction

Abstract Transfer RNA (tRNA) is one of the most abundant and popular noncoding RNA (ncRNA), which works as an adaptor molecule linking a nucleotide to an amino acid in the translation step. The 3′-end of tRNA is universally conserved as CCA-3′ and forms base pairs with ribosomal RNA during the translation. If the easy method to prepare various aa-tRNA bearing mutations in the CCA-3′ end, it is usable for analyzing the role of CCA-3′ end during the translation and engineering the translation machinery. Recently, various small noncoding RNAs have been identified and the function of those RNAs have been studied. However, it is not easy to discover the small ncRNAs with very low abundance because tRNAs are too much abundant in small RNA fraction (less than 200 nt). To overcome this problem, easy method to remove tRNAs from small RNA fraction is required. In order to solve these problems, I focused on flexizymes that are aminoacylation ribozymes developed by in vitro selection. Flexizymes have following unique characteristics: (i) substrate RNA is recognized by two consecutive base pairs between 3′-end of substrate RNA and 3′-end of flexizyme, (ii) these base pairs can be substituted with other base pairs and (iii) various activated amino acids can be used as substrates including both canonical and noncanonical amino acids. Therefore, flexizymes enable to label all endogenous tRNAs bearing CCA-3′ end with ncAAs to be removed, and to aminoacylate CCA-3′ mutated tRNAs by compensatory mutations to engineer the translation machinery.

Keywords Ribozyme · MicroRNA · SELEX · tRNA · Ribosome · Translation

1.1 Transfer RNA

Genetic information is transcribed from DNA into mRNA (messenger RNA) and mRNA is translated into protein, and this process is called as central dogma (Fig. 1.1). By human genome project, it was reported that only the 2% region of human genomic DNA is transcribed and translated to about 20,000–25,000 proteins (Collins et al. 2004), but transcriptome study revealed that about 70% region of

N. Terasaka, *Applications of Aminoacylation Ribozymes That Recognize the 3′-end of tRNA*, Springer Theses, DOI 10.1007/978-4-431-56517-8_1

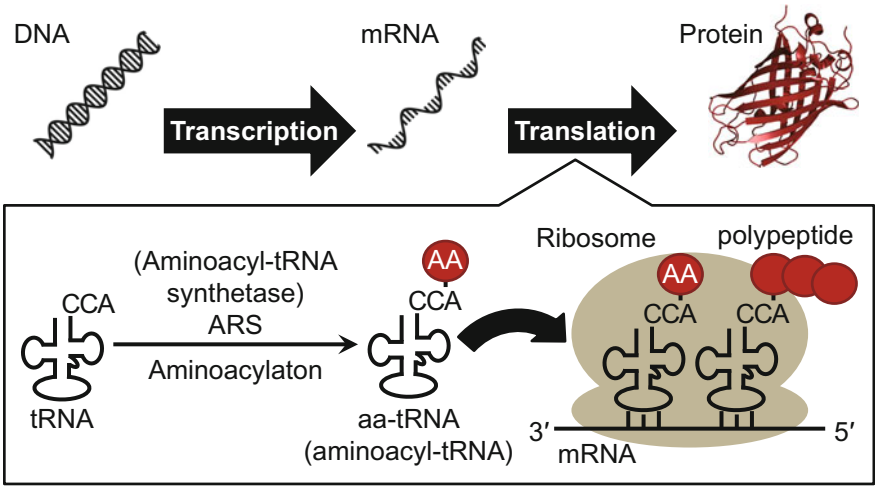

Fig. 1.1 Schematic illustration of central dogma. "AA" in the *red circle* indicates amino acid. An image of protein was prepared from crystal structure of GFP (*green* fluorescent protein) (PDB ID: 1GFL) (Yang et al. 1996)

DNA is transcribed to RNA. In addition, widespread transcription of noncoding RNAs with important functions throughout the genome have been recently discovered (Cheng et al. 2005).

Transfer RNA (tRNA) is one of the most abundant and popular noncoding RNA, which works as an adaptor molecule linking the language of nucleotide to the language of amino acid in the translation step. Canonical tRNA forms cloverleaf secondary structure and L-shaped tertiary structure as shown in Fig. 1.2. Aminoacyl-tRNA sythetase (ARS) charges corresponding amino acid onto the 3′-end of specific tRNA to produce aminoacyl-tRNA (aa-tRNA) and aa-tRNA is recruited into ribosome by translation factors (Fig. 1.1). Three consecutive nucleotides called as anticodon of tRNA form base pairs with the sequential triplet codons of mRNA in the ribosome, and corresponding amino acid is incorporated into nascent peptide chain (Figs. 1.1 and 1.2). The correspondence between codons and amino acids are defined as genetic code (Fig. 1.3). This genetic code is well conserved in the most of all organisms [some exceptions have been found (Ambrogelly et al. 2006)] and accurate translation of mRNA to protein is essential for living organisms.

CCA sequence at the 3′-end is universally conserved in all three domains, prokaryote, eukaryote, and archaea. During the translation, CCA-3′ end interacts with ribosome and translation factors, and these interactions are important for efficient translation. In the aminoacylation step, ARSs strictly recognize the body sequences of substrate tRNAs to charge specific amino acids onto specific tRNAs. In addition, because most ARSs also interact with the universally conserved CCA-3′ end of tRNAs (Cavarelli and Moras 1993; Ruff et al. 1991), it is difficult to

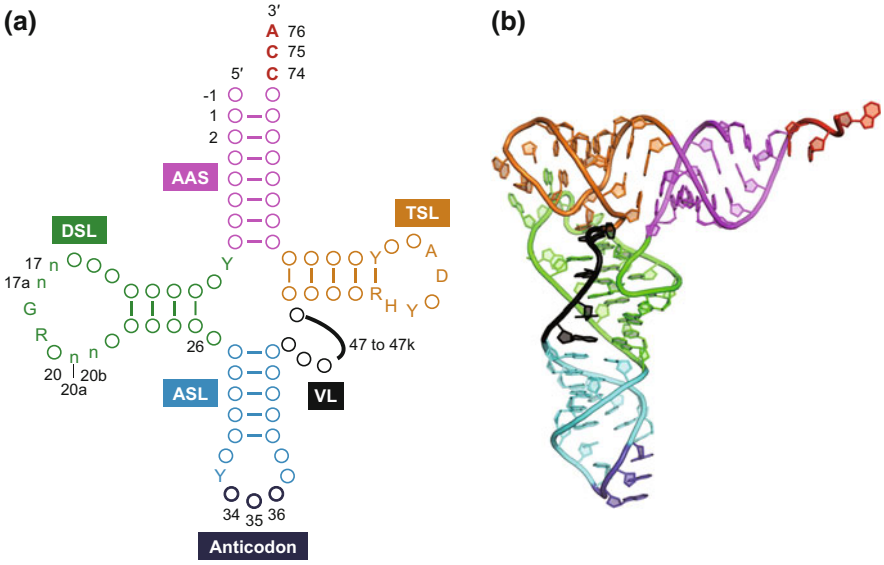

Fig. 1.2 Structure of tRNA. **a** Clover leaf structure of tRNA. Conserved bases are described, circles represent nonconserved bases, and numbers indicate the nucleotide position. Positions 34–36 (*dark blue*) are anticodon bases and positions 74–76 (*red*) are universally conserved as CCA. The sequences composing the intron and the extra bases presenting in the variable loop (position noted 47–47k) are shown as *black line*. AAS (*magenta*), the amino acid-accepting stem; DSL (*green*), the dihydrouridine stem and loop; ASL (*cyan*), the anticodon stem and loop; VL (*black*); the variable loop, TSL (*orange*); the thymidine stem and loop, Y; pyrimidine, R; purine, H; not G, D; not C. The n bases at position 17, 17a, 20a, and 20b are optional bases not present in all tRNAs. Position −1 bases are found in all cytoplasmic mature $tRNA^{His}_{GUG}$ from the three biological domains. This figure was adapted from the previous paper (Marck and Grosjean 2002). **b** L-shaped tertiary structure of tRNA. Each color indicates the same region described in Fig. 1.2a. This image was prepared from crystal structure of *Saccharomyces cerevisiae* $tRNA^{Phe}$ (PDB ID: 1EHZ) (Shi and Moore 2000)

Fig. 1.3 Standard genetic code. All 64 codons were assigned to corresponding amino acids or termination signal (termed as "Stop" in this figure)

1st base	2nd base U	2nd base C	2nd base A	2nd base G	3rd base
U	Phe	Ser	Tyr	Cys	U
					C
	Leu		Stop	Stop	A
				Trp	G
C	Leu	Pro	His	Arg	U
					C
			Gln		A
					G
A	Ile	Thr	Asn	Ser	U
					C
	Met		Lys	Arg	A
					G
G	Val	Ala	Asp	Gly	U
					C
			Glu		A
					G

prepare the various aa-tRNAs bearing mutations in the CCA-3′ end by ARSs (Schulman and Pelka 1977; Liu and Horowitz 1994; Zhou et al. 2011). To prepare such aa-tRNAs, so-called "chemical acylation" method where chemically synthesized aminoacyl-nucleotide is ligated to tRNA lacking the 3′-end by T4 RNA ligase (Hecht et al. 1978; Lodder et al. 2005) may be usable. However, in this method, it is laborious work that various aminoacyl-nuleotides are prepared by chemical synthesis. If the easy method to prepare various aa-tRNA bearing mutations in the CCA-3′ end, it is usable for analyzing the role of CCA-3′ end during the translation and engineering the translation machinery.

1.2 Other Noncoding RNAs Than tRNAs

As I mentioned above, tRNA is one of the most abundant and popular noncoding RNA (ncRNA). In addition to tRNA, ribosomal RNAs (rRNAs) are also known as popular ncRNA, which constitute a ribosome. There are three kinds of rRNAs (5S, 16S, and 23S rRNAs) in prokaryote, and four kinds of rRNAs (5S, 5.8S, 18S, and 28S rRNA) in eukaryote. Peptidyl transfer reaction, which makes a peptide bond, is catalyzed by 23S rRNA or 28S rRNA. These tRNAs and rRNAs are much abundant and account for about 95% of all RNAs in mammalian cells (Lindberg and Lundeberg 2010).

The various other ncRNAs than tRNA and rRNA have been identified mainly in mammalian (Esteller 2011). These ncRNAs are roughly classified into two groups: long ncRNA (longer than 200 nt) and small ncRNA (smaller than 200 nt) (Kapranov et al. 2007; Huang et al. 2013). Unlike small ncRNA such as microRNA, function of long ncRNA has been less studied. However, recent studies revealed the broad functional repertoire including roles in high-order chromosomal dynamics, telomere biology, and subcellular structural organization (Mercer et al. 2009; Amaral and Mattick 2008).

The class of small ncRNA includes various RNAs such as snRNAs (small nuclear RNAs), snoRNAs (small nucleolar RNAs), and miRNAs (micro RNAs) (Matera et al. 2007). snRNA makes complex with protein to form snRNP (ribonucleoprotein) and consists of spliceosome involving the reaction of mRNA splicing. snoRNA generally ranges from 60 to 300 nucleotides in length and guide the site-specific modification of nucleotide in target RNA (Mattick and Makunin 2006). In the past few years, about 22 nt short ncRNA (miRNA) has been widely studied. miRNA is loaded into Ago protein to form a RISC (RNA induced silencing complex) (Snead and Rossi 2010). A RISC binds to target mRNA via base pairs between miRNA and 3′-UTR (untranslated region) of mRNA to inhibit the translation and suppress the expression of the target gene. To date more than 1800 miRNAs in human are registered in databases (miRbase (Kozomara and Griffiths-Jones 2014), http://www.mirbase.org/) and are estimated to regulate the expression of more than 60% of genes to control a wide range of biological processes including proliferation, differentiation, apotosis, and development (Esteller 2011).

As mentioned above, various small ncRNAs have been identified and the function of those RNAs have been studied. However, it is not easy to discover the small ncRNAs with very low abundance because tRNAs are too much abundant in small RNA fraction (less than 200 nt). To overcome this problem, easy method to remove tRNAs from small RNA fraction is required.

1.3 Aminoacylation Ribozyme "Flexizyme"

In order to achieve these requirements described in former sections it is necessary (i) to easily prepare the various aa-tRNAs bearing mutations in the CCA-3′ end, and (ii) to remove endogenous tRNAs from small RNA fraction. I focused attention on the unique characteristics of flexizymes which were in vitro selected aminoacylation ribozyme (Suga et al. 2011; Terasaka and Suga 2014). First, I briefly summarize how flexizymes have been developed.

A ribozyme which is an RNA having catalytic activity was first discovered in nature in 1980s (Kruger et al. 1982; Guerrier-Takada et al. 1983). These discoveries indicate RNA can store information like DNA and catalyze chemical reaction like proteins to strongly support the "RNA world hypothesis" that the origin of life may have relied on RNA (Walter 1986). However, the chemical reactions catalyzed by natural ribozymes are limited to the cleavage or ligation of the RNA phosphodiester backbone except for peptidyl transfer by ribosome (Doudna and Cech 2002). To expand the variety of chemical reactions catalyzed by RNA, in vitro selection of ribozyme has been developed. SELEX (Systematic Evolution of Ligands by EXponential enrichment, or in vitro selection) is a method based on molecular evolution engineering to identify the active molecules having specific activities from pools of various compounds (Ellington and Szostak 1990; Tuerk and Gold 1990). It was first reported from two groups in 1990 and they discovered RNA aptamers binding to specific target molecules from random RNA library. In addition to the discovery of RNA aptamers, the ribozymes having catalytic activities have also been identified (Robertson and Joyce 1990). A general scheme of SELEX of active RNAs was shown in Fig. 1.4. DNA library containing T7 promoter sequence, 5′-constant sequence, random sequences, and 3′-constant sequence is prepared by PCR. These constant sequences are used for following reverse transcription and PCR reaction. The DNA templates are transcribed to RNAs by T7 RNA polymerase in vitro. From the RNA library, portion of RNAs are selected based on their ability to carry out a specific function (e.g., binding affinity and catalytic activity). Selected RNAs are converted to cDNAs by reverse transcription. These cDNAs are amplified by PCR and the same procedure is repeated. After the several times repeats of this process, the resulting RNA fraction will be enriched with functional molecules with the desired activity. By SELEX, many artificial ribozymes have been discovered (Johnston et al. 2001) [e.g., RNA polymerization (Johnston et al. 2001; Wochner et al. 2011; Sczepanski and Joyce 2014), alcohol

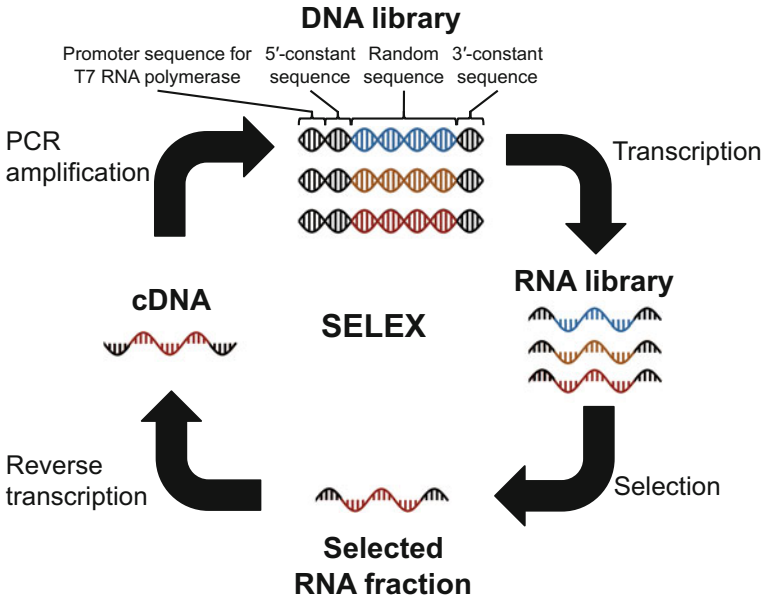

Fig. 1.4 General scheme of SELEX (in vitro selection) of functional RNAs. *Black* sequences are constant regions including the promoter sequence for T7 RNA polymerase and the 5′/3′-constant sequences necessary for reverse transcription and PCR amplification. Colored (*blue*, *orange*, and *red*) sequences indicate the random region. This figure is adapted from the previous review (Terasaka and Suga 2014)

oxidation (Tsukiji et al. 2003), Diels-Alder reaction (Agresti et al. 2005), and aminoacylation (Illangasekare et al. 1995; Lee et al. 2000; Saito et al. 2001a; Murakami et al. 2006; Chumachenko et al. 2009)]. Among them, aminoacylation ribozymes were important because these are candidates as key molecules which link the ancient RNA world with modern protein world.

In nature, protein ARS catalyzes aminoacylation reaction. Aminoacylation by ARS involves two steps: (i) activation of carboxyl group amino acids by adenylation using ATP to yield aminoacyl-adenosine monophosphate (aminoacyl-AMP), and (ii) condensation of aminoacyl-AMP and tRNA to yield aminoacyl-tRNA (aa-tRNA). Although no ribozyme catalyzing these both reactions have been discovered in nature, some artificial ribozymes catalyzing (i) or (ii) step were identified by in vitro selection. The KK13 ribozyme catalyze the activation of amino acid by using the 5′-triphosphate of RNA instead of ATP (Kumar and Yarus 2001). The #29 ribozyme family catalyzes *cis*-acyl transfer reaction using aminoacyl-AMP to produce both aminoacyl- and peptidyl-tRNAs (Illangasekare et al. 1995, 1997; Illangasekare and Yarus 1999), and the C3 ribozyme family consisting of only three essential nucleotides catalyze both *cis*- and *trans*-acyl transfer reaction using aminoacyl-AMP (Chumachenko et al. 2009; Yarus 2011). Flexizyme is also

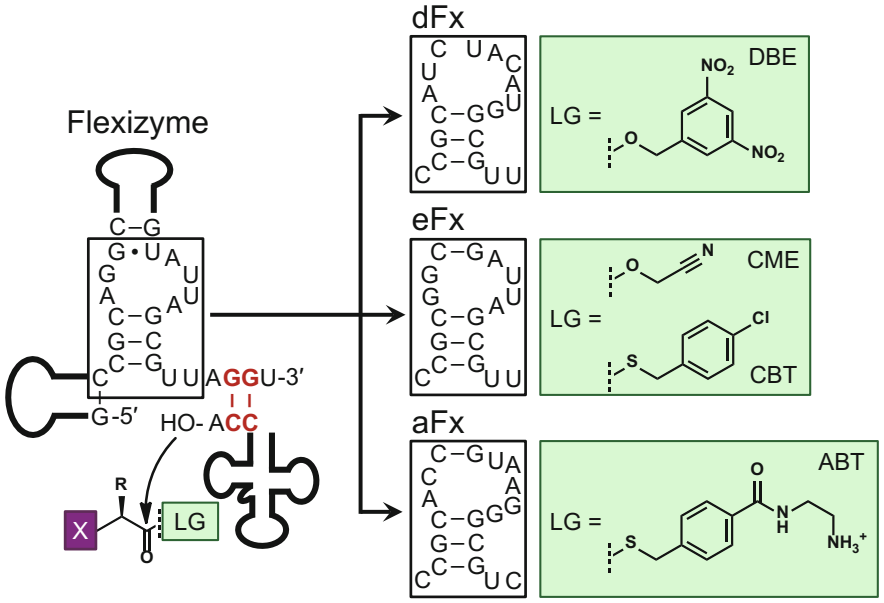

Fig. 1.5 Schematic illustration of aminoacylation by three derivatives of flexizymes and acyl-donor substrates with cognate leaving group. This figure is adapted from previous review (Terasaka and Suga 2014). *Lines* denote the Watson-Crick base pairs and bullets denote wobble base pairs. R represents amino acid side chains including noncanonical ones. X represent a-functional groups, such as amino, *N*-alkylamino, and hydroxy groups. LG: leaving group, dFx: dinitrobenzyl flexizyme, eFx: enhanced flexizyme, aFx: amino flexizyme, DBE: dinitrobenzyl ester, CME: cyanomethyl ester, CBT: *p*-chlorobenzylthioester, ABT: amino-derivatized benzyl thioester

trans-acyl-transfer ribozyme using activated amino acids, which was developed by SELEX method and was engineered to aminoacylate various activated amino acids. There are three types of flexizymes, dFx (dinitrobenzyl flexizyme) (Murakami et al. 2006), eFx (enhanced flexizyme) (Murakami et al. 2006), and aFx (amino flexizyme) (Niwa et al. 2009) (Fig. 1.5). dFx charges wide variety of amino acid whose carboxyl group is activated with 3,5-dinitrobenzyl ester (DBE), eFx charges aromatic amino acids activated with cyanomethyl ester (CME) or nonaromatic amino acids with 4-chlorobenzyl thioester (CBT), and aFx charges substrates activated with benzyl thioester group bearing a protonated primary amine (ABT).These flexizymes can charge wide variety of amino acids including noncanonical amino acids (ncAAs) such as *N*-methyl-amino acids (Kawakami et al. 2008a, 2009; Yamagishi et al. 2011), *N*-alkyl-glycines (Kawakami et al. 2008b), cyclic *N*-alkyl amino acids (Kawakami et al. 2013), *N*-acyl-amino acids (Goto et al. 2008b), exotic peptides (Goto and Suga 2009), α-hydroxy acids (Kawakami et al. 2009; Ohta et al. 2007), and D-amino acids (Goto et al. 2008a) onto tRNAs.

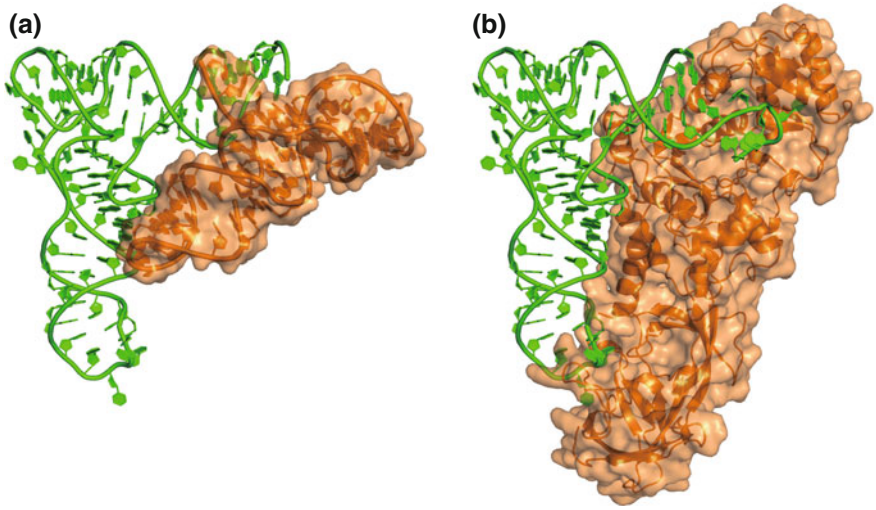

Fig. 1.6 Structures of protein and RNA aminoacyl-tRNA synthetases. **a** Crystal structure of *Escherichia coli* glutamiyl-tRNA synthetase (GlnRS; orange) and $tRNA^{Gln}$ complex (PDB ID: 1GTS) (Perona et al. 1993). **b** Crystal structure of flexizyme (*wheat color*) docked onto *E. coli* $tRNA^{Gln}$ by superimposing the minihelix on the ASL of the tRNA (PDB ID: 3CUL) (Xiao et al. 2008)

In addition to the characteristic to charge diverse kinds of amino acids, flexizymes have the flexibility to aminoacylate the substrate tRNA bearing any sequence because flexizymes recognize the CCA-3′ end by two consecutive base pairs with GGU-3′ of flexizymes (Xiao et al. 2008; Saito et al. 2001a, b) (Fig. 1.5). The crystal structure of flexizyme fused with substrate minihelix RNA docked onto the tRNAs indicated the no interaction between flexizyme and body sequence of substrate tRNA (Xiao et al. 2008) (Fig. 1.6). This is because, flexizyme can aminoacylate other RNAs different from tRNAs even if those have single-strand CCA-3′ end. In addition, in the experiment using prototype of flexizymes "pre-24," these two consecutive base pairs are important for aminoacylation and these base pairs can be substituted with other base pairs (Saito et al. 2001a, b).

In summary, flexizymes have following unique characteristics: (i) substrate RNA is recognized by two consecutive base pairs between 3′-end of substrate RNA and 3′-end of flexizyme, (ii) these base pairs can be substituted with other base pairs, and (iii) various activated amino acids can be used as substrates including both canonical and noncanonical amino acids. These features are different from natural protein ARSs and other aminoacylation ribozymes. From these characteristics of flexizymes, I considered that flexizymes enable to achieve the requirements described early in this section. In other words, flexizymes enable to label all endogenous tRNAs bearing CCA-3′ end with ncAAs to be removed, and to aminoacylate CCA-3′ mutated tRNAs by compensatory mutations (Fig. 1.7).

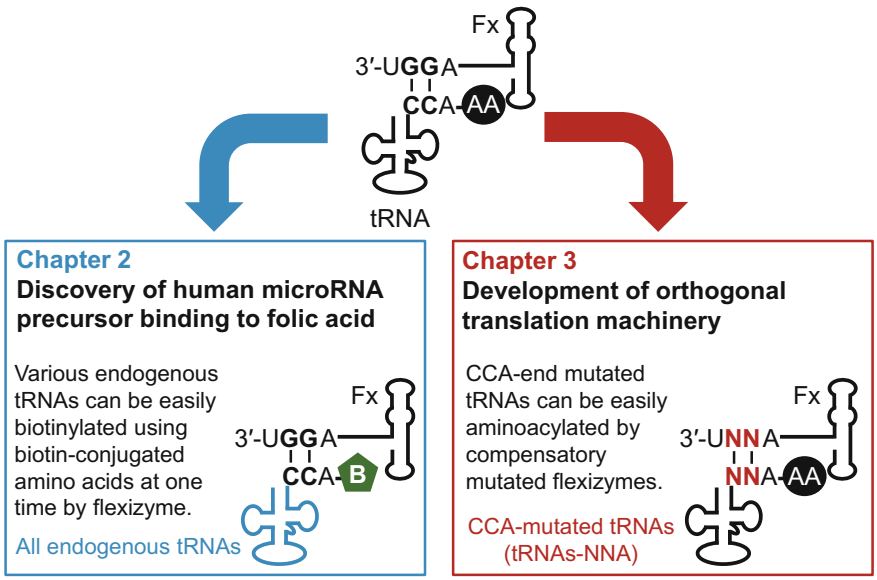

Fig. 1.7 Overview of the thesis. Discovery of human microRNA precursor binding to folic acid in Chap. 2, and development of orthogonal translation machinery in Chap. 3

References

Agresti JJ, Kelly BT, Jaschke A, Griffiths AD (2005) Selection of ribozymes that catalyse multiple-turnover Diels-Alder cycloadditions by using in vitro compartmentalization. Proc Natl Acad Sci USA 102(45):16170–16175. doi:10.1073/pnas.0503733102

Amaral PP, Mattick JS (2008) Noncoding RNA in development. Mamm Genome 19(7–8): 454–492. doi:10.1007/s00335-008-9136-7

Ambrogelly A, Palioura S, Söll D (2006) Natural expansion of the genetic code. Nat Chem Biol 3(1):29–35. doi:10.1038/nchembio847

Cavarelli J, Moras D (1993) Recognition of tRNAs by aminoacyl-tRNA synthetases. FASEB J 7(1):79–86

Cheng J, Kapranov P, Drenkow J, Dike S, Brubaker S, Patel S, Long J, Stern D, Tammana H, Helt G, Sementchenko V, Piccolboni A, Bekiranov S, Bailey DK, Ganesh M, Ghosh S, Bell I, Gerhard DS, Gingeras TR (2005) Transcriptional maps of 10 human chromosomes at 5-nucleotide resolution. Science 308(5725):1149–1154. doi:10.1126/science.1108625

Chumachenko N, Novikov Y, Yarus M (2009) Rapid and simple ribozymic aminoacylation using three conserved nucleotides. J Am Chem Soc 131(14):5257–5263. doi:10.1021/ja809419f

Collins FS, Lander ES, Rogers J, Waterston RH, Conso IHGS (2004) Finishing the euchromatic sequence of the human genome. Nature 431(7011):931–945. doi:10.1038/Nature03001

Doudna J, Cech T (2002) The chemical repertoire of natural ribozymes. Nature 418(6894):222–228. doi:10.1038/418222a

Ellington A, Szostak J (1990) In vitro selection of RNA molecules that bind specific ligands. Nature 346(6287):818–822. doi:10.1038/346818a0

Esteller M (2011) Noncoding RNAs in human disease. Nat Rev Genet 12(12):861–874. doi:10.1038/Nrg3074

Goto Y, Suga H (2009) Translation initiation with initiator tRNA charged with exotic peptides. J Am Chem Soc 131(14):5040–5041. doi:10.1021/ja900597d

Goto Y, Murakami H, Suga H (2008a) Initiating translation with D-amino acids. RNA 14(7):1390–1398. doi:10.1261/rna.1020708

Goto Y, Ohta A, Sako Y, Yamagishi Y, Murakami H, Suga H (2008b) Reprogramming the translation initiation for the synthesis of physiologically stable cyclic peptides. ACS Chem Biol 3(2):120–129. doi:10.1021/cb700233t

Guerrier-Takada C, Gardiner K, Marsh T, Pace N, Altman S (1983) The RNA moiety of ribonuclease P is the catalytic subunit of the enzyme. Cell 35(3 Pt 2):849–857. doi:10.1016/0092-8674(83)90117-4

Hecht SM, Alford BL, Kuroda Y, Kitano S (1978) "Chemical aminoacylation" of tRNA's. J Biol Chem 253(10):4517–4520

Huang Y, Zhang JL, Yu XL, Xu TS, Wang ZB, Cheng XC (2013) Molecular functions of small regulatory noncoding RNA. Biochemistry 78(3):221–230. doi:10.1134/S0006297913030024

Illangasekare M, Yarus M (1999) A tiny RNA that catalyzes both aminoacyl-RNA and peptidyl-RNA synthesis. RNA 5(11):1482–1489. doi:10.1017/S1355838299991264

Illangasekare M, Sanchez G, Nickles T, Yarus M (1995) Aminoacyl-RNA synthesis catalyzed by an RNA. Science 267(5198):643–647. doi:10.1126/science.7530860

Illangasekare M, Kovalchuke O, Yarus M (1997) Essential structures of a self-aminoacylating RNA. J Mol Biol 274(4):519–529. doi:10.1006/jmbi.1997.1414

Johnston W, Unrau P, Lawrence M, Glasner M, Bartel D (2001) RNA-catalyzed RNA polymerization: accurate and general RNA-templated primer extension. Science 292(5520):1319–1325. doi:10.1126/science.1060786

Kapranov P, Cheng J, Dike S, Nix DA, Duttagupta R, Willingham AT, Stadler PF, Hertel J, Hackermuller J, Hofacker IL, Bell I, Cheung E, Drenkow J, Dumais E, Patel S, Helt G, Ganesh M, Ghosh S, Piccolboni A, Sementchenko V, Tammana H, Gingeras TR (2007) RNA maps reveal new RNA classes and a possible function for pervasive transcription. Science 316(5830):1484–1488. doi:10.1126/science.1138341

Kawakami T, Ishizawa T, Murakami H (2013) Extensive Reprogramming of the genetic code for genetically encoded synthesis of highly N-Alkylated polycyclic peptidomimetics. J Am Chem Soc 135(33):12297–12304. doi:10.1021/Ja405044k

Kawakami T, Murakami H, Suga H (2008a) Messenger RNA-programmed incorporation of multiple N-methyl-amino acids into linear and cyclic peptides. Chem Biol 15(1):32–42. doi:10.1016/j.chembiol.2007.12.008

Kawakami T, Murakami H, Suga H (2008b) Ribosomal synthesis of polypeptoids and peptoid-peptide hybrids. J Am Chem Soc 130(50):16861–16863. doi:10.1021/ja806998v

Kawakami T, Ohta A, Ohuchi M, Ashigai H, Murakami H, Suga H (2009) Diverse backbone-cyclized peptides via codon reprogramming. Nat Chem Biol 5(12):888–890. doi:10.1038/nchembio.259

Kozomara A, Griffiths-Jones S (2014) miRBase: annotating high confidence microRNAs using deep sequencing data. Nucleic Acids Res 42(D1):D68–D73. doi:10.1093/Nar/Gkt1181

Kruger K, Grabowski P, Zaug A, Sands J, Gottschling D, Cech T (1982) Self-splicing RNA: autoexcision and autocyclization of the ribosomal RNA intervening sequence of Tetrahymena. Cell 31(1):147–157. doi:10.1016/0092-8674(82)90414-7

Kumar R, Yarus M (2001) RNA-catalyzed amino acid activation. Biochemistry 40(24):6998–7004. doi:10.1021/bi010710x

Lee N, Bessho Y, Wei K, Szostak J, Suga H (2000) Ribozyme-catalyzed tRNA aminoacylation. Nat Struct Biol 7(1):28–33. doi:10.1038/71225

Lindberg J, Lundeberg J (2010) The plasticity of the mammalian transcriptome. Genomics 95(1):1–6. doi:10.1016/j.ygeno.2009.08.010

Liu M, Horowitz J (1994) Functional transfer RNAs with modifications in the 3′-CCA end: differential effects on aminoacylation and polypeptide synthesis. Proc Natl Acad Sci USA 91(22):10389–10393. doi:10.2307/2366033

Lodder M, Wang BX, Hecht SM (2005) The N-pentenoyl protecting group for aminoacyl-tRNAs. Methods 36(3):245–251. doi:10.1016/j.ymeth.2005.04.002

Marck C, Grosjean H (2002) tRNomics: analysis of tRNA genes from 50 genomes of Eukarya, Archaea, and Bacteria reveals anticodon-sparing strategies and domain-specific features. RNA 8(10):1189–1232. doi:10.1017/S1355838202022021

Matera AG, Terns RM, Terns MP (2007) Noncoding RNAs: lessons from the small nuclear and small nucleolar RNAs. Nat Rev Mol Cell Biol 8(3):209–220. doi:10.1038/Nrm2124

Mattick JS, Makunin IV (2006) Noncoding RNA. Hum Mol Genet 15:R17–R29. doi:10.1093/Hmg/Ddl046

Mercer TR, Dinger ME, Mattick JS (2009) Long noncoding RNAs: insights into functions. Nat Rev Genet 10(3):155–159. doi:10.1038/Nrg2521

Murakami H, Ohta A, Ashigai H, Suga H (2006) A highly flexible tRNA acylation method for nonnatural polypeptide synthesis. Nat Methods 3(5):357–359. doi:10.1038/nmeth877

Niwa N, Yamagishi Y, Murakami H, Suga H (2009) A flexizyme that selectively charges amino acids activated by a water-friendly leaving group. Bioorg Med Chem Lett 19(14):3892–3894. doi:10.1016/j.bmcl.2009.03.114

Ohta A, Murakami H, Higashimura E, Suga H (2007) Synthesis of polyester by means of genetic code reprogramming. Chem Biol 14(12):1315–1322. doi:10.1016/j.chembiol.2007.10.015

Perona JJ, Rould MA, Steitz TA (1993) Structural basis for transfer RNA aminoacylation by *Escherichia Coli* glutaminyl-tRNA synthetase. Biochemistry 32(34):8758–8771. doi:10.1021/Bi00085a006

Robertson D, Joyce G (1990) Selection in vitro of an RNA enzyme that specifically cleaves single-stranded DNA. Nature 344(6265):467–468. doi:10.1038/344467a0

Ruff M, Krishnaswamy S, Boeglin M, Poterszman A, Mitschler A, Podjarny A, Rees B, Thierry JC, Moras D (1991) Class II aminoacyl transfer RNA synthetases: crystal structure of yeast aspartyl-tRNA synthetase complexed with tRNA(Asp). Science 252(5013):1682–1689. doi:10.1126/science.2047877

Saito H, Kourouklis D, Suga H (2001a) An in vitro evolved precursor tRNA with aminoacylation activity. EMBO J 20(7):1797–1806. doi:10.1093/emboj/20.7.1797

Saito H, Watanabe K, Suga H (2001b) Concurrent molecular recognition of the amino acid and tRNA by a ribozyme. RNA 7(12):1867–1878

Schulman LH, Pelka H (1977) Structural requirements for aminoacylation of *Escherichia coli* formylmethionine transfer RNA. Biochemistry 16(19):4256–4265. doi:10.1021/bi00638a020

Sczepanski JT, Joyce GF (2014) A cross-chiral RNA polymerase ribozyme. Nature 515 (7527):440–442. doi:10.1038/nature13900

Shi HJ, Moore PB (2000) The crystal structure of yeast phenylalanine tRNA at 1.93 angstrom resolution: a classic structure revisited. RNA 6(8):1091–1105. doi:10.1017/S1355838200000364

Snead NM, Rossi JJ (2010) Biogenesis and function of endogenous and exogenous siRNAs. Wires RNA 1(1):117–131. doi:10.1002/Wrna.14

Suga H, Hayashi G, Terasaka N (2011) The RNA origin of transfer RNA aminoacylation and beyond. Phil Trans R Soc B 366(1580):2959–2964. doi:10.1098/rstb.2011.0137

Terasaka N, Suga H (2014) Flexizymes-facilitated genetic code reprogramming leading to the discovery of drug-like peptides. Chem Lett 43(1):11–19. doi:10.1246/Cl.130910

Tsukiji S, Pattnaik S, Suga H (2003) An alcohol dehydrogenase ribozyme. Nat Struct Biol 10 (9):713–717. doi:10.1038/nsb964

Tuerk C, Gold L (1990) Systematic evolution of ligands by exponential enrichment: RNA ligands to bacteriophage T4 DNA polymerase. Science 249(4968):505–510. doi:10.1126/science.2200121

Walter G (1986) Origin of life: the RNA world. Nature 319. doi:10.1038/319618a0

Wochner A, Attwater J, Coulson A, Holliger P (2011) Ribozyme-catalyzed transcription of an active ribozyme. Science 332(6026):209–212. doi:10.1126/science.1200752

Xiao H, Murakami H, Suga H, Ferré-D'Amaré AR (2008) Structural basis of specific tRNA aminoacylation by a small in vitro selected ribozyme. Nature 454(7202):358–361. doi:10.1038/nature07033

Yamagishi Y, Shoji I, Miyagawa S, Kawakami T, Katoh T, Goto Y, Suga H (2011) Natural product-like macrocyclic N-methyl-peptide inhibitors against a ubiquitin ligase uncovered from a ribosome-expressed de novo library. Chem Biol 18(12):1562–1570. doi:10.1016/j.chembiol.2011.09.013

Yang F, Moss LG, Phillips GN (1996) The molecular structure of green fluorescent protein. Nat Biotechnol 14(10):1246–1251. doi:10.1038/Nbt1096-1246

Yarus M (2011) The meaning of a minuscule ribozyme. Phil Trans R Soc B 366(1580):2902–2909. doi:10.1098/rstb.2011.0139

Zhou XL, Du DH, Tan M, Lei HY, Ruan LL, Eriani G, Wang ED (2011) Role of tRNA amino acid-accepting end in aminoacylation and its quality control. Nucleic Acids Res 39(20):8857–8868. doi:10.1093/nar/gkr595

Chapter 2
Discovery of Human MicroRNA Precursor Binding to Folic Acid by Small RNA Transcriptomic SELEX

Abstract MicroRNA (miRNA) is about 22 nt single-strand RNA, which is one of the small ncRNAs (Ha and Kim in Nature Reviews Molecular Cell biology, 15 (8):509–524, 2014). miRNAs are loaded into an Argonaute protein to form the RNA-induced silencing complex (RISC) and RISC binds to target mRNA via base paring with miRNA to regulate the expression of target gene. miRNAs are transcribed from genome as part of a long primary transcripts (pri-miRNAs) and then pri-miRNAs are cleaved to produce precursor miRNAs (pre-miRNAs) which form hairpin structure. Pre-miRNAs are exported to the cytoplasm and they are cleaved to mature miRNAs. Biogenesis and functions of miRNAs are regulated by proteins and RNAs in many steps (Ha and Kim in Nature Reviews Molecular Cell Biology, 15(8):509–524, 2014). Recently, regulation of miRNA functions by binding with small molecules was discovered in human (Baselga-Escudero et al. in Nucleic Acids Research 42(2):882–892, 2014). This discovery suggests the existence of RNA aptamer elements binding to small molecules with specific biochemical activities in various human miRNAs. I will report the discovery of human microRNA precursor binding to metabolite and analyses of the function of this RNA. In my master course, tRNA- and rRNA-depleted human small ncRNA library was constructed using tRid technology (Futai et al. in Methods 106:105–111, 2016). Then, SELEX to folic acid was performed to obtain three kinds of RNAs. In my Ph.D., I measured the binding affinity of these RNAs and discovered that precursor microRNA 125a (hsa-pre-miR-125a) are bound to folic acid. Then, further mutation study revealed the essential motif of hsa-pre-miR-125a for binding to folic acid.

Keywords SELEX · Small RNA · MicroRNA · Ribozyme · Folic acid

N. Terasaka, *Applications of Aminoacylation Ribozymes That Recognize the 3′-end of tRNA*, Springer Theses, DOI 10.1007/978-4-431-56517-8_2

2.1 Introduction

Various small noncoding RNAs (ncRNAs) have been discovered in the recent years. Among them, the functions and biogenesis of microRNA (miRNA) have been extensively studied. miRNAs are about 22 nt RNAs pairing to mRNAs to regulate the translation. Canonical pathway of miRNA processing in mammalian is shown in Fig. 2.1 (Winter et al. 2009). An miRNA is initially transcribed as part of a long primary transcript, microRNA (pri-miRNA) by RNA polymerase II or III (Lee et al. 2004; Cai et al. 2004; Borchert et al. 2006). In mammalian, pri-miRNAs are cleaved by Drosha-DGCR8 microprocessor complex in nucleus to produce about 60–80 nucleotide precursor microRNA (pre-miRNA) forming hairpin structure (Lee et al. 2003; Denli et al. 2004; Gregory et al. 2004; Han et al. 2004; Landthaler et al. 2004). The pre-miRNA is then exported to the cytoplasm by Exportin-5-RanGTP (Okada et al. 2009; Yi et al. 2003). In the cytoplasm, pre-miRNA is cleaved to about 22 nt mature miRNA duplex by the RNase III enzyme Dicer (Hutvagner et al. 2001) in complex with the double-stranded RNA

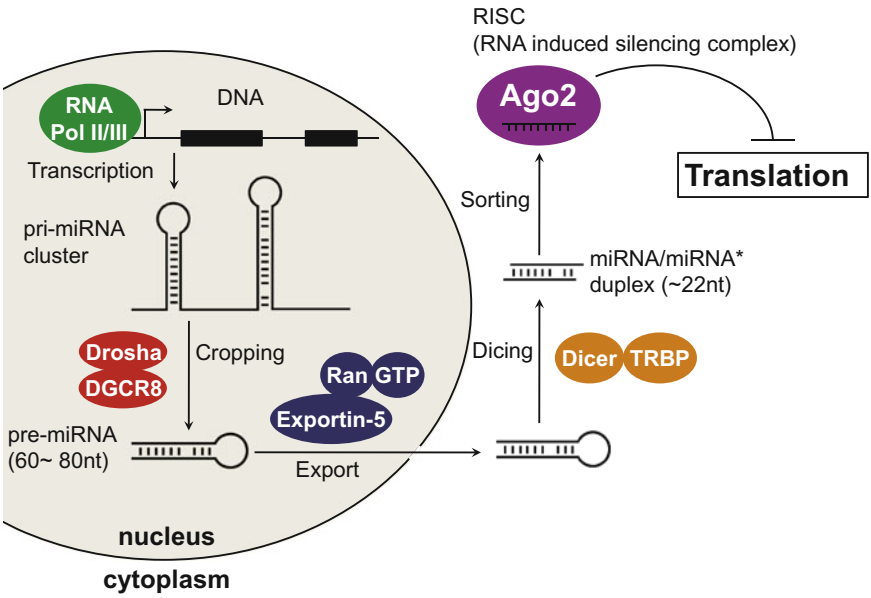

Fig. 2.1 Canonical pathway of microRNA processing. A miRNA is initially transcribed as part of a long pri-miRNA by RNA polymerase II or III. In mammalian, pri-miRNAs are cleaved by Drosha-DGCR8 microprocessor complex in nucleus to produce about 60–80 nucleotide pre-miRNA forming hairpin structure. The pre-miRNA is then exported to the cytoplasm by Exportin-5-RanGTP. In the cytoplasm, pre-miRNA is cleaved to about 22 nt mature miRNA duplex by Dicer in complex with TRBP. One strand of the duplex is loaded into an Argonaute protein (Ago2) to form RISC. RISC binds to target mRNA via base paring with miRNA, whereas Ago2 functions as effectors by recruiting factors that induce translational repression

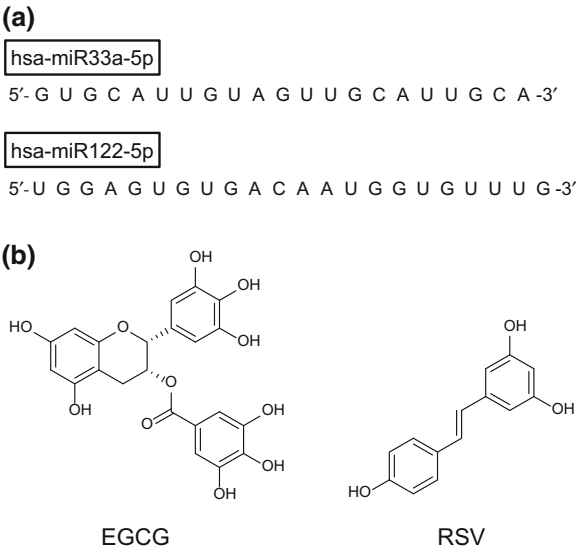

Fig. 2.2 Human miRNAs directly binding to polyphenols. **a** Sequences of hsa-miR-33a-5p and hsa-miR-122-5p which directly bind to specific polyphenols. **b** Chemical structures of epigallocatechin gallate (EGCG) and resveratrol (RSV)

binding protein TRBP (Haase et al. 2005). One strand of the duplex is loaded into an Argonaute protein to form the RNA-induced silencing complex (RISC) and the other strand is discarded (Khvorova et al. 2003; Schwarz et al. 2003; Liu et al. 2004). RISC binds to target mRNA via base paring with miRNA, whereas Argonaute protein functions as effectors by recruiting factors that induce translational repression, mRNA deadenylation and mRNA decay (Huntzinger and Izaurralde 2011).

Biogenesis and functions of miRNAs are regulated by proteins and RNAs in many steps including their transcription, their processing by Drosha and Dicer, their loading onto Argonaute proteins and miRNA turn over, and their dysregulation which are associated with many human diseases including cancer (Ha and Kim 2014; Hansen et al. 2013). Recently, it was reported that direct binding of specific polyphenols (epigallocatechin gallate and resveratrol) to hsa-miR-33a-5p and hsa-miR-122-5p ("hsa" indicates *Homo sapiens*, "5p" indicates mature miRNA derived from 5′-end of pre-miRNA) modulates divergently their levels in hepatic cells (Fig. 2.2) (Baselga-Escudero et al. 2014). This is the first report about post-transcriptional regulation of miRNAs by binding of natural small molecules. In addition to these miRNAs, the RNA elements in human mRNAs binding to ATP or GTP have been discovered by genomic SELEX (Fig. 2.3) (Curtis and Liu 2013; Vu et al. 2012). From these discoveries, I considered that more RNA aptamer elements binding to metabolites with specific biochemical activities exist in other human small ncRNAs. In this chapter, I aimed to discover human small ncRNA including microRNAs and these precursors which bind to metabolite.

Many 145 miRNAs involved in the control of a variety of carcinogenesis mechanisms, were modulated by natural agents, including vitamins, oligoelements,

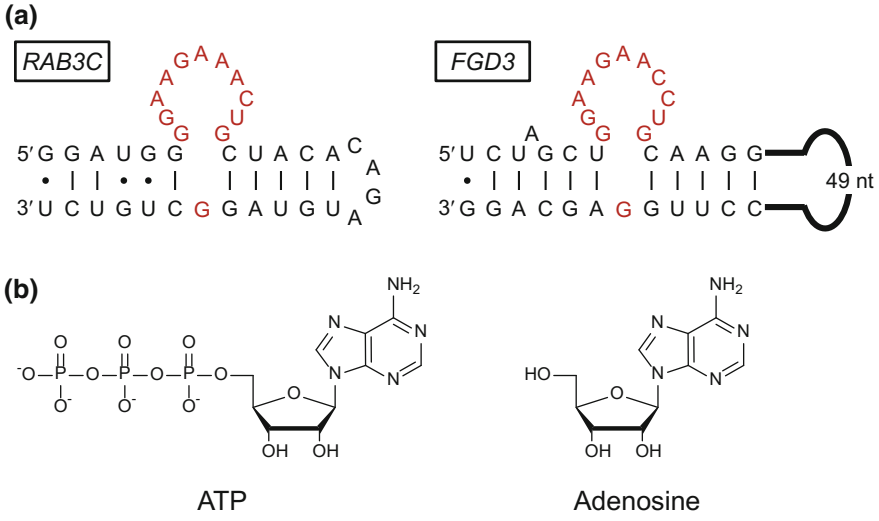

Fig. 2.3 Adenosine aptamers discovered in human transcripts. **a** Secondary structures of the regions containing adenosine aptamers of human *RAB3C* gene and human *FGD3* intron (Vu et al. 2012). *Red* bases are essential motifs binding to adenosine. **b** Chemical structures of adenosine 5′-triphosphate and adenosine

polyphenols, isoflavones, indoles, isothiocyanates, phospholipids, saponins, anthraquinones, and polyunsaturated fatty acids (Izzotti et al. 2012). Although the detailed mechanisms of how to modulate expression of miRNAs by these molecules are unknown, there is a possibility that some of these molecules directly bind to miRNAs or those precursors to regulate the functions. Among these natural agents, I focused my attention on folic acid (vitamin B9), which is one of the water soluble vitamins. The term "folic acid" refers to the synthetic form of the vitamin whereas "folate" refers to the natural forms, such as those present in food (Melse-Boonstra et al. 2004). Folate includes oxidized, reduced, polyglutamylated, methylated, and formylated forms of folic acid (Selhub 1989). Deficiency of dietary folate has been linked to developmental anomalies (Mulinare et al. 1988) as well as increased risk for a number of cancers (Jiang et al. 2003). In addition, folic acid deficient culture medium changes the expression level of many human miRNAs and folic acid supplementation in the culture medium restored miRNA levels, which indicate that modulation of miRNAs by folate is reversible (Marsit et al. 2006). From these results, I chose folic acid as a candidate molecule binding to miRNA.

In order to discover the certain RNAs interacting with small molecules or proteins, pull down method, computational prediction (Barrick et al. 2004) and genomic SELEX (Singer et al. 1997) have been widely used. These approaches have been very successful, but they have some limitations. By classical pull down method, although RNAs expressing in vivo can be discovered, it is difficult to detect RNAs with low abundance in vivo. Computational predictions rely primarily on conservation and structural stability as signal for an active molecule, thus constraining the

range of possible predictions (Zimmermann et al. 2010; Dinger et al. 2008). Genomic SELEX is one of the SELEX methods, where libraries are derived from genomic DNA. This methodology enables to identify new RNA aptamer elements even if the RNA is less abundant. However posttranscriptionally processed RNA sequences [e.g., splicing, nontemplated addition of nucleotides (Koppers-Lalic et al. 2014) and circular permutation (Pan and Uhlenbeck 1993)] cannot be obtained by genomic SELEX because the library was derived from genome. In addition, obtained sequence may not be transcribed from genome in vivo. To overcome these problems, I decided to perform SELEX using library prepared from natural transcript, which is called as cDNA-SELEX (Chen et al. 2003; Dobbelstein and Shenk 1995) or transcriptomic SELEX (Fujimoto et al. 2012). This method enables to discover the small molecule-binding RNAs transcribed in vivo even if the level of expression is very low.

In the small RNA fraction (shorter than 200 nt), tRNAs and rRNAs are much abundant (Lindberg and Lundeberg 2010). Therefore, it is necessary to remove tRNAs and rRNAs from small RNAs in order to construct a cDNA library of high quality, which enables every potential small ncRNAs binding to metabolite equal candidacy for selection. Although several kits to remove the rRNAs using hybridization probes or ribonuclease are commercially available, the reported methods to deplete tRNAs require each sequence to be individually identified and prepared about 30 different probes (Yuan et al. 2003; Liu et al. 2009). In my master course, tRNAs in the small RNA fraction were labeled with biotin-conjugated amino acids using flexizymes and were depleted, which is called as tRid (Futai et al. 2016). From this small RNA library, cDNA library for SELEX was constructed and then selection to folic acid was performed to obtain three kinds of RNA sequences. To my knowledge, this is the first example of transcriptomic SELEX using small RNA library and this method of SELEX was named as small RNA transcriptomic SELEX.

In this chapter, the study during my master course will be briefly summarized and I will report binding analyses of RNAs obtained from small RNA transcriptomic SELEX performed during my Ph.D.

2.2 Results and Discussions

2.2.1 Summary of Master Course Study

In my master course, tRNA-depleted small RNA library was constructed using tRid technology (Futai et al. 2016) and some RNAs binding to folic acid were discovered using small RNA transcriptomic SELEX. First, I briefly summarize the study during my master course.

Because the expression level of miRNAs and precursors are totally different among the cells and conditions, eight human cell lines (BeWo, HuH-7,

Table 2.1 Human miRNA precursor profile [adapted from Landgraf et al. (2007)] and cell lines used in this chapter

Organ systems and cell types	Numbers of miRNA precursors	Corresponding cell lines used in this chapter
hsa_Osteosarcoma-U2Os-uninduced	168	HuO-3N1
hsa_Placenta	152	BeWo
hsa_renal_carcinoma-DH1-diff-3d	159	VMRC-RCW
hsa_Teratocarcinoma-NT2-norm	111	NEC14
hsa_Hepatoma-PLC	139	HuH-7
hsa_Breast-adenocarcinoma-MCF7	100	MCF7
hsa_Cervix-HeLa-IFNa	120	HeLaS3
hsa_Burkitt-patient3	128	RAJI

VMRC-RCW, NEC14, HuO-3N1, RAJI, MCF7 and HeLaS3 cells) were chosen based on the expression levels of miRNAs to include various miRNAs into the library (Table 2.1) (Landgraf et al. 2007). After extracting small RNAs from these cell lines, rRNAs were removed by hybridization with complementary nucleotide probe (Ribominus) and tRNAs were depleted by tRid (Fig. 2.4) (Futai et al. 2016). Consequently tRNA-/rRNA-depleted small RNA library was constructed. Next, tRNA-/rRNA-depleted small RNA library was converted to cDNA library. RNA library was ligated with 3′- and 5′-adaptors containing promoter sequence for T7 RNA polymerase. Then, RNA library ligated with adaptors was reverse transcribed to cDNA and amplified by PCR (Fig. 2.4). In comparison with the crude fraction of small RNAs, the population of non-rRNA/tRNA small RNAs was suitably enriched, with only 24 and 9% of tRNAs (including non-CCA tRNA fragments and pre-tRNAs) and rRNAs, respectively, remaining in the final fraction (the total number of sequences was 89, Fig. 2.5). This small-RNA-enriched library was deemed to be applicable to smaRt-SELEX against a target molecule.

Folic acid (Fig. 2.6a) was immobilized onto the magnetic beads via ester bond, whose surface is covered by hydroxyl group. Small RNA transcriptomic SELEX using the folic acid-immobilized beads and the library described above was performed four rounds. PAGE analysis of RNA library indicated the fractions of small RNAs bound to the folic acid beads were enriched over the background and several discrete bands appeared (Fig. 2.6b and c). The RNA pool at the fourth round was then cloned and sequenced and three RNA sequences (hsa-pre-miR-125a, FA1 and FA2) were enriched (Table 2.2). FA1 is antisense sequence to mitochondrial mRNA of ND1 (NADH dehydrogenase 1) bearing additional poly-A/C sequence at the 3′-end, which is not coded in genome. FA2 is 5′-fragment of $tRNA^{Gly}_{GCC}$, whose 3′-fragment was discovered as small RNA (tRF3006) (Lee et al. 2009).

Because 3′- and 5′-adaptors were ligated with naturally transcribed RNA sequences for reverse transcription and PCR during SELEX, it was possible that these adaptors are essential for binding to folic acid. The secondary structures predicted using mfold software (Zuker 2003) are shown in Fig. 2.7. In the case of FA1 and FA2, ligation of adaptors dramatically changed the secondary structure

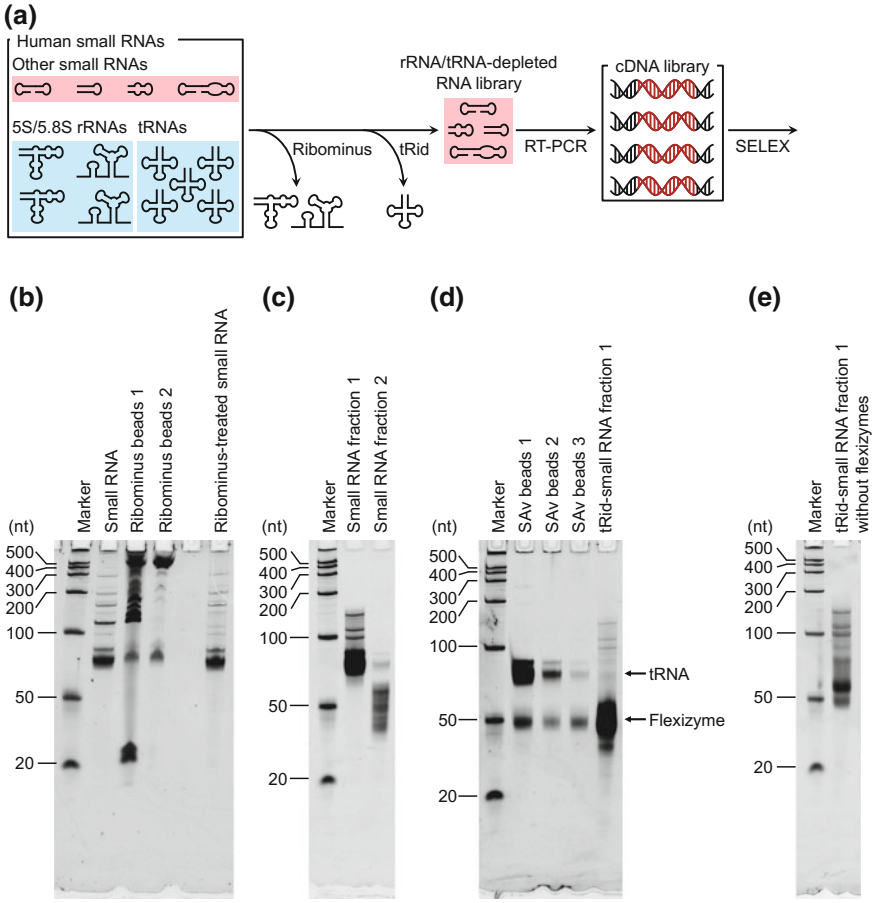

Fig. 2.4 Construction of a human tRNA-depleted small RNA library. **a** Schematic illustration of small RNA transcriptomic SELEX. From the small RNA fraction, the 5S and 5.8S rRNAs were removed using probes complementary to these rRNAs (RiboMinus, Life technologies), and then tRNAs were depleted using the tRid method. The rRNA-/tRNA-depleted small RNA library was converted to cDNA by RT-PCR and SELEX was performed. **b** RiboMinus™ treated human small RNA. Lanes marked Ribominus beads 1 and 2, indicate magnetic beads after RiboMinus treatment which were directly loaded onto the polyacrylamide gel. **c** Separation of rRNA-depleted small RNA into fraction 1 (lager than about 60 nt) and 2 (smaller than about 60 nt). **d** Depletion of tRNAs from small RNA fraction 1 by tRid. In the lanes marked streptavidin (SAv) beads 1, 2, and 3, the magnetic beads after the tRid treatment were directly loaded onto the polyacrylamide gel. **e** Removal of flexizymes after the tRid treatment

(referred as FA1 + adp and FA2 + adp). On the other hand, the structure of hsa-pre-miR-125a was retained when adaptors were ligated (named as hsa-pre-miR-125a + adp). Therefore, it was necessary to investigate whether these RNAs can bind to folic acid without adaptor sequences.

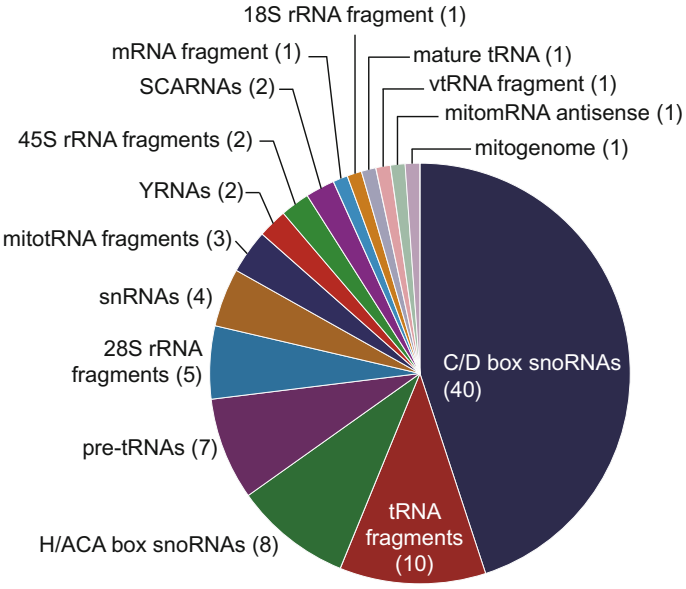

Fig. 2.5 The proportion of rRNA-/tRNA-depleted human small RNA library. Total sequence number was 89. The numbers after the name of RNAs indicate the number of sequences

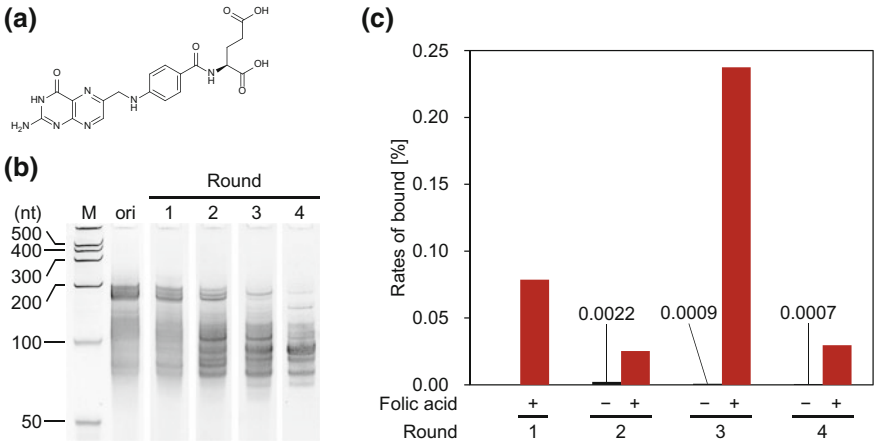

Fig. 2.6 Isolation of folic acid binding small RNAs using small RNA transcriptomic SELEX. **a** Chemical structure of folic acid. **b** Polyacrylamide gel analysis of the RNA library from each round of smaRt-SELEX. M indicates the RNA marker, "ori" indicates the RNA library before smaRt-SELEX. **c** Bead-binding activity of RNAs from each round of the smaRt-SELEX. Proportional binding was determined by normalizing bound quantities to input quantities of RNA. *Black bars* indicate binding of RNA to hydroxyl-beads that were not conjugated to folic acid, and *red bars* indicate binding of RNA to folic acid-immobilized beads. Hydroxyl-beads were not used in the first round

Table 2.2 RNAs obtained from SELEX

Sequence (5′ to 3′)	Remarks	Frequency
TTTTATGGCGTCAGCGAAGGGTT GTAGTAGCCCGTAAAAACCAAAAAAACC	FA1 (Antisense of MT-ND1 mRNA)	20/40
GCATTGGTGGTTCAGTGGTAGAA TTCTCGCCTGCCACGCGGGAGGCCCGGGT	FA2 (5′-fragment of $tRNA^{Gly}_{GCC}$)	7/40
TCCCTGAGACCCTTTAACCTGTGAGG ACATCCAGGGTCACAGGTGAGGTTCTT GGGAGCC	Hsa-pre-miR-125a	3/40
TCCTCTTTAGTATAGTGGTGAGTATC CCCGCCTGTCACGCGGGAGACCGG	5′-fragment of $tRNA^{Asp}_{GTC}$	1/40
CCTGTCACGCGGGAGACCGGGGTT CGATTCCCCGACGGGGAGCCA	3′-fragment of $tRNA^{Asp}_{GTC}$	1/40
TCACTGACTGTCTTGGGAGGAGGGG CTGGGTGTGGCACACAGTGA	Chromosome 22 Antisense of MYH9 gene	1/40
GGGAGGGTGCCTGGAGGAGTGGAG GGATTGGATTTACACCCTCTTA	Chromosome 2	1/40
CAGCCGCAAGGGAGGCTGGGAAG TACAGTCATGCCTTCAGGTAGCCGT GAGCCCTG	Chromosome 1	1/40
GAAAAAGTCATGGAGGCCATGGGGT TGGCTTGAAACCAGCTTTGGGGGGTTCGAT TCCTTCCTTTTTTTGCCA	$tRNA^{Ser}_{UGA}$	1/40
TACGGACTCACTATAGGGAGCTATCG ACGTAACGCTGGGGATTGTGGGTTCGTCCCA TCTGGGTCGCCA	Similar to $tRNA^{Arg}_{CCG}$	1/40
TTTTGGGGTTTGGCAAAAACCAAA AAAACCAACCCAAACCCACCAAAAACCAA	No match in the databases	1/40
TTGGCTGAGGATGCGGAGGGGAGGAG GCTGAGTA	Chromosome 11 Intron of TAF6L gene	1/40
TGAGGATGGTGGTCAAGGGACCCCTATCACAC CACCACCACCAA	Mitochondrial genome	1/40

2.2.2 K_D Determination and Mutation Study Using Biolayer Interferometry

During my doctor course, binding interaction between folic acid and RNAs obtained from SELEX was investigated. Three RNAs ligated with adaptors were prepared by in vitro transcription and three RNAs without adaptors which were chemically synthesized were purchased from Gene design Inc. Dissociation constant (K_D) values were measured using biolayer interferometory (BLI). In order to immobilize folic acid onto the biosensors, ethylenediamine was immobilized onto

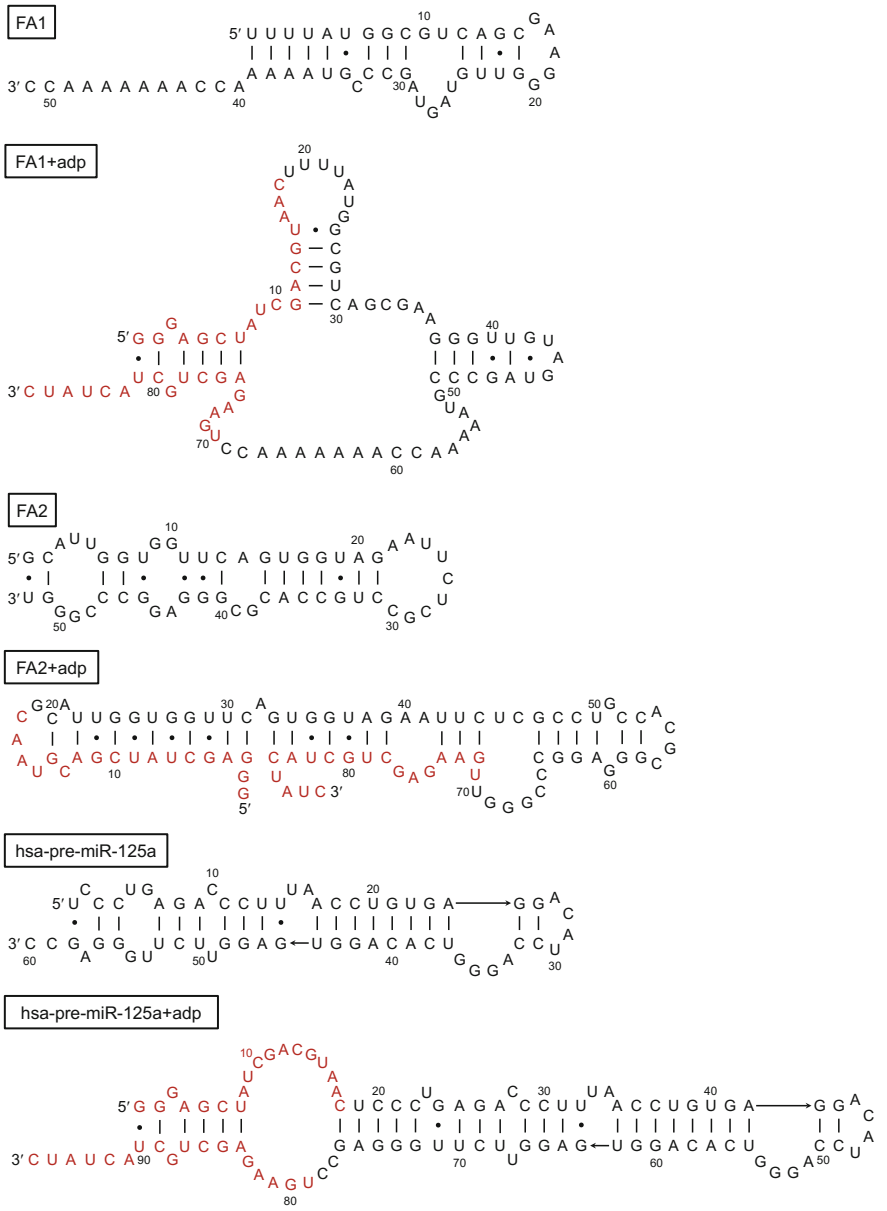

Fig. 2.7 Predicted secondary structure of RNAs obtained from SELEX to folic acid. Secondary structures were predicted using mfold software (Zuker 2003). *Red* bases indicated adaptor sequences and *numbers* indicate the nucleotide positions. *Lines* denote the Watson–Crick base pairs and *bullets* denote wobble base pairs

Table 2.3 Dissociation constant of RNAs obtained from SELEX

RNA	K_D (μM)	R^2
FA1 + Adp	3.8	0.98
FA2 + Adp	ND	
FA1	ND	
FA2	ND	

ND indicates "not determined" and R^2 value is derived from curve fitting in the steady-state analysis

AR2G (Amine Reactive Second-Generation) biosensors whose surface bears carboxyl group. Then, folic acid was conjugated with this sensor via amide bond. Six to eight different concentrations of RNA were used for steady-state analysis to determine the K_D values.

The results of binding analysis about FA1 and FA2 were shown in Table 2.3. FA1 was bound to folic acid only when adaptors were ligated (K_D value was 3.8 μM). This indicates that ligation of adaptors is essential for FA1 to bind to folic acid, which is consistent with the difference of predicted structure between FA1 and FA1 + adp (Fig. 2.6). On the other hand, FA2 did not bind to folic acid with or without adaptors. This result indicates that it was false positive when FA2 sequence was obtained by SELEX to folic acid. During SELEX, cDNAs are amplified by PCR. However, each cDNA is not uniformly amplified at the same efficiency by PCR, which means that the sequences whose PCR efficiency is higher could easily be amplified and therefore such sequences are obtained from final round as false positive (Tsuji et al. 2009).

The results of binding analysis about hsa-pre-miR-125a were shown in Table 2.4. In contrast to FA1 and FA2, hsa-pre-miR-125a can bind to folic acid with or without adaptors, and both hsa-pre-miR-125a and hsa-pre-miR-125a + adp showed the almost the same binding affinity (K_D values were 2.8 μM and 1.9 μM each). These results indicate that adaptors do not affect the binding affinity of hsa-pre-miR-125a to folic acid.

To identify the essential motif of hsa-pre-miR-125a to bind to folic acid, mutants were prepared by in vitro transcription and K_D values of those mutants were measured. Because 5′-end base of the wild-type hsa-pre-miR-125a is not G, the efficiency of in vitro transcription by T7 RNA polymerase was too low. Therefore, U1G/G58C mutant hsa-pre-miR-125a whose predicted secondary structure was the same as that of wild-type was prepared to enhance the T7 transcription efficiency, and U1G/G58C mutant showed the almost the same K_D value as that of wild-type (2.6 μM) (Fig. 2.8 and Table 2.4). Therefore, I introduced the same mutations (U1G/G58C) into other mutants except for m1 mutant (Fig. 2.8 and Table 2.4). First, as a negative control hsa-pre-miR-21 U1G mutant was prepared. The binding affinity of hsa-pre-miR-21 U1G was too low to determine the K_D value. Next, the

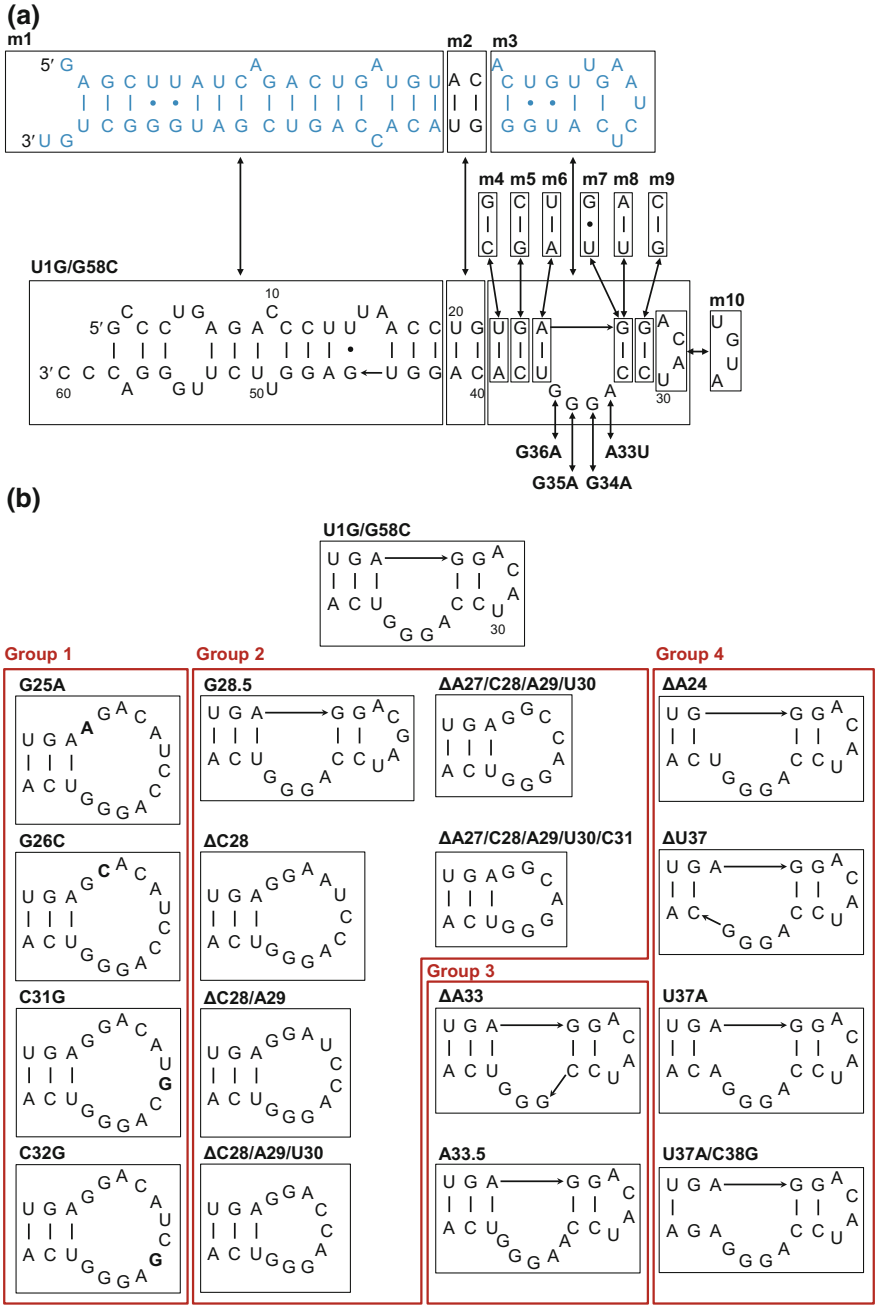

Fig. 2.8 Mutants of hsa-pre-miR-125a. *Lines* denote the Watson–Crick base pairs and *bullets* denote wobble base pairs. Secondary structures were predicted using mfold software (Zuker 2003). **a** Roughly mutated hsa-pre-miR-125a mutants. *Cyan* bases denote corresponding regions to hsa-pre-miR-21 used as negative control. **b** Loop region mutants were divided into four groups. *Bold* bases in group 1 are mutated bases

Table 2.4 Dissociation constant of hsa-pre-miR-125a mutants

RNA	Mutation	K_D (μM)	R^2
hsa-pre-miR-21	U1G	ND	
hsa-pre-miR-125a	WT	2.8	0.98
	Adp+	1.9	0.97
	U1G/G58C	2.6	0.99
hsa-pre-miR-125a U1G/G58C	m1	4.6	0.98
	m2	6.2	0.99
	m3	ND	
	m4	2.1	0.98
	m5	3.2	1.00
	m6	3.2	0.99
	m7	32	0.98
	m8	62	0.96
	m9	48	0.95
	m10	4.2	0.88
	A33U	3.0	0.96
	G34A	38	0.94
	G35A	ND	
	G36A	35	0.99
	G25A	73	0.99
	G26C	62	0.99
	C31G	6.0	0.99
	C32G	11	0.99
	G28.5	5.9	0.98
	ΔC28	1.8	0.96
	ΔC28/A29	1.4	0.94
	ΔC28/A29/U30	1.2	0.93
	ΔA27/C28/A29/U30	5.2	0.97
	ΔA27/C28/A29/U30/C31	12	0.98
	ΔA33	11	1.00
	A33.5	48	0.93
	ΔA24	ND	
	ΔU37	ND	
	U37A	2.1	0.95
	U37A/C38G	ND	

ND indicates "not determined"

some regions of pre-miR-125a U1G/G58C mutant were replaced from pre-miR-21 U1G mutant to prepare m1 and m3 mutant, and the region of pre-miR-125a which is same as hsa-pre-miR-21 was substituted with other bases to prepare m2 mutant (Fig. 2.8a). Mutant m1 and m2 had comparable K_D value but the binding affinity of

m3 was too low to be determined (Table 2.4). In addition, mutations at three base pairs next to the terminal loop did not change the binding affinity (mutants m4, m5 and m6 in Fig. 2.8a). These results indicate that terminal loop region of hsa-pre-miR-125a is important for binding to folic acid. Therefore binding affinity of several mutants whose bases of terminal loop region were substituted with other bases was measured (Fig. 2.8a). Mutants m10 and A33U showed almost the same binding affinity (K_D = 4.2 μM and 3 μM each in Table 2.4) as that of wild-type, but the K_D values of other mutants (m7, m8, m9, G34A, G35A and G36A) increased about 10 to 20 times more than that of wild-type (Fig. 2.8 and Table 2.4).

For further analysis, several point mutants, deletion mutants, and insertion mutants were prepared and divided into four groups (Fig. 2.8b). Each mutant in group 1 has a point mutation in the terminal loop to disrupt a structure of terminal loop. Mutants G25A, G26C, and C32G showed decreased binding affinity but C31G had the comparable binding affinity (K_D = 6.0 μM in Fig. 2.8b and Table 2.4), which indicate that G24, G26, and C32 are important but the predicted structure of terminal loop is not essential for binding. Next, the other bases than important bases for binding observed in mutation study of group 1 were deleted or a base was inserted (mutants in group 2 in Fig. 2.8b). All these mutants except for ΔA27/C28/A29/U30/C31 mutant showed the comparable K_D values, which indicates that minimal length of terminal loop necessary for binding is 8 nt. Both mutants ΔA33 and G34.5 (group 3 in Fig. 2.8b) had weak binding affinity (K_D = 11 and 48 μM each in Table 2.4). This result and the fact that A33U showed the comparable affinity (Table 2.4) indicate that one nucleotide between C32 and G34 is important but the variety of bases is not. Deletion of a base at the next to the terminal loop (ΔA24 and ΔU37 in group 4) and two mispairs next to the terminal loop (U37A/C38G in group 4) abolished the binding affinity but one mispair at the same position (U37A in group 4) did not show the decrease of binding affinity.

From mutation study described above, the essential motif for binding to folic acid was shown in Fig. 2.9. This motif was not observed in other RNAs obtained by SELEX (Table 2.2). By searching the structure of human miRNA precursors registered in the database of microRNA (miRbase (Kozomara and Griffiths-Jones 2014), http://www.mirbase.org/), this motif was discovered only in miR-125a precursors.

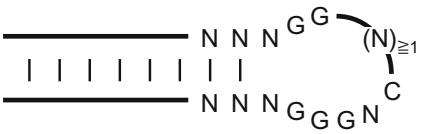

Fig. 2.9 Essential motif for binding to folic acid. N means A/U/G/C. *Black bold lines* indicate RNA and *lines* between bases denote base pairs

2.3 Conclusion

In this chapter, novel interaction between hsa-pre-miR-125a and folic acid was identified using small RNA transcriptomic SELEX. Because the abundance of miRNA precursors including both pri- and pre-miRNAs is too low, the methods to discover the interaction of these RNAs and small molecules have been limited. This small RNA transcriptomic SELEX has great potential to identify the interaction of low abundant small RNAs. In addition, new RNA motif for binding to folic acid was discovered, which is difficult to be discovered by computational analysis.

However, there are still some problems in this method. The first problem is the influence of the ligation of adaptor sequences. Because these adaptors may dramatically change the structure of natural transcript, the potential RNA aptamer elements whose structures are changed by adaptors cannot be identified by this method. To overcome this problem, it is necessary to cleavage the adaptors after PCR or transcription and re-ligate these before RT-PCR (reverse transcription-PCR), or perform multiple selections using different adaptor sets. Second problem is diversity of transcripts extracted from cells. The expression levels of RNAs are different among the cells and conditions of culture. To include all RNAs transcribed in various cells, it is necessary to extract RNAs from various cells or organs including both cancer cells and normal cells.

Analysis of binding affinity of hsa-pre-miR-125a revealed the essential motif in the terminal loop region for binding to folic acid. Because this loop region is common in both pri- and pre-miR-125a, folic acid binds to both precursors. In addition, this motif is conserved in mammalian (Fig. 2.10). It was reported the terminal loop region controls miRNA processing by Drosha and Dicer (Zhang and Zeng 2010). In addition, several regions of pri-miRNAs are important for processing by Dorhsa, apical stem and terminal loop elements of pri-miR-125a have

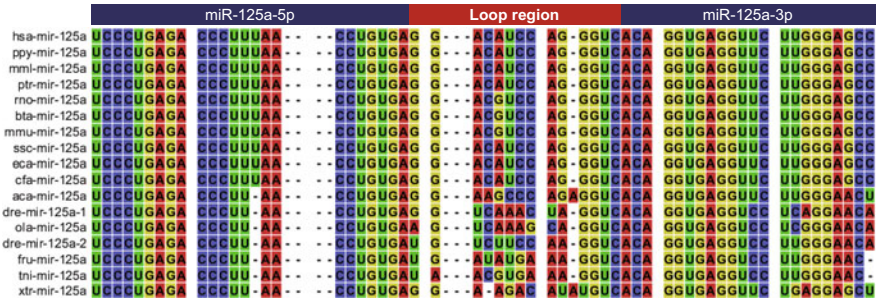

Fig. 2.10 The sequences of pre-miR-125a of various species. These sequences were from miRbase (Kozomara and Griffiths-Jones 2014) (http://www.mirbase.org/). The abbreviations indicate as follows, Hsa: *Homo sapiens*, ppy: *Pongo pygmaeus*, mml: *Macaca mulatta*, ptr: *Pan troglodytes*, rno: *Rattus norvegicus*, bta: *Bos taurus*, mmu: *Mus musculus*, ssc: *Sus scrofa*, eca: *Equus caballus*, cfa: *Canis familiaris*, aca: *Anolis carolinensis*, dre: *Danio rerio*, ola: *Oryzias latipes*, fru: *Fugu rubripes*, tni: *Tetraodon nigroviridis*, xtr: *Xenopus tropicalis*

significant contributions on processing by Drosha (Auyeung et al. 2013). These reports suggested the potential of folic acid binding to terminal loop of miR-125a precursors to regulate the processing. Nonetheless, further studies are necessary to elucidate whether the interaction between folic acid and miR-125a precursors regulate the processing.

In conclusion, I here described the small RNA transcriptomic SELEX methodology, which enabled us to uncover potential aptamers against a metabolite, folic acid in this report, from a pool of small RNAs in a length range of 10–200 nt. This method is certainly extendable to other metabolites as well as various intracellular macromolecules such as proteins for the discovery of potential aptamers derived from naturally occurring small RNAs, including pre- and pri-miRNAs.

2.4 Materials and Methods

Chemical synthesis of α-*N*-biotinyl-phenylalanine cyanomethyl ester (Biotin-Phe-CME)

Biotin-Phe-CME was synthesized as previously described (Saito et al. 2001).

Preparation of RNAs

The Fx3 + N1 and RNAs for BLI analysis were prepared using runoff in vitro transcription with T7 RNA polymerase and purified by denaturing PAGE (8 M Urea, 1 × TBE, %T = 8 and %C = 5). The primers for preparing transcription templates and RNAs are shown in Tables 2.5 and 2.6. All primers were purchased from Eurofins Genomics K.K. (Japan). FA1, FA2, and hsa-pre-miR-125a RNAs were purchased from Gene Design Inc. (Japan). The concentrations of RNAs were determined by absorbance at 260 nm.

Preparation of dial-Fx3

In order to avoid the amplification of Fx3 during the construction of small RNA library, 3′-end of Fx3 + N1 purified by denaturing PAGE was oxidized to dialdehyde group (named as dial-Fx3 + N1) under the following conditions; 20 μM Fx3 + N1 was incubated with 30 mM $NaIO_4$ on ice for 20 min and then 2% (w/v) $LiClO_4$ in acetone was added. The mixture was centrifuged at 15,000 × *g* (room temperature) for 10 min to precipitate dial-Fx3 + N1. The pellet was rinsed with acetone and centrifuged at 15,000 × *g* (room temperature) for 3 min two times, and dissolved in water. The concentrations of RNAs were determined by absorbance at 260 nm.

Cell cultures for construction of small RNA library

BeWo cells (RIKEN Cell Bank, code RCB1644) were grown in Ham's F-12 medium (17458-65, Nacalai Tesque Inc.) supplemented with 100 unit/mL penicillin, 100 μg/mL streptomycin (15140-122, Thermo Fisher Scientific Inc.) and

Table 2.5 Primers and adaptors used in this chapter

Name	Sequence (5′ to 3′)	Remarks
Primer Fx3-1	TAATACGACTCACTATAGGATCGAAAGATTTCCG CAGGCC	Transcription of Fx3 + N1
Primer Fx3-2	NACCTAACGCCAATACCCTTTCGGGCCTGCGGAA ATCTTT	Transcription of Fx3 + N1
Primer Fx3-3	GGCGTAATACGACTCACTATAGG	Transcription of Fx3 + N1
primer Fx3-4	NACCTAACGCCAATACCCTT	Transcription of Fx3 + N1
Primer seq-1	GCCTCTTCGCTATTACGCCAGC	Sequencing
Primer seq-2	TGTTGTGTGGAATTGTGAGCGG	Sequencing
3′-adaptor	*A*pp-TGAAGAGCTGCTACTATC-ddC	Construction of the cDNA library
5′-adaptor	*GGCGUAAUACGACUCACUAUAGGGAGCUAUCGACGUAAC*	Construction of the cDNA library
Primer sele-1	GGCGTAATACGACTCACTATAGGGAGCTATCGACGTAAC	Construction of the cDNA library and selection
Primer sele-2	GATAGTAGCAGCTCTTCA	Construction of the cDNA library and selection
Primer FA1 + Adp-1	GGGAGCTATCGACGTAACTTTTATGGCGTCAGCGA AGGGTTG	Transcription of FA1 + Adp
Primer FA1 + Adp-2	GGTTTTTTTGGTTTTTACGGGCTACTACAACCCTTC GCTGACGCC	Transcription of FA1 + Adp
Primer FA1 + Adp-3	GATAGTAGCAGCTCTTCAGGTTTTTTTGGTTTTTA CGGGCTAC	Transcription of FA1 + Adp
Primer FA2 + Adp-1	GGGAGCTATCGACGTAACGCATTGGTGGTTCAGTG GTAGAATTC	Transcription of FA2 + Adp
Primer FA2 + Adp-2	ACCCGGGCCTCCCGCGTGGCAGGCGAGAATTCTACC ACTGAACCACC	Transcription of FA2 + Adp
Primer FA2 + Adp-3	GATAGTAGCAGCTCTTCAACCCGGGCCTCCCGC	Transcription of FA2 + Adp

(continued)

Table 2.5 (continued)

Name	Sequence (5′ to 3′)	Remarks
Primer hsa-pre-miR-125a + Adp-1	GGGAGCTATCGACGTAACTCCCTGAGACCCTTTAACCTG	Transcription of hsa-pre-miR-125a + Adp
Primer hsa-pre-miR-125a + Adp-2	GGCTCCCAAGAACCTCACCTGTGACCCTGGATGTCCTCAC	Transcription of hsa-pre-miR-125a + Adp
Primer hsa-pre-miR-125a + Adp-3	GATAGTAGCAGCTCTTCAGGCTCCCAAGAACCTCACC	Transcription of hsa-pre-miR-125a + Adp
Primer T7 + Adp	GGCGTAATACGACTCACTATAGGGAGCTATCGACGTAAC	Transcription of FA1/FA2/hsa-pre-miR-125a + Adp
Primer T7	GGCGTAATACGACTCACTATAG	Transcription of pre-miRNAs
pre-miRNA template 1	ACAGCCCATCGACTGGTGTTGCCATGAGATTCAACAGTCAACAT CAGTCTGATAAGCTCTATAGTGAGTCGTATTACGCC	Transcription of pre-miRNAs
pre-miRNA template 2	GGGCTCCAAGAACCTCACCTGTGACCCTGGATGTCCTCACAGGTT AAAGGGTCTCAGGGCTATAGTGAGTCGTATTACGCC	Transcription of pre-miRNAs
pre-miRNA template 3	ACAGCCCATCGACTGGTGTTGTGACCCTGGATGTCCTCACAACAT CAGTCTGATAAGCTCTATAGTGAGTCGTATTACGCC	Transcription of pre-miRNAs
pre-miRNA template 4	GGGCTCCAAGAACCTCACCACTGACCCTGGATGTCCTCAGTGGT TAAAGGGTCTCAGGGCTATAGTGAGTCGTATTACGCC	Transcription of pre-miRNAs
pre-miRNA template 5	GGGTCCCAAGAACCTCACCTGCCATGAGATTCAACAGTCAGGTT AAAGGGTCTCAGGGCTATAGTGAGTCGTATTACGCC	Transcription of pre-miRNAs
pre-miRNA template 6	GGGCTCCAAGAACCTCACCTGGGACCCTGGATGTCCTCCCAGGTT AAAGGGTCTCAGGGCTATAGTGAGTCGTATTACGCC	Transcription of pre-miRNAs
pre-miRNA template 7	GGGCTCCAAGAACCTCACCTGTCACCCTGGATGTCCTGACAGGTT AAAGGGTCTCAGGGCTATAGTGAGTCGTATTACGCC	Transcription of pre-miRNAs
pre-miRNA template 8	GGGCTCCAAGAACCTCACCTGTGTCCCTGGATGTCCACACAGGT TAAAGGGTCTCAGGGCTATAGTGAGTCGTATTACGCC	Transcription of pre-miRNAs

(continued)

Table 2.5 (continued)

Name	Sequence (5′ to 3′)	Remarks
pre-miRNA template 9	GGGCTCCAAGAACCTCACCTGTGACCCTAGATGTCCTCACAGGT TAAAGGGTCTCAGGGCTATAGTGAGTCGTATTACGCC	Transcription of pre-miRNAs
pre-miRNA template 10	GGGCTCCAAGAACCTCACCTGTGACCCTAGATGTCTTCACAGGT TAAAGGGTCTCAGGGCTATAGTGAGTCGTATTACGCC	Transcription of pre-miRNAs
pre-miRNA template 11	GGGCTCCAAGAACCTCACCTGTGACCCTGCATGTGCTCACAGGTT AAAGGGTCTCAGGGCTATAGTGAGTCGTATTACGCC	Transcription of pre-miRNAs
pre-miRNA template 12	GGGCTCCAAGAACCTCACCTGTGACCCTGGTACACCTCACAGGTT AAAGGGTCTCAGGGCTATAGTGAGTCGTATTACGCC	Transcription of pre-miRNAs
pre-miRNA template 13	GGGCTCCAAGAACCTCACCTGTGACCCAGGATGTCCTCACAGGT TAAAGGGTCTCAGGGCTATAGTGAGTCGTATTACGCC	Transcription of pre-miRNAs
pre-miRNA template 14	GGGCTCCAAGAACCTCACCTGTGACCTTGGATGTCCTCACAGGTT AAAGGGTCTCAGGGCTATAGTGAGTCGTATTACGCC	Transcription of pre-miRNAs
pre-miRNA template 15	GGGCTCCAAGAACCTCACCTGTGACTCTGGATGTCCTCACAGGTT AAAGGGTCTCAGGGCTATAGTGAGTCGTATTACGCC	Transcription of pre-miRNAs
pre-miRNA template 16	GGGCTCCAAGAACCTCACCTGTGATCCTGGATGTCCTCACAGGTT AAAGGGTCTCAGGGCTATAGTGAGTCGTATTACGCC	Transcription of pre-miRNAs
pre-miRNA template 17	GGGCTCCAAGAACCTCACCTGTGACCCTGGATGTCTTCACAGGTT AAAGGGTCTCAGGGCTATAGTGAGTCGTATTACGCC	Transcription of pre-miRNAs
pre-miRNA template 18	GGGCTCCAAGAACCTCACCTGTGACCCTGGATGTGCTCACAGGT TAAAGGGTCTCAGGGCTATAGTGAGTCGTATTACGCC	Transcription of pre-miRNAs
pre-miRNA template 19	GGGCTCCAAGAACCTCACCTGTGACCCTGCATGTCCTCACAGGT TAAAGGGTCTCAGGGCTATAGTGAGTCGTATTACGCC	Transcription of pre-miRNAs
pre-miRNA template 20	GGGCTCCAAGAACCTCACCTGTGACCCTCGATGTCCTCACAGGTT AAAGGGTCTCAGGGCTATAGTGAGTCGTATTACGCC	Transcription of pre-miRNAs
pre-miRNA template 21	GGGCTCCAAGAACCTCACCTGTGACCCTGGATCGTCCTCACAGG TTAAAGGGTCTCAGGGCTATAGTGAGTCGTATTACGCC	Transcription of pre-miRNAs

(continued)

Table 2.5 (continued)

Name	Sequence (5′ to 3′)	Remarks
pre-miRNA template 22	GGGCTCCAAGAACCTCACCTGTGACCCTGGATTCCTCACAGGTTA AAGGGTCTCAGGGCTATAGTGAGTCGTATTACGCC	Transcription of pre-miRNAs
pre-miRNA template 23	GGGCTCCAAGAACCTCACCTGTGACCCTGGATCCTCACAGGTTAA AGGGTCTCAGGGCTATAGTGAGTCGTATTACGCC	Transcription of pre-miRNAs
pre-miRNA template 24	GGGCTCCAAGAACCTCACCTGTGACCCTGGTCCTCACAGGTTAAAG GGTCTCAGGGCTATAGTGAGTCGTATTACGCC	Transcription of pre-miRNAs
pre-miRNA template 25	GGGCTCCAAGAACCTCACCTGTGACCCTGGCCTCACAGGTTAAAG GGTCTCAGGGCTATAGTGAGTCGTATTACGCC	Transcription of pre-miRNAs
pre-miRNA template 26	GGGCTCCAAGAACCTCACCTGTGACCCTGCCTCACAGGTTAAAGG GTCTCAGGGCTATAGTGAGTCGTATTACGCC	Transcription of pre-miRNAs
pre-miRNA template 27	GGGCTCCAAGAACCTCACCTGTGACCCGGATGTCCTCACAGGTTA AAGGGTCTCAGGGCTATAGTGAGTCGTATTACGCC	Transcription of pre-miRNAs
pre-miRNA template 28	GGGCTCCAAGAACCTCACCTGTGACCCTTGGATGTCCTCACAGGT TAAAGGGTCTCAGGGCTATAGTGAGTCGTATTACGCC	Transcription of pre-miRNAs
pre-miRNA template 29	GGGCTCCAAGAACCTCACCTGTGACCCTGGATGTCCCACAGGTTA AAGGGTCTCAGGGCTATAGTGAGTCGTATTACGCC	Transcription of pre-miRNAs
pre-miRNA template 30	GGGCTCCAAGAACCTCACCTGTGCCCTGGATGTCCTCACAGGTT AAAGGGTCTCAGGGCTATAGTGAGTCGTATTACGCC	Transcription of pre-miRNAs
pre-miRNA template 31	GGGCTCCAAGAACCTCACCTGTGTCCCTGGATGTCCTCACAGGT TAAAGGGTCTCAGGGCTATAGTGAGTCGTATTACGCC	Transcription of pre-miRNAs
pre-miRNA template 32	GGGCTCCAAGAACCTCACCTGTCTCCCTGGATGTCCTCACAGGTT AAAGGGTCTCAGGGCTATAGTGAGTCGTATTACGCC	Transcription of pre-miRNAs

N means A/T/G/C, italic types indicate ribonucleotides, ddC indicates dideoxyribocytidine

Table 2.6 RNAs used in this chapter

Name	Sequence (5′ to 3′)
Fx3 + N1	*GGAUCGAAAGAUUUCCGCAGGCCCGAAAGGGUAUUGG CGUUAGGUN*
FA1 + Adp	*GGGAGCUAUCGACGUAACUUUUAUGGC GUCAGCGAAGGGUUGUAGUAGCCCGUAAAAACCAAAAAAA CCUGAAGAGCUGCUACUAUC*
FA2 + Adp	*GGGAGCUAUCGACGUAACGCAUUGGUG GUUCAGUGGUAGAAUUCUCGCCUGCCACGCGGGAGGCCC GGGUUGAAGAGCUGCUACUAUC*
FA1	*UUUUAUGGCGUCAGCGAAGGGUUGUA GUAGCCCGUAAAAACCAAAAAAACC*
FA2	*GCAUUGGUGGUUCAGUGGUAGAAUUC UCGCCUGCCACGCGGGAGGCCCGGGU*
hsa-pre-miR-21G U1G	*GAGCUUAUCAGACUGAUGUUGACUGU UGAAUCUCAUGGCAACACCAGUCGAUGGGCUGU*
hsa-pre-miR-125a	*UCCCUGAGACCCUUUAACCUGUGAGG ACAUCCAGGGUCACAGGUGAGGUUCUUGGGAGCC*
hsa-pre-miR-125a + Adp	*GGGAGCUAUCGACGUAACUCCCUGAGACCCUUUAACCU GUGAGGACAUCCAGGGUCACAGGUGAGGUUCUUGGGAGC CUGAAGAGCUGCUACUAUC*
hsa-pre-miR-125a U1G/G58C	*GCCCUGAGACCCUUUAACCUGUGAGG ACAUCCAGGGUCACAGGUGAGGUUCUUGGAGCCC*
m1	*GAGCUUAUCAGACUGAUGUUGUGAGG ACAUCCAGGGUCACAACACCAGUCGAUGGGCUGU*
m2	*GCCCUGAGACCCUUUAACCACUGAGG ACAUCCAGGGUCAGUGGUGAGGUUCUUGGAGCCC*
m3	*GCCCUGAGACCCUUUAACCUGACUGU UGAAUCUCAUGGCAGGUGAGGUUCUUGGGACCC*
m4	*GCCCUGAGACCCUUUAACCUGGGAGG ACAUCCAGGGUCCCAGGUGAGGUUCUUGGAGCCC*
m5	*GCCCUGAGACCCUUUAACCUGUCAGG ACAUCCAGGGUGACAGGUGAGGUUCUUGGAGCCC*
m6	*GCCCUGAGACCCUUUAACCUGUGUGG ACAUCCAGGGACACAGGUGAGGUUCUUGGAGCCC*
m7	*GCCCUGAGACCCUUUAACCUGUGAGGACAUCUAGGG UCACAGGUGAGGUUCUUGGAGCCC*
m8	*GCCCUGAGACCCUUUAACCUGUGAAGA CAUCUAGGGUCACAGGUGAGGUUCUUGGAGCCC*
m9	*GCCCUGAGACCCUUUAACCUGUGAGC ACAUGCAGGGUCACAGGUGAGGUUCUUGGAGCCC*
m10	*GCCCUGAGACCCUUUAACCUGUGAGG UGUACCAGGGUCACAGGUGAGGUUCUUGGAGCCC*
A33U	*GCCCUGAGACCCUUUAACCUGUGAGG ACAUCCUGGGUCACAGGUGAGGUUCUUGGAGCCC*
G34A	*GCCCUGAGACCCUUUAACCUGUGAGG ACAUCCAAGGUCACAGGUGAGGUUCUUGGAGCCC*

(continued)

Table 2.6 (continued)

Name	Sequence (5′ to 3′)
G35A	*GCCCUGAGACCCUUUAACCUGUGAGGA CAUCCAGAGUCACAGGUGAGGUUCUUGGAGCCC*
G36A	*GCCCUGAGACCCUUUAACCUGUGAGGA CAUCCAGGAUCACAGGUGAGGUUCUUGGAGCCC*
G25A	*GCCCUGAGACCCUUUAACCUGUGAAGA CAUCCAGGGUCACAGGUGAGGUUCUUGGAGCCC*
G26C	*GCCCUGAGACCCUUUAACCUGUGAGCA CAUCCAGGGUCACAGGUGAGGUUCUUGGAGCCC*
C31G	*GCCCUGAGACCCUUUAACCUGUGAGGA CAUGCAGGGUCACAGGUGAGGUUCUUGGAGCCC*
C32G	*GCCCUGAGACCCUUUAACCUGUGAGGA CAUCGAGGGUCACAGGUGAGGUUCUUGGAGCCC*
G28.5	*GCCCUGAGACCCUUUAACCUGUGAGGA CGAUCCAGGGUCACAGGUGAGGUUCUUGGAGCCC*
ΔC28	*GCCCUGAGACCCUUUAACCUGUGAGGA AUCCAGGGUCACAGGUGAGGUUCUUGGAGCCC*
ΔC28/A29	*GCCCUGAGACCCUUUAACCUGUGAGGA UCCAGGGUCACAGGUGAGGUUCUUGGAGCCC*
ΔC28/A29/U30	*GCCCUGAGACCCUUUAACCUGUGAGGA CCAGGGUCACAGGUGAGGUUCUUGGAGCCC*
ΔA27/C28/A29/U30	*GCCCUGAGACCCUUUAACCUGUGAGGC CAGGGUCACAGGUGAGGUUCUUGGAGCCC*
ΔA27/C28/A29/U30/C31	*GCCCUGAGACCCUUUAACCUGUGAGGC AGGGUCACAGGUGAGGUUCUUGGAGCCC*
ΔA33	*GCCCUGAGACCCUUUAACCUGUGAGGACAUCCGGGUC ACAGGUGAGGUUCUUGGAGCCC*
A33.5	*GCCCUGAGACCCUUUAACCUGUGAGGA CAUCCAAGGGUCACAGGUGAGGUUCUUGGAGCCC*
ΔA24	*GCCCUGAGACCCUUUAACCUGUGGGAC AUCCAGGGUCACAGGUGAGGUUCUUGGAGCCC*
ΔU37	*GCCCUGAGACCCUUUAACCUGUGAGGA CAUCCAGGGCACAGGUGAGGUUCUUGGAGCCC*
U37A	*GCCCUGAGACCCUUUAACCUGUGAGGA CAUCCAGGGACACAGGUGAGGUUCUUGGAGCCC*
U37A/C38G	*GCCCUGAGACCCUUUAACCUGUGAGGA CAUCCAGGGAGACAGGUGAGGUUCUUGGAGCCC*

N means A/U/G/C, italic types indicate ribonucleotides

10% fetal bovine serum (10437-010, Thermo Fisher Scientific Inc.) in an incubator with 5% CO_2 at 37 °C. HuH-7, VMRC-RCW, NEC14, HuO-3N1, and RAJI Cells (RIKEN Cell Bank, code RCB1942, RCB1963, RCB0490, RCB2104, RCB1647) were grown in RPMI 1640 medium (30264-85, Nacalai Tesque Inc.) supplemented with 100 unit/mL penicillin, 100 μg/mL streptomycin (15140-122, Thermo Fisher Scientific Inc.) and 10% fetal bovine serum (10437-010, Thermo Fisher Scientific

Inc.) in an incubator with 5% CO_2 at 37 °C. MCF7 cells (RIKEN Cell Bank, code RCB1940) were grown in MEM (21442-25, Nacalai Tesque Inc.) supplemented with 100 unit/mL penicillin, 100 μg/mL streptomycin (15140-122, Thermo Fisher Scientific Inc.), 0.1 mM nonessential amino acids (M71455, Sigma-Aldrich Co. LLC.), 1 mM sodium pyruvate (S8636, Sigma-Aldrich Co. LLC.), and 10% fetal bovine serum (10437-010, Thermo Fisher Scientific Inc.) in an incubator with 5% CO_2 at 37 °C. HeLa S3 cells (JCRB Cell Bank, JCRB0713) were grown in DMEM (08458-45, Nacalai Tesque Inc.) supplemented with 100 unit/mL penicillin, 100 μg/mL streptomycin (15140-122, Thermo Fisher Scientific Inc.) and 10% fetal bovine serum (10437-010, Thermo Fisher Scientific Inc.) in an incubator with 5% CO_2 at 37 °C.

Construction of the rRNA-/tRNA-depleted human small RNA library

Once cells arrived to about 20% of confluence, the media were removed and ISOGEN II (311-07361, NIPPON GENE) was added to dissolve cells. Small RNAs (10-200 nt) were isolated according to the attached protocol. The concentrations were determined by absorbance at 260 nm.

Small RNAs extracted from each cell lines were mixed with an equal ratio and 10 μg small RNAs were treated with Ribominus^{TM} Eykaryote kit (A10837-08, Thermo Fisher Scientific Inc.) according to the attached protocol. Ribosomal RNA-depleted small RNAs were separated to 10–60 nt fraction and 60–200 nt fraction by denaturing PAGE (8 M Urea, 1 × TBE, %T = 8 and %C = 5). tRNAs in the 60–200 nt fraction of small RNAs were removed under the following conditions; a mixture of 48 μL of 73.3 ng/μL 60–200 nt fraction of small RNAs and 33.3 μM dial-Fx3 + N1 in 166.7 mM HEPES-KOH (pH 7.5) was heated at 95 °C for 2 min and cooled to room temperature over 5 min. Sixteen μL of 3 M $MgCl_2$ was added, and the mixture was transferred to an ice bath, 16 μL of 25 mM Biotin-Phe-CME in DMSO was added, and the mixture was incubated on ice for 2 h. After 2 h incubation, 8 μL of 3 M NaCl and 220 μL of ethanol were added, and then precipitated. To capture biotin-Phe-tRNAs, the RNA was dissolved with 120 μL SAv binding buffer (5 mM HEPES-KOH (pH 7.5), 500 μM EDTA, 1 M NaCl and 0.1% tween-20) and then mixed with 1.2 mg Dynabeads M-280 Streptavidin (11205D, Thermo Fisher Scientific Inc.) which were prewashed with SAv wash buffer (5 mM Tris-HCl (pH 7.5), 500 μM EDTA and 1 M NaCl) three times before use, SAv solution A (0.1 M NaOH and 50 mM NaCl) two times and 0.1 M NaCl one time. After 15 min incubation using rotary shaker at room temperature, supernatant was recovered and precipitated with ethanol. For the second aminoacylation, the RNA was dissolved in 32 μL of 125 mM HEPES-KOH (pH 7.5) with 0.75 M $MgCl_2$ and incubated at room temperature for 5 min. The mixture was transferred to an ice bath, 8 μL of 25 mM Biotin-Phe-CME was added. After 2 h incubation on ice, 48 μL of 500 mM NaCl and 220 μL of ethanol were added. RNAs were precipitated and dissolved in 80 μL SAv binding buffer. To capture biotin-Phe-tRNAs, the same procedure described above was performed using 800 μg beads. Supernatant was precipitated with ethanol and dissolved in 16 μL of 125 mM HEPES-KOH (pH 7.5) with 0.75 M $MgCl_2$ and incubated at room

temperature for 5 min. The mixture was transferred to an ice bath, 4 μL of 25 mM Biotin-Phe-CME was added. After 2 h incubation on ice, 68 μL of 500 mM NaCl and 220 μL of ethanol were added. RNAs were precipitated and dissolved in 40 μL SAv binding buffer. To capture biotin-Phe-tRNAs, the same procedure described above was performed using 400 μg beads. Supernatant was precipitated with ethanol and dissolved in water. The concentrations were determined by absorbance at 260 nm.

A dial-Fx3 + N1 in the tRNA-depleted small RNA fraction was removed by denaturing PAGE (8 M Urea, 1 × TBE, %T = 8 and %C = 5). All amount of rRNA-/tRNA-depleted small RNA fraction and 10–60 nt fraction were mixed and used for preparation of cDNA library.

Construction of the cDNA library from rRNA-/tRNA-depleted human small RNA library

The 3′-adaptor (purchased from Integrated DNA Technologies) and 5′-adaptor (purchased from Japan Bio Service) were purified by denaturing PAGE (8 M Urea, 1 × TBE, %T = 20 and %C = 5) before use. For ligation of 3′-adaptor, 6.67 μL mixture of 70 ng/μL rRNA-/tRNA-depleted human small RNA library, 15 μM 3′-adaptor, 25% (v/v) PEG8000, 40 U/μL T4 RNA ligase 2 truncated (M0242S, New England BioLabs), and 1 × reaction buffer attached with T4 RNA ligase 2 truncated was incubated at 16 °C for 12 h. After the incubation, RNAs were extracted with phenol–chloroform mixture and precipitated with ethanol. Nonreacted 3′-adaptor was removed by denaturing PAGE (8 M Urea, 1 × TBE, %T = 8 and %C = 5). RNA library ligated with 3′-adaptor was treated with $NaIO_4$ according to protocol described above, in order to avoid the ligation of contaminated RNA library not ligated with 3′-adaptor in the next step. For ligation of 5′-adaptor, 10 μL mixture of all amount of RNA library ligated with 3′-adaptor, 20 μM 5′-adaptor, 15% (v/v) PEG8000, 30 U/μL T4 RNA ligase 1 (M0204S, New England BioLabs), and 1 × reaction buffer attached with T4 RNA ligase 1 was incubated at 37 °C for 30 min and then at 16 °C for 12 h. After the incubation, RNAs were extracted with phenol–chloroform mixture and precipitated with ethanol. Nonreacted 5′-adaptor was removed by denaturing PAGE (8 M Urea, 1 × TBE, %T = 8 and %C = 5). RNA library ligated with 3′/5′-adaptors was converted to cDNA by reverse transcription and PCR using primers sele-1 and sele-2 and PrimeScript™ One Step RT-PCR Kit Ver.2 (RR055A, TaKaRa), and cDNA was purified by Native-PAGE (1 × TBE, %T = 8 and %C = 5).

Immobilization of folic acid onto the magnetic beads

Magnetic beads whose surface was modified with hydroxyl group (FG-beads, TAS8848 N1120, Tamagawa Seiki) were used for immobilization of folic acid. FG-beads were suspended in *N*,*N*-dimethylformamide (DMF, 10344-00, KANTO CHEMICAL) at 5 μg/μL and washed with DMF three times. FG-beads (5 μg/μL) were incubated at 25 °C for 24 h with 10 mM folic acid (16221-91, Nacalai Tesque

Inc.) in DMF in the presence of 10 mM EDC (1-ethyl-3-(3-dimethylaminopropyl) carbodiimide hydrochloride, 15022-86, Nacalai Tesque Inc.) and 10% (v/v) triethylamine (202-02641, WAKO). Thereafter, the folic acid-immobilized beads were washed with DMF three times and suspended in DMF at 10 μg/μL.

Small RNA transcriptomic SELEX

cDNA library was transcribed to RNA library by runoff in vitro transcription with T7 RNA polymerase and purified by denaturing PAGE (8 M Urea, 1× TBE, %T = 8 and %C = 5). A 10 μL of 510 ng/μL RNA library and 1× selection buffer (50 mM HEPES-KOH (pH 7.5), 300 mM KCl, 5 mM $MgCl_2$ and 0.05% tween-20) was mixed with of FG-beads whose surface is modified with hydroxyl group which prewashed by 1× selection buffer three times before use, and this mixture was incubated using rotary shaker at 4 °C for 30 min (referred to as "pre-clear" process). After the incubation, the supernatant was added to folic acid-immobilized beads which were washed by 1× selection buffer three times before use, and this mixture was incubated using rotary shaker at 4 °C for 1 h. After the incubation, the supernatant was discarded and the beads were washed with 100 μL of 1× selection buffer (referred to as "wash" process). The beads were suspended in 1 mM folic acid in 1× selection buffer and incubated using rotary shaker at 4 °C for 30 min to elute the RNAs binding to folic acid-immobilized beads. The supernatant was recovered and this elution cycle repeated three times. All of the supernatants were mixed and precipitated with ethanol. The pellet was dissolved in 10 μL of water.

To quantify the amount of recovered RNAs from beads, quantitative RT-PCR was performed as follows: 0.5% of recovered RNAs were mixed with 10 μL of RT mix (500 μM dNTP, 5 μM primer sele-2, 8 U/μL M-MLV Reverse Transcriptase (M1701, Promega K.K.) and 1× reaction buffer attached with reverse transcriptase), and this mixture was incubated at 50 °C for 1 h. After the incubation, 1 μL of reverse transcription reaction solution was mixed with 19 μL of qPCR mix (5 μM primer sele-1, 5 μM primer sele-2 10 mM Tris-HCl (pH 9.0), 50 mM KCl, 0.1% Triton-X100, 2.5 mM $MgCl_2$, 0.25 mM dNTP, 1/1,000,000 SYBR® Green I (50512, LONZA), Taq DNA polymerase) and qPCR was performed using LightCycler® 1.5 (Roche Diagnostics K.K.) at 94 °C (20 °C/sec) for 1 min, followed by 35 cycles of 94 °C for 10 s (20 °C/s), 51 °C for 10 s (20 °C/s), and 72 °C for 30 s (0.5 °C/s) to measure C_p values.

The all amount of recovered RNAs not used for qPCR was mixed with RT mix and this mixture was incubated at 50 °C for 1 h. After the incubation, all of the reverse transcription reaction solution was mixed with 200 μL of qPCR mix without SYBR® Green I and DNA was amplified by PCR by C_p + 2 cycle of 94 °C for 10 s, 51 °C for 10 s, and 72 °C for 30 s. DNA was extracted with phenol–chloroform mixture and precipitated with ethanol, and then used for next round of selection.

For the first round of selection, preclear process was not performed, wash process was performed one time and 200 μg beads were used. For the second round of

selection, preclear process was performed one time, wash process was performed one time and 100 μg beads were used. For the third round of selection, preclear process was performed one time, wash process was repeated three times, and 100 μg beads were used. For the fourth round of selection, preclear process was performed one time, wash process was repeated three times and 20 μg beads were used.

Sequencing

The cDNAs of tRNA-depleted human small RNA library and RNAs after SELEX were TA cloned into pGEM®-T Easy Vectors (A1360, Promega K.K.). These vectors were used to transform *E. coli* DH5α cells in LB medium with 100 μg/mL. Inserted cDNAs in the vectors were amplified by colony-PCR using primers seq-1 and seq-2, and sequenced by FASMAC Co., Ltd. (Japan).

To annotate the sequenced RNAs, BLAST search (Altschul et al. 1990) using NCBI human genomic plus transcript database (http://blast.ncbi.nlm.nih.gov/Blast.cgi), fRNA database (Mituyama et al. 2009) (http://www.ncrna.org/frnadb/), genomic tRNA database (Chan and Lowe 2009) (http://gtrnadb.ucsc.edu/), snoRNABase (Lestrade and Weber 2006) (https://www-snorna.biotoul.fr/) and miRbase (Kozomara and Griffiths-Jones 2014) (http://www.mirbase.org/) was performed.

Biolayer interferometry (BLI)

Binding of RNAs to folic acid was measured using the Octet RED96 biolayer interferometry (BLI) instrument (ForteBio, Inc.) and all measurement were conducted at 30 °C and agitation rate is 1000 rpm.

Folic acid was immobilized onto the amine reactive second-generation (AR2G) biosensor from ForteBio as follows; each AR2G sensor was prewet for more than 10 min in water prior to use. Each AR2G sensor was equilibrated in water for 3 min, then activated with EDC/NHS solution (200 mM EDC and 50 mM *N*-hydroxysuccinimide (NHS, A00013, Watanabe Chemical Industries) in water) for 10 min. The activated sensors was modified with amine group by incubating with EDA solution [100 mM ethylenediamine (15020-22, Nacalai Tesque Inc.), 10 mM boric acid buffer (pH 8.5) and 1 M NaCl] for 150 s, then quenched with 1 M ethanolamine (E6133, Sigma-Aldrich Co. LLC., pH 8.5 adjusted by KOH) for 3 min. The amine group-immobilized sensors were equilibrated with 250 mM phosphate buffer (pH 7.0) for 3 min and then folic acid was immobilized by incubating with FA/EDC/NHS/Phos solution [20 mM folic acid, 200 mM EDC, 50 mM NHS and 250 mM phosphate buffer (pH 7.0)] for 20 min. The folic acid-immobilized sensors were incubated with water for 3 min. Reference sensors for the binding analysis were prepared following the same protocols described above using EDC/NHS/Phos solution [200 mM EDC, 50 mM NHS and 250 mM phosphate buffer (pH 7.0)] instead of FA/EDC/NHS/Phos solution.

Binding of RNAs to folic acid was measured as follows: folic acid-immobilized sensors or reference sensors were prewet for more than 10 min in Octet buffer

(50 mM HEPES-KOH (pH 7.5), 300 mM KCl, 50 mM $MgCl_2$, 0.05% tween-20) prior to use. The sensors were equilibrated in Octet buffer for 3 min, then incubated in Octet buffer for 1 min to generate baseline. As an association step, the sensors were incubated in RNA dissolved in Octet buffer. After an association step, the sensors were incubated in Octet buffer as a dissociation step. The sensors were regenerated by incubating in R buffer (20 mM EDTA and 0.05% tween-20) for 10 s 5 times. The ForteBio Data Analysis Octet software was used to perform steady-state analysis. For each RNA, six to eight concentrations were used, from 200 nM to 240 μM (depending on the affinity of each RNAs).

References

Altschul SF, Gish W, Miller W, Myers EW, Lipman DJ (1990) Basic local alignment search tool. J Mol Biol 215(3):403–410. doi:10.1016/S0022-2836(05)80360-2

Auyeung VC, Ulitsky I, McGeary SE, Bartel DP (2013) Beyond secondary structure: primary-sequence determinants license pri-miRNA hairpins for processing. Cell 152(4):844–858. doi:10.1016/j.cell.2013.01.031

Barrick JE, Corbino KA, Winkler WC, Nahvi A, Mandal M, Collins J, Lee M, Roth A, Sudarsan N, Jona I, Wickiser JK, Breaker RR (2004) New RNA motifs suggest an expanded scope for riboswitches in bacterial genetic control. Proc Natl Acad Sci USA 101(17):6421–6426. doi:10.1073/pnas.0308014101

Baselga-Escudero L, Blade C, Ribas-Latre A, Casanova E, Suarez M, Torres JL, Salvado MJ, Arola L, Arola-Arnal A (2014) Resveratrol and EGCG bind directly and distinctively to miR-33a and miR-122 and modulate divergently their levels in hepatic cells. Nucleic Acids Res 42(2):882–892. doi:10.1093/nar/gkt1011

Borchert GM, Lanier W, Davidson BL (2006) RNA polymerase III transcribes human microRNAs. Nat Struct Mol Biol 13(12):1097–1101. doi:10.1038/Nsmb1174

Cai XZ, Hagedorn CH, Cullen BR (2004) Human microRNAs are processed from capped, polyadenylated transcripts that can also function as mRNAs. RNA 10(12):1957–1966. doi:10.1261/Rna.7135204

Chan PP, Lowe TM (2009) GtRNAdb: a database of transfer RNA genes detected in genomic sequence. Nucleic Acids Res 37:D93–D97. doi:10.1093/Nar/Gkn787

Chen L, Yun SW, Seto J, Liu W, Toth M (2003) The fragile X mental retardation protein binds and regulates a novel class of mRNAs containing U rich target sequences. Neuroscience 120(4):1005–1017. doi:10.1016/S0306-4522(03)00406-8

Curtis E, Liu D (2013) Discovery of widespread GTP-binding Motifs in genomic DNA and RNA. Chem Biol 20(4):521–532. doi:10.1016/j.chembiol.2013.02.015

Denli AM, Tops BBJ, Plasterk RHA, Ketting RF, Hannon GJ (2004) Processing of primary microRNAs by the microprocessor complex. Nature 432(7014):231–235. doi:10.1038/Nature03049

Dinger ME, Pang KC, Mercer TR, Mattick JS (2008) Differentiating protein-coding and noncoding RNA: challenges and ambiguities. PLoS Comput Biol 4(11):e1000176. doi:10.1371/journal.pcbi.1000176

Dobbelstein M, Shenk T (1995) In vitro selection of RNA ligands for the ribosomal L22 protein associated with Epstein-Barr virus-expressed RNA by using randomized and cDNA-derived RNA libraries. J Virol 69(12):8027–8034

Fujimoto Y, Nakamura Y, Ohuchi S (2012) HEXIM1-binding elements on mRNAs identified through transcriptomic SELEX and computational screening. Biochimie 94(9):1900–1909. doi:10.1016/j.biochi.2012.05.003

Futai K, Terasaka N, Katoh T, Suga H (2016) tRid, an enabling method to isolate previously inaccessible small RNA fractions. Methods 106:105–111. doi:10.1016/j.ymeth.2016.04.033

Gregory RI, Yan KP, Amuthan G, Chendrimada T, Doratotaj B, Cooch N, Shiekhattar R (2004) The Microprocessor complex mediates the genesis of microRNAs. Nature 432(7014):235–240. doi:10.1038/Nature03120

Ha M, Kim VN (2014) Regulation of microRNA biogenesis. Nat Rev Mol Cell Biol 15(8):509–524. doi:10.1038/nrm3838

Haase AD, Jaskiewicz L, Zhang HD, Laine S, Sack R, Gatignol A, Filipowicz W (2005) TRBP, a regulator of cellular PKR and HIV-1 virus expression, interacts with Dicer and functions in RNA silencing. EMBO Rep 6(10):961–967. doi:10.1038/sj.embor.7400509

Han JJ, Lee Y, Yeom KH, Kim YK, Jin H, Kim VN (2004) The Drosha-DGCR8 complex in primary microRNA processing. Genes Dev 18(24):3016–3027. doi:10.1101/Gad.1262504

Hansen TB, Jensen TI, Clausen BH, Bramsen JB, Finsen B, Damgaard CK, Kjems J (2013) Natural RNA circles function as efficient microRNA sponges. Nature 495(7441):384–388. doi:10.1038/Nature11993

Huntzinger E, Izaurralde E (2011) Gene silencing by microRNAs: contributions of translational repression and mRNA decay. Nat Rev Genet 12(2):99–110. doi:10.1038/nrg2936

Hutvagner G, McLachlan J, Pasquinelli AE, Balint E, Tuschl T, Zamore PD (2001) A cellular function for the RNA-interference enzyme Dicer in the maturation of the let-7 small temporal RNA. Science 293(5531):834–838. doi:10.1126/science.1062961

Izzotti A, Cartiglia C, Steele VE, De Flora S (2012) MicroRNAs as targets for dietary and pharmacological inhibitors of mutagenesis and carcinogenesis. Mutat Res 751(2):287–303. doi:10.1016/j.mrrev.2012.05.004

Jiang R, Hu FB, Giovannucci EL, Rimm EB, Stampfer MJ, Spiegelman D, Rosner BA, Willett WC (2003) Joint association of alcohol and folate intake with risk of major chronic disease in women. Am J Epidemiol 158(8):760–771. doi:10.1098/Aje/Kwg221

Khvorova A, Reynolds A, Jayasena SD (2003) Functional siRNAs and miRNAs exhibit strand bias. Cell 115(2):209–216. doi:10.1016/S0092-8674(03)00893-6

Koppers-Lalic D, Hackenberg M, Bijnsdorp IV, van Eijndhoven MA, Sadek P, Sie D, Zini N, Middeldorp JM, Ylstra B, de Menezes RX, Wurdinger T, Meijer GA, Pegtel DM (2014) Nontemplated nucleotide additions distinguish the small RNA composition in cells from exosomes. Cell reports 8(6):1649–1658. doi:10.1016/j.celrep.2014.08.027

Kozomara A, Griffiths-Jones S (2014) miRBase: annotating high confidence microRNAs using deep sequencing data. Nucleic Acids Res 42(D1):D68–D73. doi:10.1093/Nar/Gkt1181

Landgraf P, Rusu M, Sheridan R, Sewer A, Iovino N, Aravin A, Pfeffer S, Rice A, Kamphorst AO, Landthaler M, Lin C, Socci ND, Hermida L, Fulci V, Chiaretti S, Foa R, Schliwka J, Fuchs U, Novosel A, Muller RU, Schermer B, Bissels U, Inman J, Phan Q, Chien MC, Weir DB, Choksi R, De Vita G, Frezzetti D, Trompeter HI, Hornung V, Teng G, Hartmann G, Palkovits M, Di Lauro R, Wernet P, Macino G, Rogler CE, Nagle JW, Ju JY, Papavasiliou FN, Benzing T, Lichter P, Tam W, Brownstein MJ, Bosio A, Borkhardt A, Russo JJ, Sander C, Zavolan M, Tuschl T (2007) A mammalian microRNA expression atlas based on small RNA library sequencing. Cell 129(7):1401–1414. doi:10.1016/j.cell.2007.04.040

Landthaler M, Yalcin A, Tuschl T (2004) The human DiGeorge syndrome critical region gene 8 and its D. melanogaster homolog are required for miRNA biogenesis. Curr Biol 14(23):2162–2167. doi:10.1016/j.cub.2004.11.001

Lee Y, Ahn C, Han JJ, Choi H, Kim J, Yim J, Lee J, Provost P, Radmark O, Kim S, Kim VN (2003) The nuclear RNase III Drosha initiates microRNA processing. Nature 425(6956):415–419. doi:10.1038/Nature01957

Lee Y, Kim M, Han JJ, Yeom KH, Lee S, Baek SH, Kim VN (2004) MicroRNA genes are transcribed by RNA polymerase II. EMBO J 23(20):4051–4060. doi:10.1038/sj.emboj.7600385

Lee YS, Shibata Y, Malhotra A, Dutta A (2009) A novel class of small RNAs: tRNA-derived RNA fragments (tRFs). Genes Dev 23(22):2639–2649. doi:10.1101/Gad.1837609

Lestrade L, Weber MJ (2006) snoRNA-LBME-db, a comprehensive database of human H/ACA and C/D box snoRNAs. Nucleic Acids Res 34:D158–D162. doi:10.1093/Nar/Gkj002

Lindberg J, Lundeberg J (2010) The plasticity of the mammalian transcriptome. Genomics 95 (1):1–6. doi:10.1016/j.ygeno.2009.08.010

Liu JD, Carmell MA, Rivas FV, Marsden CG, Thomson JM, Song JJ, Hammond SM, Joshua-Tor L, Hannon GJ (2004) Argonaute2 is the catalytic engine of mammalian RNAi. Science 305 (5689):1437–1441. doi:10.1126/science.1102513

Liu JM, Livny J, Lawrence MS, Kimball MD, Waldor MK, Camilli A (2009) Experimental discovery of sRNAs in Vibrio cholerae by direct cloning, 5S/tRNA depletion and parallel sequencing. Nucleic Acids Res 37(6):e46. doi:10.1093/nar/gkp080

Marsit CJ, Eddy K, Kelsey KT (2006) MicroRNA responses to cellular stress. Cancer Res 66 (22):10843–10848. doi:10.1158/0008-5472.CAN-06-1894

Melse-Boonstra A, West CE, Katan MB, Kok FJ, Verhoef P (2004) Bioavailability of heptaglutamyl relative to monoglutamyl folic acid in healthy adults. Am J Clin Nutr 79 (3):424–429

Mituyama T, Yamada K, Hattori E, Okida H, Ono Y, Terai G, Yoshizawa A, Komori T, Asai K (2009) The Functional RNA Database 3.0: databases to support mining and annotation of functional RNAs. Nucleic Acids Res 37(Database issue):D89–D92. doi:10.1093/nar/gkn805

Mulinare J, Cordero JF, Erickson JD, Berry RJ (1988) Periconceptional use of multivitamins and the occurrence of neural tube defects. JAMA 260(21):3141–3145. doi:10.1001/jama.260.21.3141

Okada C, Yamashita E, Lee SJ, Shibata S, Katahira J, Nakagawa A, Yoneda Y, Tsukihara T (2009) A high-resolution structure of the pre-microRNA nuclear export machinery. Science 326(5957):1275–1279. doi:10.1126/science.1178705

Pan T, Uhlenbeck OC (1993) Circularly permuted DNA, RNA and proteins—a review. Gene 125 (2):111–114. doi:10.1016/0378-1119(93)90317-V

Saito H, Kourouklis D, Suga H (2001) An in vitro evolved precursor tRNA with aminoacylation activity. EMBO J 20(7):1797–1806. doi:10.1093/emboj/20.7.1797

Schwarz DS, Hutvagner G, Du T, Xu ZS, Aronin N, Zamore PD (2003) Asymmetry in the assembly of the RNAi enzyme complex. Cell 115(2):199–208. doi:10.1016/S0092-8674(03)00759-1

Selhub J (1989) Determination of tissue folate composition by affinity-chromatography followed by high-pressure ion-pair liquid-chromatography. Anal Biochem 182(1):84–93. doi:10.1016/0003-2697(89)90722-7

Singer B, Shtatland T, Brown D, Gold L (1997) Libraries for genomic SELEX. Nucleic Acids Res 25(4):781–786. doi:10.1093/nar/25.4.781

Tsuji S, Hirabayashi N, Kato S, Akitomi J, Egashira H, Tanaka T, Waga I, Ohtsu T (2009) Effective isolation of RNA aptamer through suppression of PCR bias. Biochem Biophys Res Commun 386(1):223–226. doi:10.1016/j.bbrc.2009.06.013

Vu MM, Jameson NE, Masuda SJ, Lin D, Larralde-Ridaura R, Luptak A (2012) Convergent evolution of adenosine aptamers spanning bacterial, human, and random sequences revealed by structure-based bioinformatics and genomic SELEX. Chem Biol 19(10):1247–1254. doi:10.1016/j.chembiol.2012.08.010

Winter J, Jung S, Keller S, Gregory RI, Diederichs S (2009) Many roads to maturity: microRNA biogenesis pathways and their regulation. Nat Cell Biol 11(3):228–234. doi:10.1038/Ncb0309-228

Yi R, Qin Y, Macara IG, Cullen BR (2003) Exportin-5 mediates the nuclear export of pre-microRNAs and short hairpin RNAs. Genes Dev 17(24):3011–3016. doi:10.1101/Gad.1158803

Yuan G, Klambt C, Bachellerie JP, Brosius J, Huttenhofer A (2003) RNomics in Drosophila melanogaster: identification of 66 candidates for novel non-messenger RNAs. Nucleic Acids Res 31(10):2495–2507

Zhang XX, Zeng Y (2010) The terminal loop region controls microRNA processing by Drosha and Dicer. Nucleic Acids Res 38(21):7689–7697. doi:10.1093/Nar/Gkq645

Zimmermann B, Bilusic I, Lorenz C, Schroeder R (2010) Genomic SELEX: A discovery tool for genomic aptamers. Methods 52(2):125–132. doi:10.1016/j.ymeth.2010.06.004

Zuker M (2003) Mfold web server for nucleic acid folding and hybridization prediction. Nucleic Acids Res 31(13):3406–3415. doi:10.1093/Nar/Gkg595

Chapter 3
Orthogonal Ribosome–tRNAs Pair by Engineering of Peptidyl Transferase Center

Abstract The CCA-3′ sequence of tRNA is conserved among all organisms and is important for aminoacylation and translation. In bacteria, the CCA-3′ end makes Watson–Crick base pairs with bases of 23S rRNA in the peptidyl transferase center (PTC) in the classical state (Voorhees et al. in Nat Struct Mol Biol 16:528–533, 2009) and translocation (Dorner et al. in Nat Struct Mol Biol 13:234–241, 2006) during translation. These base pairs are important for translation activity, and the compensatory mutations in these base pairs are tolerated during peptidyl transfer reaction (Kim and Green in Molecular Cell 4(5):859–864, 1999) and translocation (Dorner et al. in Nat Struct Mol Biol 13:234–241, 2006). However, it is yet empirically unknown whether such mutations accommodates translation in its entirety. I will report development of orthogonal translation machinery (Terasaka et al. in Nat Chem Biol 10(7):555–557, 2014). First, I developed a method to easily aminoacylate various amino acids onto tRNAs bearing mutation (or mutations) in CCA-3′ end using compensatory mutated flexizymes. Then the translation activity of the PTC-mutated ribosomes and tRNAs were measured. Consequently, I developed the mutant ribosome–tRNA pair which had comparable translation activity and orthogonality to the wild-type ribosome–tRNA pair. Finally, two different peptides were expressed simultaneously in one pot from a single mRNA template using the mutant and wild-type ribosome–tRNA pairs.

Keywords tRNA · Ribosome · Translation · Peptide · Synthetic biology

3.1 Introduction

Assignment of 20 canonical amino acids to codons, is achieved by specific acylation of tRNA with cognate amino acid catalyzed by aminoacyl-tRNA synthetase (ARS). Since each tRNA has an anticodon that pairs with the codon, the codons on mRNA can be decoded by the cognate aminoacyl-tRNAs (aa-tRNAs) according to the genetic code; and thus ribosome is able to catalyze the formation of peptide bond along the mRNA template, to yield a polypeptide with the encoded

N. Terasaka, *Applications of Aminoacylation Ribozymes That Recognize the 3′-end of tRNA*, Springer Theses, DOI 10.1007/978-4-431-56517-8_3

sequence. While 20 canonical amino acids are used in the natural translation system, it has been demonstrated that more than hundreds of different noncanonical amino acids (ncAAs) can be incorporated into nascent polypeptide chain by engineering of the genetic code (Liu and Schultz 2010). Assignment of ncAAs in the genetic code has been achieved by two methodologies: genetic code expansion (Magliery et al. 2001; Wang et al. 2001) and genetic code reprogramming (Forster et al. 2003). The former method generally assigns a ncAA (or multiple ncAAs) to a nonsense codon(s) such as stop codons and an artificially programmed quadruplet codon(s). Genetic code expansion has been applied for both in vivo and in vitro expression of proteins with ncAAs.

When the genetic code expansion is performed in vivo, availability of ncAA-tRNA generally relies on an exogenously introduced ARS specifically paired with an orthogonal tRNA. The orthogonal tRNA should not be aminoacylated by endogenous ARSs. At the same time, the exogenous ARS should be engineered to specifically charge the ncAA onto the orthogonal tRNA, but not onto endogenous tRNAs. Several orthogonal ARS–tRNA pairs have been successfully developed (Liu and Schultz 2010), and thus far demonstrated expression of proteins containing ncAAs. However, the choices of usable ncAAs are yet limited to a few subgroups, because the majority examples of the engineered ARSs are based on *Methanococcus jannaschii* TyrRS (Wang et al. 2001), *Methanosarcina barkeri* PylRS (Polycarpo et al. 2006; Neumann et al. 2008), or *Methanosarcina mazei* PylRS (Mukai et al. 2008; Yanagisawa et al. 2008); therefore, the usable ncAAs for these mutant enzymes are limited to Phe or Lys analogs.

In addition to orthogonal ARS–tRNA pair, orthogonal ribosome–mRNA pair has been developed (Rackham and Chin 2005). In this system engineered ribosome containing orthogonal 16S rRNA which does not recognizes endogenous mRNA but recognizes engineered mRNA bearing mutated Shine–Dalgarno (SD) sequence, was used (Rackham and Chin 2005). Decoding center of this orthogonal 16S rRNAs have been further evolved for efficient amber codon decoding (Wang et al. 2007) and quadruplet codon (Neumann et al. 2010). These orthogonal ribosome–mRNA pairs enabled to express specific protein-containing ncAAs in vivo (Wang et al. 2014). However, the numbers of usable ncAAs and codons were still limited.

On the other hand, in the genetic code reprograming, multiple sense codons can be simultaneously reassigned with various ncAAs. Genetic code reprogramming has been dominantly utilized in in vitro reconstituted translation system (Shimizu et al. 2001) to produce short polypeptides containing diverse exotic ncAAs, such as D-amino acids (Goto et al. 2008) and *N*-methyl-amino acids (Kawakami et al. 2008, 2009; Yamagishi et al. 2011). Although in the genetic code reprogramming method, multiple ncAAs can be incorporated, some canonical amino acids cannot be used simultaneously. It is because the canonical amino acids originally assigned in natural genetic code need to be removed to suppress the incorporation of canonical amino acids instead of ncAAs (Goto et al. 2011). To overcome this problem in genetic code reprogramming, I conceived the new concept of orthogonal translation system, which is orthogonal ribosome–tRNA pair. This engineered translation system means that wild-type ribosome only use canonical aa-tRNAs and the

engineered ribosome only use ncAA-tRNAs as substrates. In this system, it is not necessary to deplete canonical amino acids and to change the original genetic code in order to incorporate ncAAs.

To develop the orthogonal ribosome–tRNA pair, the interaction between ribosome and tRNA needs to be engineered. During the elongation cycle of bacterial translation, where amino acids were sequentially added to the growing peptide chain, CCA-end of tRNA interacts with 23S rRNA of 50S subunit (Fig. 3.1). The elongation cycle is divided to three steps (Moazed and Noller 1989; Schmeing and Ramakrishnan 2009) (Fig. 3.2). First step is accommodation of an aa-tRNA into the A-site of ribosome. An aa-tRNA is delivered to the A-site by EF-Tu•GTP in the A/T state, where the anticodon forms base pairs with codon in the A-site of 30S and the acceptor end is bound to EF-Tu (the first letter represents the binding site on the 30S and the second letter the site on the 50S). Then GTP is hydrolyzed to GDP to release EF-Tu•GDP and the accommodation of the acceptor end of the aa-tRNA into the A-site of the 50S (A/A state, the classical state). Second is peptide bond formation between aa-tRNA in A/A state and peptidyl-tRNA in the P/P state, which is catalyzed in the peptidyl transferase center (PTC). After the peptide bond formation, peptidyl-tRNA in the A/A state is translocated to the P/P state and deacylated tRNA in the P/P state is translocated to the E/E state facilitated by EF-G with associated GTP hydrolysis, which is the third step.

In the PTC of classical state of *Escherichia coli* ribosome complex, critical Watson–Crick base pairs occur between the universally conserved 3′-end of tRNAs

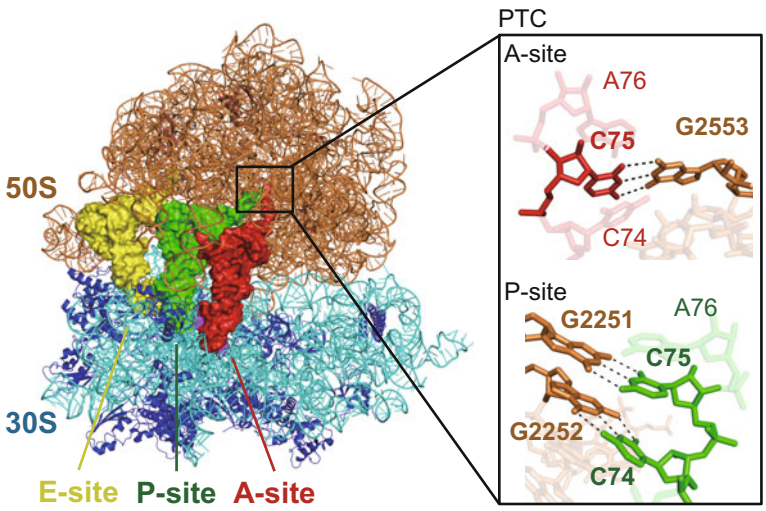

Fig. 3.1 Crystal structure of classical state of bacterial ribosome–tRNAs–mRNA complex. The interaction between 23S rRNA and CCA-end of tRNAs at the peptidyl transferase center (PTC) is shown in black rectangle. *Black dashed lines* indicate hydrogen bonds. This structure was reported in previous paper (Voorhees et al. 2009) (PDB ID: 2WDK/2WDL)

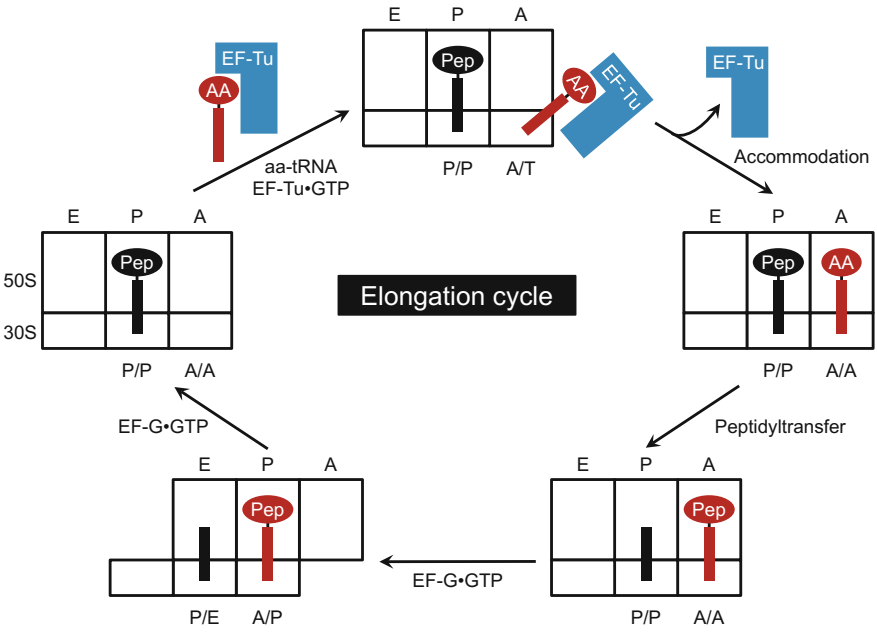

Fig. 3.2 Schematic illustration of elongation cycle of bacterial translation. The ribosomes are described as *black rectangles* and divided into 30S and 50S subunits and partitioned into the A-, P- and E-sites. The biding states of the tRNAs as previously defined (Moazed and Noller 1989) are indicated at the bottom of each sites. "Pep" means peptide and "AA" means amino acid. Bold lines indicate tRNAs

(C74 and C75) and 23S rRNA G2251 and G2252 at the P site as well as G2553 at the A site, which were revealed by biochemical experiments and crystal structural analyses (Bashan et al. 2003; Nissen et al. 2000; Steitz 2008; Moazed and Noller 1991; Samaha et al. 1995; Lescoute and Westhof 2006; Green et al. 1998; Voorhees et al. 2009; Polikanov et al. 2014) (Figs. 3.1 and 3.3a). Using an analogue of aa-tRNA fragment (C75 mutant puromycin derivatives of the form NPm) as an A-site substrate (Fig. 3.3b and c), peptidyl transfer activity of wild-type and G2553N mutant ribosome 50S subunits was measured (Kim and Green 1999). They reported that the wild-type ribosome preferred the wild-type substrate (CPm) by about 2- to 5-fold relative to the other substrates (APm, GPm, and UPm) (Fig. 3.3b). Furthermore, G2553C ribosome preferred the compensatory mutated substrate (GPm) by at least 20-fold relative to the other three substrates (Fig. 3.3c). These results indicated that G2253C ribosome–GPm pair has weak orthogonality to wild-type ribosome–CPm pair in peptidyl transfer reaction.

The first step of translocation is movement of acceptor end of peptidyl-tRNA in the A/A state into the A/P state and acceptor end of deacylated tRNA in the P/P state into the P/E state, which is called as hybrid state (Moazed and Noller 1989) (Figs. 3.2 and 3.4). This first step is promoted by EF-G•GTP but it can occur in the

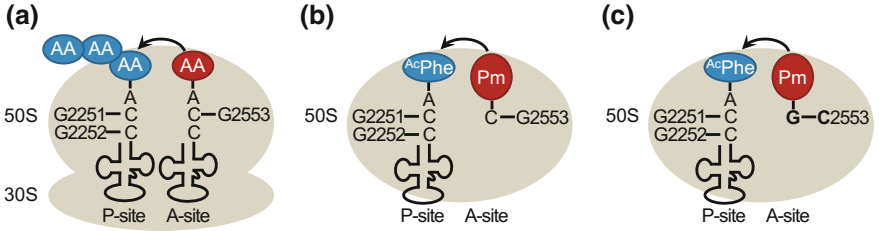

Fig. 3.3 Peptidyl transfer reaction using G2553 N mutant ribosome and C75 mutant puromycin derivatives (Kim and Green 1999). The ribosomes are described as wheat ellipse and divided into 50S and 30S subunits. **a** Schematic illustration of natural peptidyl transfer between peptidyl-tRNA at P-site and aa-tRNA at A-site. **b** Schematic illustration of peptidyl transfer between *N*-acetyl-phenylalanyl-tRNA (^{Ac}Phe-tRNA) at P-site and C75 puromycin derivatives shown as CPm at A-site using reconstituted wild-type 50S subunit. **c** Schematic illustration of peptidyl transfer between *N*-acetyl-phenylalanyl-tRNA (^{Ac}Phe-tRNA) at P-site and C75G puromycin derivatives shown as GPm at A-site using reconstituted G2553C mutant 50S subunit

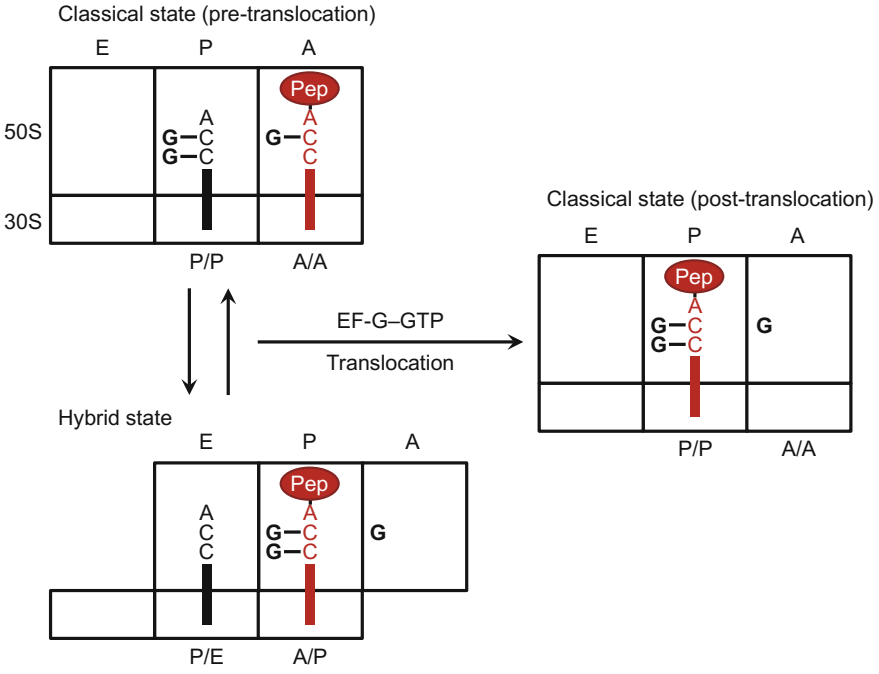

Fig. 3.4 Schematic illustration of classical and hybrid state of tRNA-ribosome complex and translocation induced by EF-G–GTP (Dorner et al. 2006; Cornish et al. 2008). The ribosomes are described as black rectangles and divided into 30S and 50S subunits and partitioned into the A-, P-, and E-sites. The biding states of the tRNAs as previously defined (Moazed and Noller 1989) are indicated at the bottom of each sites. "Pep" in red circle means peptidyl-tRNA. Bold lines indicate tRNAs and bold Gs indicate G2251, G2252, and G2553 of 23S rRNA interacting with CCA-end of tRNAs. This figure was adapted from previous report

Table 3.1 EF-G translocation of WT, G2252C, and G2251C mutant ribosomes

		Translocation rate (s^{-1})				Translocation rate (s^{-1})	
P-site tRNA	A-site tRNA	WT	G2252C	P-site tRNA	A-site tRNA	WT	G2251C
WT	WT	3.8	1.5	WT	WT	3.8	2.1
WT	C74G	1.5	5.0	WT	C75G	1.4	9.3

This table was adapted from previous report (Dorner et al. 2006)

absence of GTP (Spiegel et al. 2007). Then EF-G promotes translocation of peptidyl-tRNA from the A/P state to the P/P state and deacylated tRNA from the P/E state to the E/E state to be released from the ribosome. To my knowledge, there is no direct evidence of the interaction between 23S rRNA and CCA-end of tRNAs during the hybrid state. However, Dorner et al. indicated the potential pairs between C74/C75 of peptidyl-tRNA in the A/P state and G2252/G2251 of 23S rRNA in the P-site (Dorner et al. 2006) (Fig. 3.4). In this report, they measured EF-G translocation rate with the pairs of wild-type and mutant ribosomes and tRNAs (Tables 3.1 and 3.2). When C74G tRNA is in the A-site of wild-type ribosome, translocation rate reduced (Table 3.1). When potential pairing between tRNA in the A/P state and 23S rRNA in the P-site was restored (the pair of C74G tRNA and G2252C ribosome), translocation rate was restored (Table 3.1). Similar result was observed about the interaction between C75 of tRNA in the A/P state and G2251 of 23S rRNA (Table 3.1). These results indicates that the pair of G2251C or G2252C ribosome and C75G or C74G tRNA have weak orthogonality to the pair of wild-type ribosome and tRNA in translocation step.

On the other hand, disruption of the interaction in the A/A state (the pairs of wild-type tRNA and G2253C/U/A ribosomes) increased the rate of translocation (Table 3.2) and restoring the base pair in the A/A state (the pair of C75G tRNA and G2253C ribosome) diminished the translocation rate. These results indicate that ribosome and tRNAs favored the stable state forming base pairs.

These studies described above showed that engineering the base pairs between G2251/G2252/G2553 of ribosome and C74/C75 of tRNAs in the PTC had potential to develop the orthogonal ribosome–tRNA pairs. However, it was unknown

Table 3.2 EF-G translocation with WT and G2553 mutant ribosomes. ND indicates "not determined"

		Translocation rate (s^{-1})			
P-site tRNA	A-site tRNA	WT	G2553C	G2553U	G2553A
WT	WT	3.8	10.7	12.2	12.4
WT	C75G	1.4	1.1	ND	ND

This table was adapted from previous report (Dorner et al. 2006)

whether a mutation (or mutations) of 23S rRNA and CCA-3′ end of tRNAs in the PTC affect the whole translation reaction to produce polypeptides using aa-tRNAs as substrates in an mRNA-dependent manner, including other steps.

In this chapter, I measured the translation activity of the PTC-mutated ribosome–tRNA pairs using an *E. coli* custom-made in vitro translation system that was integrated with the flexizyme technology, referred to as the FIT (Flexible In vitro Translation) system (Goto et al. 2011). In natural, tRNAs are aminoacylated by protein aminoacyl-tRNA synthetases (ARSs) and ARSs specifically recognize the sequence of cognate tRNAs. Because most ARSs also interact with the universally conserved CCA-3′ end of tRNAs (Cavarelli and Moras 1993; Ruff et al. 1991), ARSs are not suitable for preparation of aminoacyl-tRNA (aa-tRNA) bearing mutation in the CCA-3′ end (Schulman and Pelka 1977; Liu and Horowitz 1994; Zhou et al. 2011). In order to overcome this problem, flexizymes (eFx and dFx) bearing compensatory mutated 3′-ends were used because flexizymes recognize CCA-3′ end of substrate RNA via base pairs as described in Chap. 1. Finally, the pair of mutant ribosome and tRNAs which acted orthogonally and used only the cognate genetic code consisting of ncAAs were developed (Terasaka et al. 2014).

3.2 Results and Discussions

3.2.1 Aminoacylation of CCA-Mutated tRNAs

To confirm that CCA-3′ end mutated tRNAs (denoted as tRNAs-NNA) can be aminoacylated by compensatory mutated flexizymes, I arbitrarily chose lysine and tyrosine as amino acids substrates (Fig. 3.5), and $tRNA_{CUU}^{AsnE2}$ and $tRNA_{GUA}^{AsnE2}$ (Fig. 3.6) bearing corresponding anticodons. Three mutant tRNAs derived from $tRNA_{CUU}^{AsnE2}$ and $tRNA_{GUA}^{AsnE2}$ bearing single or double mutation (or mutations) (C74G, C75G, or C74G/C75G) and the compensatory single or double mutated flexizymes derived from dFx and eFx were prepared by in vitro transcription. The aminoacylation efficiency was measured by acid-PAGE, which indicates the cognate mutant dFxs and eFxs can aminoacylate the tRNAs-NNA in the presence of Lys-DBE and Tyr-CME (Fig. 3.7). On the other hand, wild-type flexizymes could not aminoacylate non-cognate tRNA mutants (Fig. 3.7). In the case of C75U tRNA mutant, aminoacylation efficiency of mutant flexizymes bearing GAU-3′ end, which form two Watson–Crick base pairs with tRNAs, was lower than that of wild-type bearing GGU-3′ end, which forms one Watson–Crick base pair and one G•U wobble base pair (Fig. 3.8). This result indicates that G•U wobble base pair is more suitable for aminoacylation by flexizymes than A-U Watson–Crick base pair. Mutant flexizymes could also charge several other amino acids (Fig. 3.5) onto the corresponding mutant tRNAs (Fig. 3.9).

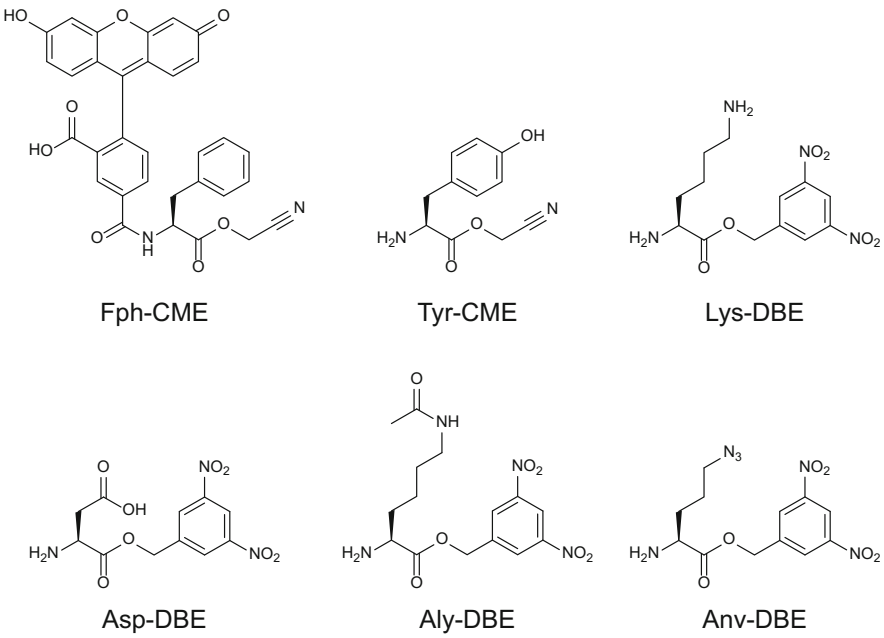

Fig. 3.5 Amino acid substrates used in this chapter. The abbreviations of Fph, Aly, and Anv represent *N*-(5-FAM)-L-phenylalanine, L-acetyllysine, and L-azidonorvaline, respectively. Carboxyl groups were activated using cyanomethyl ester (CME) or 3,5-dinitrobenzyl ester (DBE)

3.2.2 Preparation of Tagged Ribosomes

Mutant ribosomes bearing a mutation (or mutations) at the PTC were prepared using an MS2-tag affinity purification method (Youngman and Green 2005). Professor Rachel Green in Johns Hopkins University kindly gifted me a plasmid p278 MS2 (Amp^R) encoding 23S rRNA inserted with MS2-tag sequence in helix 98 of 23S rRNA (Fig. 3.10a), pcI^{857} (Kan^R) encoding a temperature-sensitive mutant of the lambda repressor protein cI and a plasmid pMAL-c2g (Amp^R) encoding His_6-tagged MS2 coat protein fused with maltose binding protein (His_6-MS2-MBP).

The plasmids p278 MS2 bearing mutations at PTC were constructed by site-directed mutagenesis. First, the plasmid pMAL-c2g was used to transform *E. coli* and His_6-MS2-MBP was expressed to be purified by FPLC using Ni-NTA affinity column. Next, the plasmids pcI^{857} and p278 MS2 were used to transform *E. coli*. Because the mutant ribosomes may be toxic to *E. coli*, this transformed *E. coli* was pre-cultured at 30 °C where mutant ribosomes were not expressed and the temperature was increased to 42 °C to express the mutant ribosomes. His_6-MS2-MBP was immobilized onto the MBP column by FPLC and the

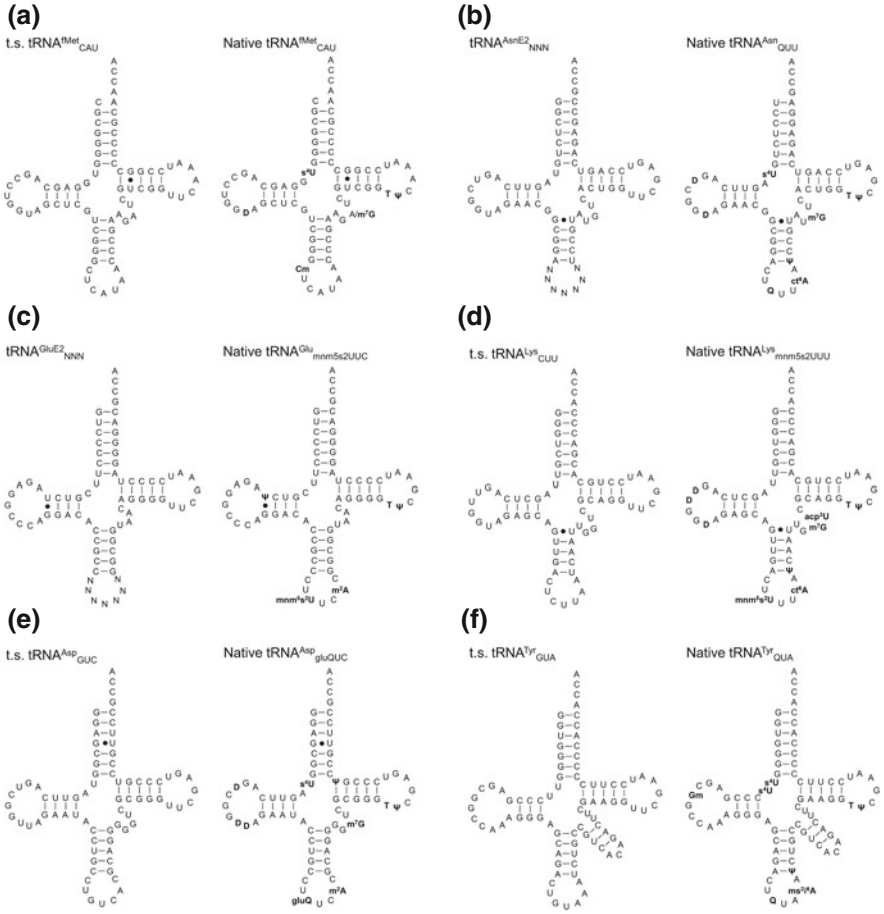

Fig. 3.6 Secondary structures of transcribed (t.s.) tRNAs compared with native tRNAs of *E. coli*. The figure presents the secondary structures of $tRNA_{CAU}^{fMet}$ (**a**), $tRNA_{NNN}^{AsnE2}$ (**b**), $tRNA_{NNN}^{GluE2}$ (**c**), $tRNA_{CUU}^{Lys}$ (**d**), $tRNA_{GUC}^{Asp}$ (**e**), and $tRNA_{GUA}^{Tyr}$ (**f**). s^4U; 4-thiouridine, D; dihydrouridine, Cm; 2′-O-methylcytidine, m^7G; 7-methylguanosine, ψ; pseudouridine, Q; queuosine, ct^6A: cyclic N^6-threonylcarbamoyladenosine, mnm^5s^2U; 5-methylaminomethyl-2-thiouridine, m^2A; 2-methyladenosine, acp^3U; 3-(3-amino-3-carboxypropyl)uridine, T; ribothymidine, gluQ; glutamyl-queuosine, ms^2i^6A; 2-methylthio-N^6-isopentenyladenosine. The sequences are based on the Modomics database (Machnicka et al. 2013) (http://modomics.genesilico.pl/)

expressed tagged-ribosomes (wild-type, G2251C, G2252C, G2553C, G2251C/G2553C, G2251C/G2252C/G2553C, and G2251A/G2553A) were purified by MS2 affinity purification using FPLC (Fig. 3.10b). Contamination of wild-type untagged-ribosome into the purified tagged-ribosomes were quantified by primer extension method (Youngman and Green 2005). This result showed the negligible contamination rate less than 3% (Fig. 3.11).

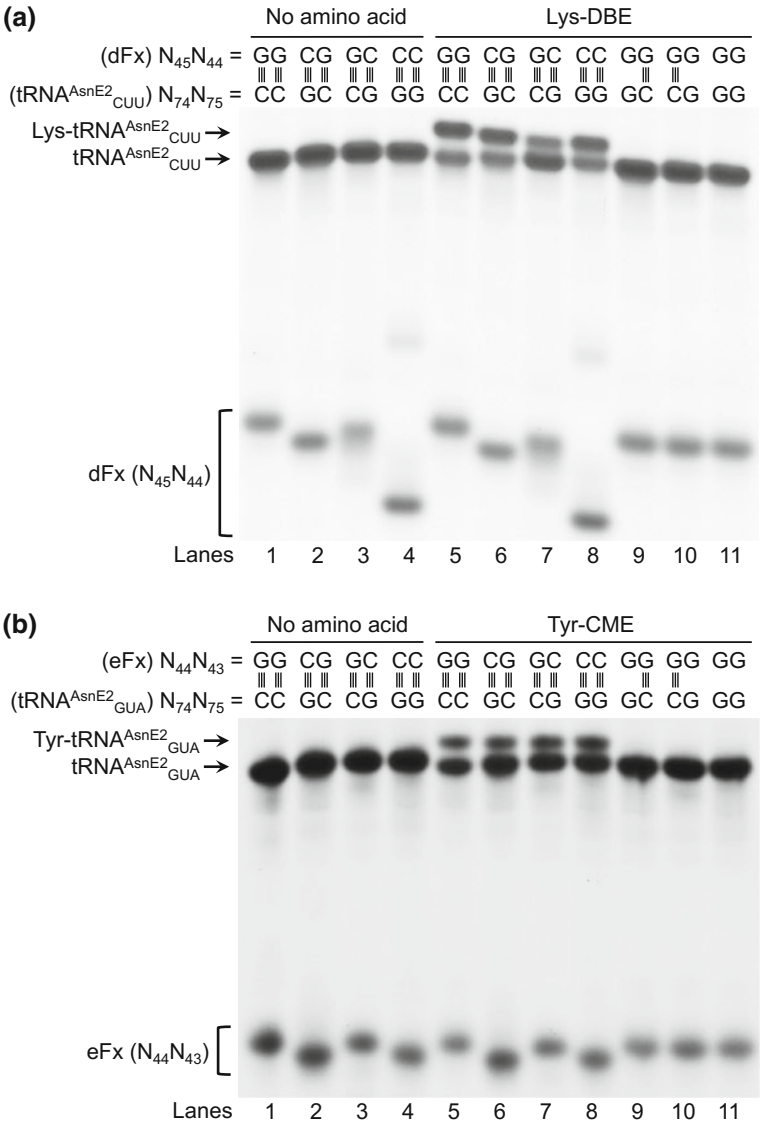

Fig. 3.7 A model study of aminoacylation of tRNAs-NNA derived from $tRNA^{AsnE2}$. tRNAs were acylated by dFx in the presence of Lys-DBE (**a**), and eFx in the presence of Tyr-CME (**b**). Acid-PAGE separated the bands of aa-tRNA (*upper*) and uncharged tRNA (*lower*). The data were generated from a sample of the end product of aminoacylation reaction. Note that the mobility of flexizymes was different depending on the 3′-terminal mutations

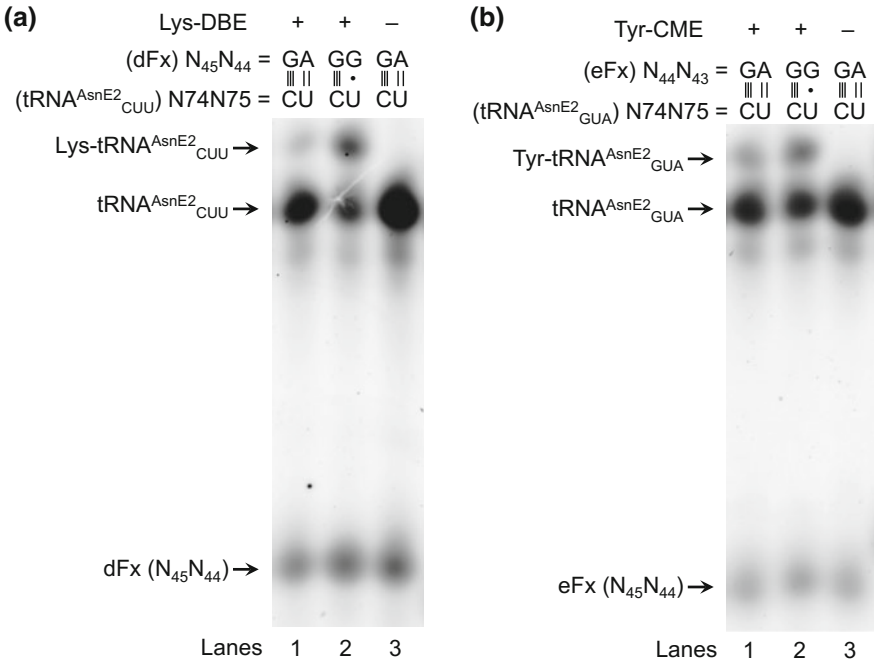

Fig. 3.8 Aminoacylation of tRNA-CUA derived from $tRNA^{AsnE2}$. tRNAs were acylated by dFx in the presence of Lys-DBE (**a**), and eFx in the presence of Tyr-CME (**b**). Acid-PAGE separated the bands of aa-tRNA (*upper*) and uncharged tRNA (*lower*). The data were generated from a sample of the end product of aminoacylation reaction

3.2.3 *Translation Activity of Wild-type/Mutant Ribosome–tRNA Pairs*

An assay system to detect peptides translated by tagged-ribosomes and aa-tRNAs-NNA was established. Because *E. coli* ARSs do not uniformly charge amino acids onto tRNAs-NNA (Liu and Horowitz 1994; Schulman and Pelka 1977; Zhou et al. 2011), a conventional methods using radioisotope-labeling amino acids is unsuitable. Instead, fluorescently labeled amino acid (*N*-(5-FAM)-L-phenylalanine, Fph, Fig. 3.5) was aminoacylated onto initiator $tRNA_{CAU}^{fMet}$ and incorporated at N-terminus of peptide by FIT system (Goto et al. 2011) to reassign the initiation codon from fMet to Fph. Lysine and tyrosine were charged onto $tRNA_{CUU}^{AsnE2}$-CCA and $tRNA_{GUA}^{AsnE2}$-CCA by cognate dFx and eFx, respectively. As a model template, a DNA template encoding the heptapeptide-1 (Fph-Lys-Tyr-Lys-Lys-Tyr-Lys) was prepared and the expression of heptapeptide-1 in the FIT system, whose components were described in the section of materials and methods, was confirmed. Tricine-SDS-PAGE analysis of the translated product enabled to visualize a fluorescent band (Fig. 3.12a) and quantify an expressed peptide by comparison with a

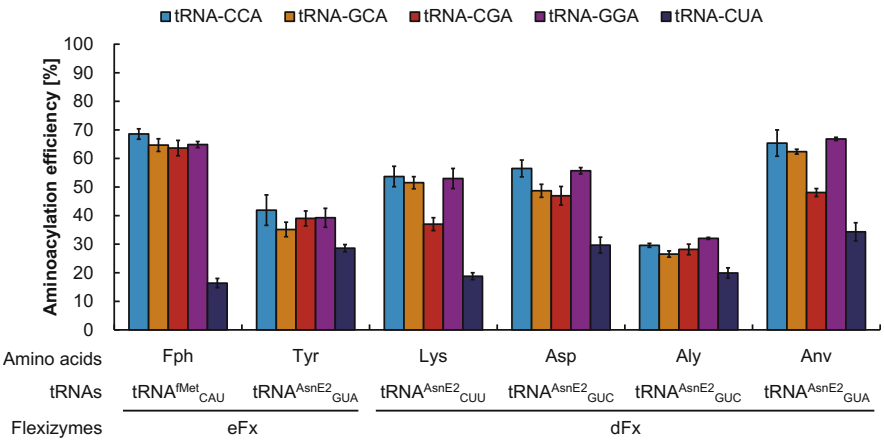

Fig. 3.9 Efficiency of flexizymes-catalyzed aminoacylation with canonical (Tyr, Lys, and Asp) and non-canonical (Fph, Aly, and Anv) amino acids. The tRNAs-CCA, -GCA, -CGA, -GGA, and -CUA were acylated by the compensatory flexizymes, dFx/eFx-GGU, -GCU, -CGU, -CCU, and -AGU. The data represent the average of three independent reactions. The error bars represent the standard deviation. The data were generated from a sample of the end product of aminoacylation reaction

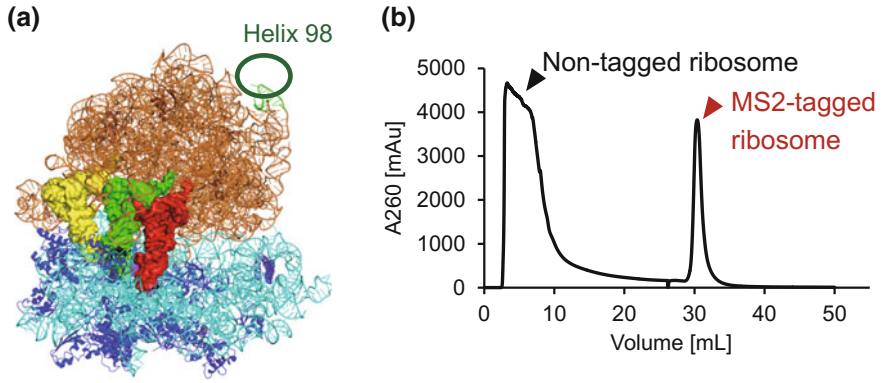

Fig. 3.10 Schematic illustration of the insertion sites for the MS2 tag and purification of tagged ribosome. **a** Helix 98 in 23S rRNA which is the insertion sites for the MS2 tag was indicated as *green circle*. The image of structure was produced from the previous report (Voorhees et al. 2009) (PDB ID: 2WDK/2WDL). **b** Representative results of FPLC purification of MS2-tagged ribosome

band generated by a known concentration of Fph (Fig. 3.12b), and the peak corresponding to heptatpeptide-1 was confirmed by MALDI-TOF-MS (Fig. 3.12c). The production of heptapeptide-1 plateaued at 30 min, with a final concentration of approximately 1.0 μM. We also examined expression of heptapeptide-1 using Lys-$tRNA_{CUU}^{GluE2}$-CCA and Tyr-$tRNA_{GUA}^{GluE2}$-CCA under the same condition, and the amount of expressed peptide increased to 3.5 μM (Fig. 3.13a and b).

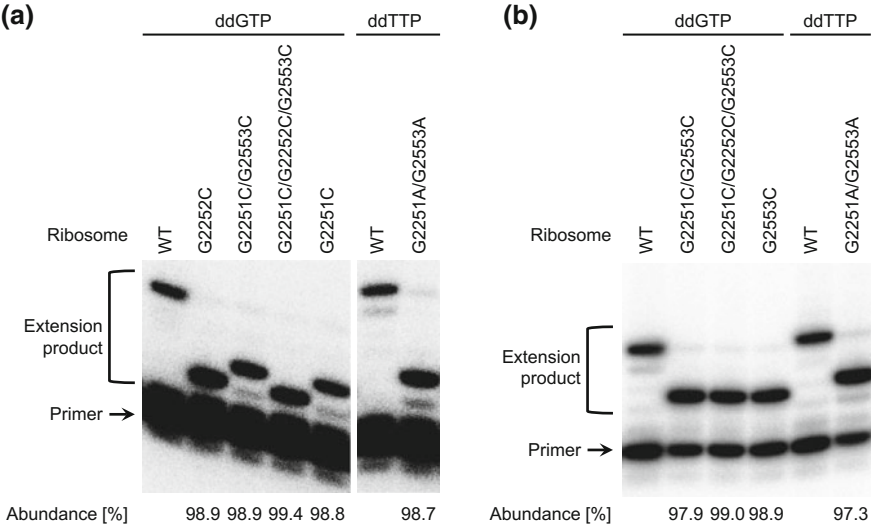

Fig. 3.11 Primer extension analysis of rRNAs extracted from MS2-tagged ribosomes purified by FPLC. **a** A primer that is complementary to the bases of 2254–2273 in 23S rRNA was used for the detection of mutations of 2251 and 2252. **b** A primer that is complementary to the bases of 2556–2575 in 23S rRNA was used for the detection of mutation of 2553. MS2-tagged ribosomes bearing mutations produced different ddGTP or ddTTP stops from those produced by WT ribosome. The abundance of tagged ribosomes relative to untagged wild-type in each population was shown below the gel. The calculated values of abundance were derived from a single experimental data set

The increase of expression rate could be attributed to the higher binding affinity of aa-tRNAs^{GluE2}-CCA to EF-Tu compared to that of aa-tRNA^{AsnE2}-CCA (Fig. 3.14). Therefore, we decided to use tRNA^{GluE2} for further translation experiments.

Next, I investigated whether tRNAs-NNA can be used by the wild-type ribosome for mRNA-dependent translation. Four mutant aa-tRNAs bearing GCA-3′, CGA-3′, and GGA-3′ were prepared by cognate dFxs and eFxs (Fig. 3.9) and measured peptide expression. Surprisingly tRNA-GCA could be used by wild-type ribosome to express heptapeptide-1 even only one base pair forms at P-site and the final concentration of the peptide was 2.7 μM (Fig. 3.13). On the other hand, tRNAs-CGA and -GGA were inactive with wild-type ribosome (Fig. 3.13). These results indicate that tRNAs-CGA and tRNAs-GGA but not tRNAs-GCA are orthogonal to the wild-type tRNAs-CCA (Fig. 3.15).

Then, I measured the translation activity of mutant ribosomes and tRNAs. As predicted from the results with the pair of wild-type ribosome and non-cognate tRNAs-GCA, the G2252C ribosome was also active with both cognate tRNAs-GCA and non-cognate tRNAs-CCA, but not with tRNAs-CGA and tRNAs-GGA (Fig. 3.13a). The expression rate of cognate pair of G2252C ribosome and tRNAs-GCA was almost the same as that of wild-type pair, and that of non-cognate pair of G2252C ribosome and tRNAs-CCA was also the same as that

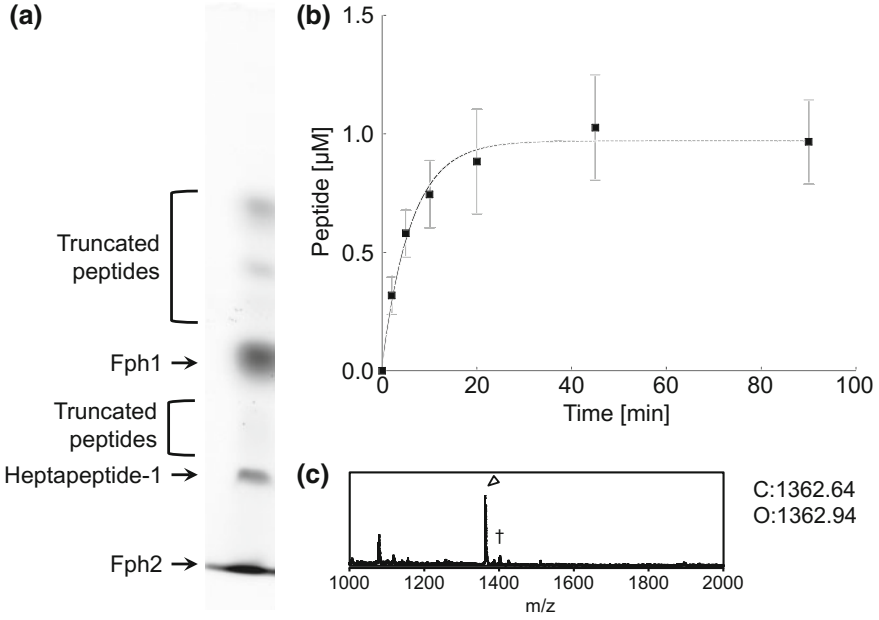

Fig. 3.12 Translation activity of pairs of wild-type ribosome–tRNA using $tRNAs^{AsnE2}$ as elongator tRNAs. **a** Tricine-SDS-PAGE analysis of heptapeptide-1 (FphLysTyrLysLysTyrLys) synthesized using the wild-type pairs of ribosome–tRNAs. $tRNA_{CAU}^{fMet}$ bearing the CCA-3′ end were used as initiator tRNAs, and $tRNAs_{NNN}^{AsnE2}$ (NNN denotes CUU and GUA designating Lys and Tyr, respectively) bearing the CCA-3′ end were used as elongator tRNAs. This image showed the result of the end of the translation reaction. Two bands were observed for Fph (indicated by Fph1 and Fph2), presumably due to the presence of Fph, Fph-CME, and Fph-$tRNA_{CAU}^{fMet}$. The bands above and below of Fph1 showed truncated peptides generated by peptidyl-tRNA drop-off (Kang and Suga 2011). **b** Time-course analysis of heptapeptide-1 production. The data represents the average of three independent reactions and error bars represent the standard deviation of the individual measurements. **c** MALDI-TOF MS analysis of heptapeptide-1. C and O denotes calculated and observed mass values, respectively. † indicates a potassium adduct of heptapeptide-1. Other minor peaks were also present in the non-templated translation product likely originating from the translation system. The data were generated from a sample of the end product of translation reaction

of non-cognate pair of wild-type ribosome and tRNAs-GCA (Fig. 3.13b). These both cognate and non-cognate pairs yielded heptapeptide-1 as major products (Fig. 3.13c). These results indicated that mispair between G2252 and G74 or C2252 and C74 could be tolerated during the translation reaction.

The double mutant ribosome G2251C/G2553C ribosome was sufficiently active with only cognate tRNAs-CGA to yield heptapeptide-1 (Fig. 3.13). Time-course analysis indicated that expression plateaued at a final concentration of 1.7 μM. This suggests that the cognate pair of G2251C/G2553C ribosome and tRNAs-CGA

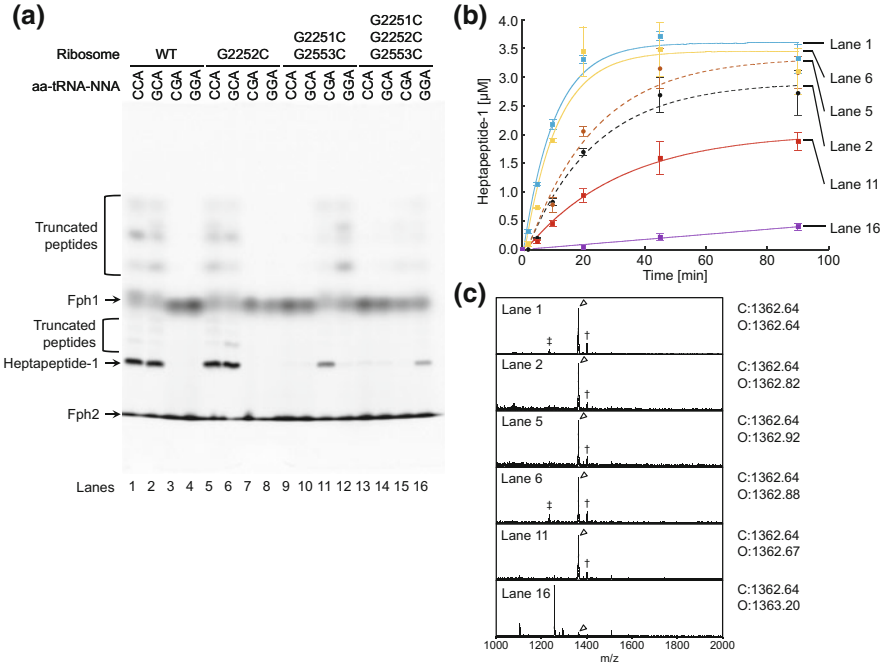

Fig. 3.13 Translational activity of pairs of ribosome and tRNA mutants. **a** Tricine-SDS-PAGE analysis of heptapeptide-1 (Fph-Lys-Tyr-Lys-Lys-Tyr-Lys) synthesized using the designated pairs of ribosome–tRNA mutants. $tRNAs_{CAU}^{fMet}$ bearing the respective NNA-3′ end were used as initiator tRNAs, and $tRNAs_{NNN}^{GluE2}$ (NNN denotes CUU and GUA designating Lys and Tyr, respectively) bearing the respective NNA-3′ end were used as elongator tRNAs. This image showed the result of the end of the translation reaction. **b** Time-course analysis of heptapeptide-1 production by active pairs of ribosomes and tRNAs. I investigated four cognate pairs of the wild-type ribosome–tRNAs-CCA (cyan solid line), G2252C-ribosome–tRNAs-GCA (yellow solid), G2251C/G2553C-ribosome–tRNAs-CGA (red solid), and G2251C/G2252C/G2553C-ribosome–tRNAs-GGA (purple solid), and two non-cognate pairs of the wild-type ribosome–tRNAs-GCA (black dashed) and G2252C-ribosome–tRNAs-CCA (brown dashed). The data represents the average of three independent reactions. The error bars represent the standard deviation. **c** MALDI-TOF MS analysis of heptapeptide-1 synthesized using cognate and non-cognate ribosome–tRNA pairs. Lane numbers are those of the tricine-SDS-PAGE gel described in Fig. 3.13. C and O denotes calculated and observed mass values, respectively. † indicates a potassium adduct of heptapeptide-1. ‡ indicates the molecular mass value consistent with FphLysTyrLysLysTyr, which was presumably produced by peptidyl-tRNA drop-off (Kang and Suga 2011). The identity of major peak in lane 16 is unknown; however, since this peaks as well as other minor peaks were also present in the sample of G2251C/G225C/G2553C-ribosome alone, it could be originated from a contaminant of the G2251C/G225C/G2553C-ribosome preparation. The data were generated from a sample of the end product of translation reaction

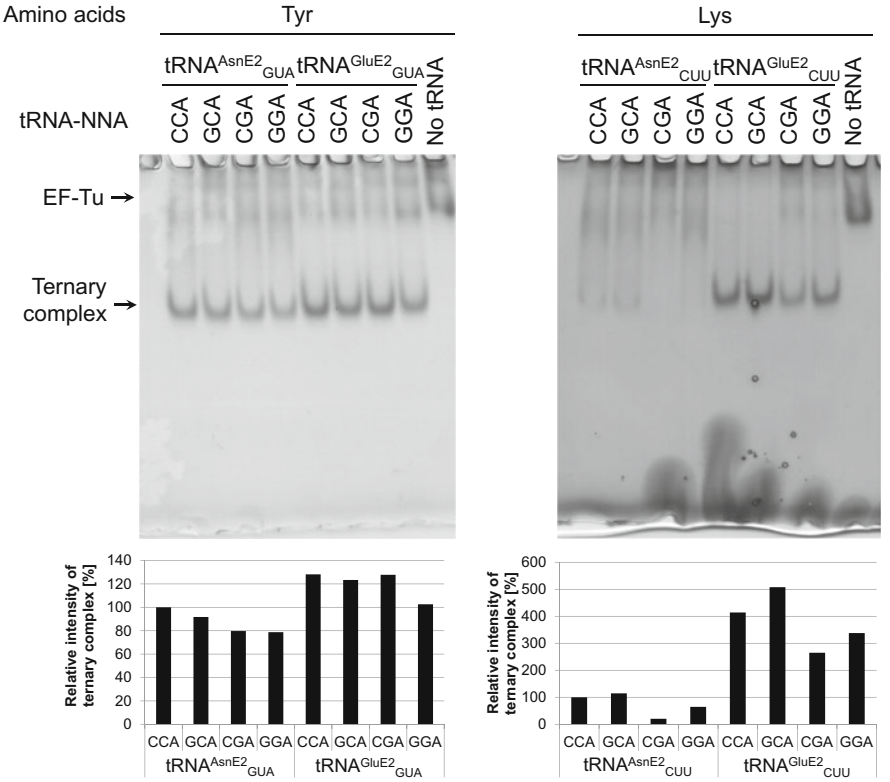

Fig. 3.14 Gel-shift assay for ternary complex of elongation factor Tu (EF-Tu), guanosine triphosphate (GTP) and aa-tRNAs-CCA, GCA, CGA, and GGA. Tyrosine was charged onto $tRNA_{GUA}^{AsnE2}$ and $tRNA_{GUA}^{GluE2}$, and lysine was charged onto $tRNA_{CUU}^{AsnE2}$ and $tRNA_{CUU}^{GluE2}$. Band intensities of the ternary complexes were normalized relative to EF-Tu, GTP, and aa-tRNAs-CCA complexes. The values of the relative intensity of the ternary complex (*y*-axis) were derived from a single experimental set

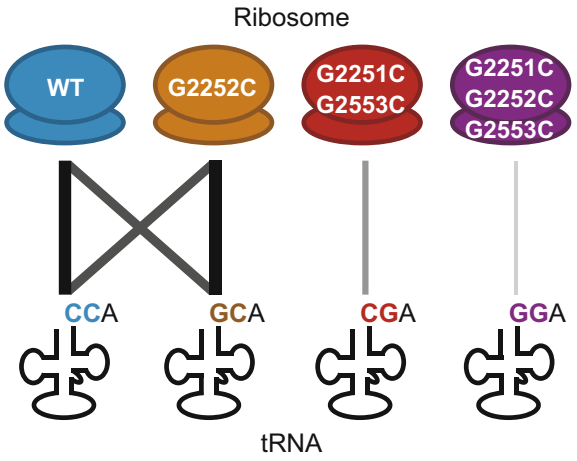

Fig. 3.15 Illustration of compatibility and orthogonality of the ribosome–tRNAs mutant pairs. Line thickness indicates the compatibility of translational activity between each ribosome–tRNA pair

functions orthogonally to the wild-type pair (Fig. 3.15). However, this mutant pair has a slower translation rate than the wild-type pair, resulting in a lower yield of peptide due to the hydrolysis of the aa-tRNAs. Faint bands observed when using tRNAs-CCA and tRNAs-GCA could be ascribed to a peptide originating from the background translation by little amount (<3%) of wild-type ribosome contamination to the respective mutant ribosome (Fig. 3.11). When tRNAs-GGA was used, a very faint band was detected because mispair between G2252 and G74 was tolerated as described above. However, these bands were too faint to reliably quantify the intensity for the time-course experiment below and determine the product identity by MALDI-TOF analysis.

The triple mutant ribosome (G2251C/G2252C/G2553C) was active with only cognate tRNAs-GGA to yield heptapeptide-1 like the double mutant ribosome (Fig. 3.13). However, the translation rate dramatically decreased and the final concentration of heptapeptide-1 was 0.4 μM, which was reflected as a tiny peak of heptapaptide-1 in MALDI-TOF-MS spectrum (Fig. 3.13c).

I also tested the translational activity of other ribosome mutants (G2251A/G2553A, G2251C, and G2553C) and tRNA mutant (tRNA-CUA) (Fig. 3.16). Like G2251C/G2553 ribosome and G2251C/G2252C/G2553C ribosome, G2251A/G2553A ribosome was active with only cognate tRNA-CUA, but the band was too faint to reliably quantify the intensity for the time-course experiment and determine the product identity by MALDI-TOF analysis. A very faint band observed when using tRNAs-CCA could be due to the contamination of wild-type ribosome (Fig. 3.11). These results indicate that A-U pair between 23S rRNA and tRNA is not appropriate for translation. In addition, wild-type ribosome was inactive with tRNAs-CUA, which suggests that G•U wobble pair between ribosome and tRNA at the PTC is not tolerated. In the case of G2251C and G2553C ribosomes, translation activity was not restored when using tRNA-CCA or tRNA-CGA. This result and the fact that the pair of G2251C/G2553C ribosome and tRNA-CGA had comparable translation activity to wild-type pair, combination of two base pairs, G2553-C75 at the A-site and G2251-C75 at the P-site, is essential for translation.

These decrease of translation rate of cognate pair of mutant ribosome and tRNAs indicates that, despite the fact that PT activity and translocation activity of mutant ribosomes bearing mutations at PTC was restored by the compensatory mutations into CCA end of tRNAs (Kim and Green 1999; Dorner et al. 2006), these compensatory mutations did not fully restore the whole translation activity. This further suggests that these bases have crucial roles in not only the PT reaction and translocation but also other steps of translation, potentially involving interactions with other rRNAs or protein factors. It was confirmed that the binding affinity of

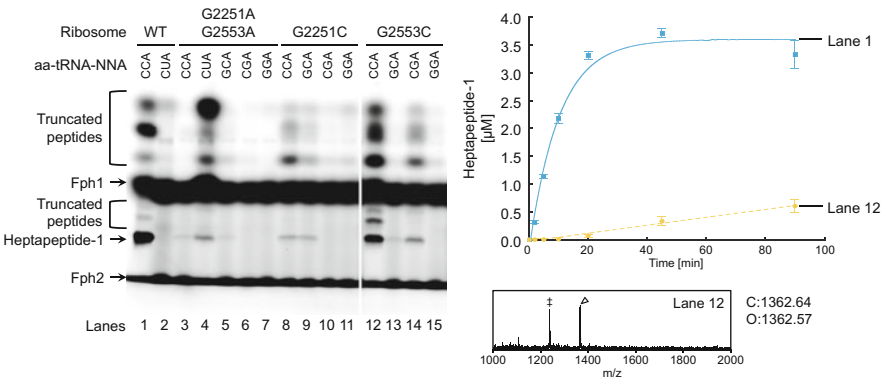

Fig. 3.16 Translational activity of pairs of ribosome–tRNA mutants bearing CCA, GCA, CGA, GGA, and CUA-3′ ends. $tRNAs^{fMet}$ were used as initiator tRNAs and $tRNAs^{GluE2}$ as elongator tRNAs. **a** The entire image of the tricine-SDS-PAGE analysis of a heptapeptide-1 (FphLysTyrLys LysTyrLys) synthesized using pairs of ribosome–tRNA mutants. This image showed the result of the end of the translation reaction. The bands above and below of Fph1 showed truncated peptides generated by peptidyl-tRNA drop-off (Kang and Suga 2011), which were also observed for the wild-type control of lane 1. The faint bands in lanes 3, 8, 9, and 13 could be ascribed to a peptide originating from the background translation by little amount (<3%) of wild-type ribosome contamination to the respective mutant ribosome (Fig. 3.12). **b** Time-course analysis of heptapeptide-1 production by active pairs of ribosomes and tRNAs. Lane numbers are those of the tricine-SDS-PAGE gel described in Fig. 3.16a, in which the solid line in cyan indicates the reaction of a cognate pairs of the wild-type ribosome–tRNAs-CCA (the identical result shown in Fig. 3.13b) while the *dashed line* in *yellow* shows that of a non-cognate pair G2253C-ribosome–tRNAs-CCA. The data represents the mean value of each sample (n = 3) and error bars show the standard deviations obtained from independent measurements. **c** MALDI-TOF MS analysis of heptapeptide-1 synthesized using a non-cognate pair G2253C-ribosome–tRNAs-CCA. Lane numbers are those of the Tricine-SDS-PAGE gel described in Fig. 3.16a. C and O denotes calculated and observed mass values, respectively. ‡ indicates the molecular mass value consistent with FphLysTyrLysLysTyr, which could be one of the bands corresponding to the truncated peptides appeared in the tricine-SDS-PAGE. The data shown in Fig. 3.16a and c were generated from a sample of the end product of translation reaction

aa-tRNAs-NNA to form ternary complexes (EF-TU•GTP•aa-tRNA) were almost the same as that of wild-type, which was coincident with the previous report (Nissen et al. 2000; Liu et al. 1998). In the accommodation step, C75 of tRNA packs between EF-Tu residue 219 and the flipped base of A55 of 16S rRNA, which is 99.5% conserved in all species of known sequence (Schmeing et al. 2009). It is possible that these interaction is critical for efficient translation reaction. Nonetheless, further studies are necessary to elucidate why compensatory mutations at CCA-end could not fully restore the translation activity of mutant ribosomes.

3.2.4 *Simultaneous Expression of Two Different Peptides from Single mRNA Template*

Because the pair of G2251C/G2553C ribosome and tRNAs-CGA had comparable translation activity and orthogonality to the wild-type ribosome and tRNA-CCA pair, I examined whether two distinct peptides could be expressed from a single mRNA template under artificially programmed genetic code in one pot. Four amino acids were assigned to the respective genetic codes as follows; For the wild-type ribosome–tRNAs pair, a genetic code (referred to as WT-code) assigned Fph (AUG, initiation), lysine (AAG), tyrosine (UAC), and aspartic acid (GAC), and for the G2251C/G2553C ribosome–tRNAs-CGA pair, an orthogonal genetic code (referred to as OR-code) assigned Fph (AUG, initiation), lysine (AAG), L-azidonorvaline (Anv; UAC) and L-acetyllysine (Aly; GAC) (Fig. 3.17). The tRNAs-CCA and tRNAs-CGA were aminoacylated with respective amino acids using wild-type or compensatory mutated flexizymes. The DNA template encoding heptapeptide-2

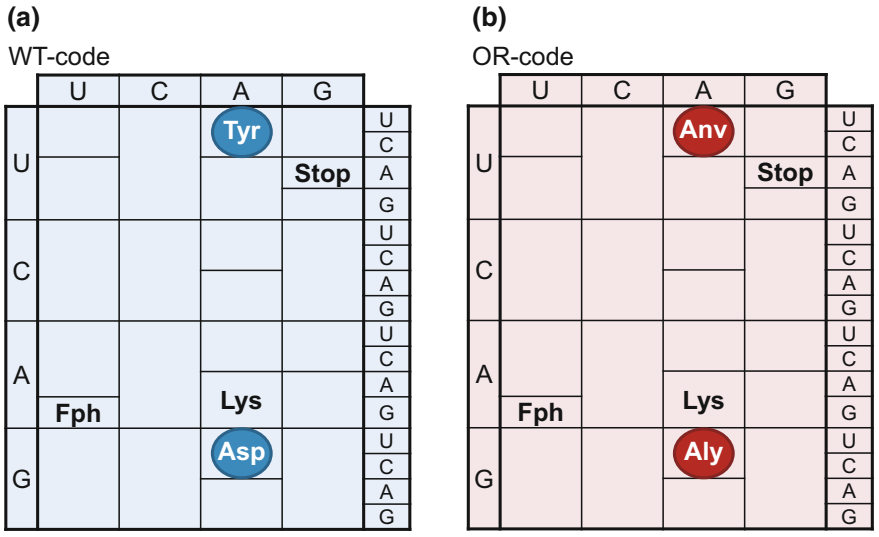

Fig. 3.17 Two genetic codes programmed for simultaneous expression of two distinct peptides from a single mRNA sequence. **a** WT-code. This code comprises the wild-type ribosome–tRNAs-CCA pair. **b** OR-code. This code comprises the G2251C/G2553C-ribosome–tRNAs-CGA pair

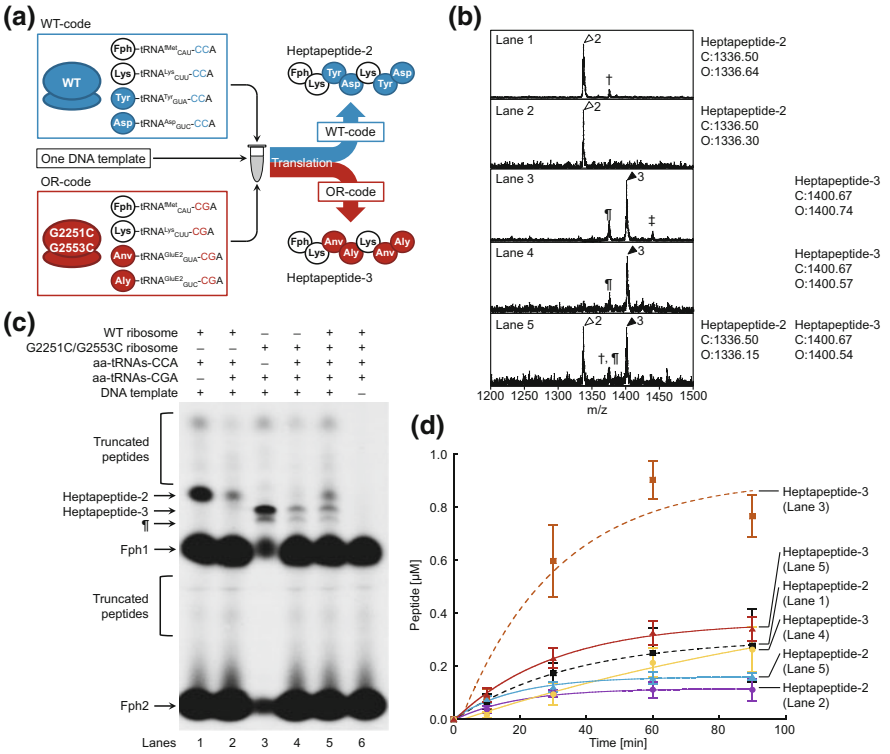

Fig. 3.18 Simultaneous expression of two distinct peptides from a single mRNA sequence under two artificially programmed genetic codes. **a** Schematic illustration of simultaneous expression. The wild-type ribosome–tRNAs-CCA and G2251C/G2553C-ribosome–tRNA-CGA pairs generated heptapeptide-2 and heptapeptide-3, respectively, according to the WT- and OR-codes. **b** MALDI-TOF MS analysis of translational products. Calculated (C) and observed mass (O) values are shown in the right panel of the spectra. † and ‡ denote a potassium adduct of heptapeptide-2 and heptapeptide-3, respectively. ¶ denotes heptapeptide-3 whose azide group was reduced to a primary amino group presumably by thiols present in the FIT system (Sako et al. 2008). Since other minor unidentified peaks were present in the non-templated translation product, they are likely present in the translation system. The data shown in Fig. 3.18b and c were generated from a sample of the end product of translation reaction. **c** Tricine-SDS-PAGE analysis of the respective heptapeptides. **d** Time-course analysis of simultaneous expression of heptapeptides. Heptapeptide-2 expression is seen in lane 1 (*black dashed line*), lane 2 (*purple*) and lane 5 (*cyan*, simultaneous expression); heptapeptide-3 expression is seen in lane 3 (*brown dashed line*) lane 4 (*yellow*) and lane 5 (*red*, simultaneous expression). Lane numbers are those described in Fig. 3.18c. The data represents the average of three independent reactions and error bars represent the standard deviation

according to the WT-code and heptapeptide-3 according to the OR-code was added to the FIT system, which comprised the combination of the wild-type ribosomes. G2251C/G2553C ribosomes and/or the above aa-tRNAs (Fig. 3.18a).

In the presence of wild-type ribosome and wild-type aa-tRNAs-CCA, heptapeptide-2 was expressed according to WT-code (Fig. 3.18b–d). When aa-tRNAs-CGA was added into wild-type pair of ribosome and aa-tRNAs-CCA, only heptapeptide-2 was observed in tricine-SDS-PAGE and MALDI-TOF-MS spectrum without any hybrid products (for example, Fph-Lys-Anv-Asp-Lys-Tyr-Aly, $[M + H]^+ = 1313.51$) generated from potential cross-reading (or readings) of codons in non-cognate genetic code (Fig. 3.18b and c). This indicates that aa-tRNAs-CGA was not used as translation substrates by wild-type ribosome. Similarly, the mutant pair of G2251C/G2553C ribosome and aa-tRNAs-CGA or this pair with the wild-type aa-tRNAs-CCA yielded only heptapeptide-2 (Fig. 3.18b–d). The decrease of peptide expression was observed in the presence of one ribosome with both cognate and non-cognate aa-tRNAs (Fig. 3.18c and d). This decreased expression of peptide could not be restored by increasing EF-Tu concentrations from 10 to 20 μM, which rules out EF-Tu sequestration by the non-cognate aa-tRNAs as an explanation for this effect (Fig. 3.19). From this result and the fact that the affinity of aa-tRNAs-CCA to EF-Tu was almost the same as that of aa-tRNAs-CGA (Fig. 3.14), it is possible that ternary complex including non-cognate aa-tRNAs compete with that including cognate aa-tRNAs in accommodation step. Nonetheless, further studies are necessary to restore this decrease of expression rate.

In the presence of both wild-type and mutant pair of ribosome and aa-tRNAs, the desired both heptapeptide-2 and -3 were expressed from a single DNA template in one pot according to the WT- and OR-codes (Fig. 3.18). In the absence of DNA template, no peptide was observed (Fig. 3.18c), which is consistent with the observation that translation proceeded in an mRNA-dependent manner. Moreover, the same experiment using different DNA template and aa-tRNAs produced two different heptapeptides from one DNA template (Figs. 3.20 and 3.21).

In these experiments, two distinct peptides can be expressed from one DNA template without any hybrid products. These results indicate that these coexisting translational machineries acted orthogonally and used only the cognate genetic codes.

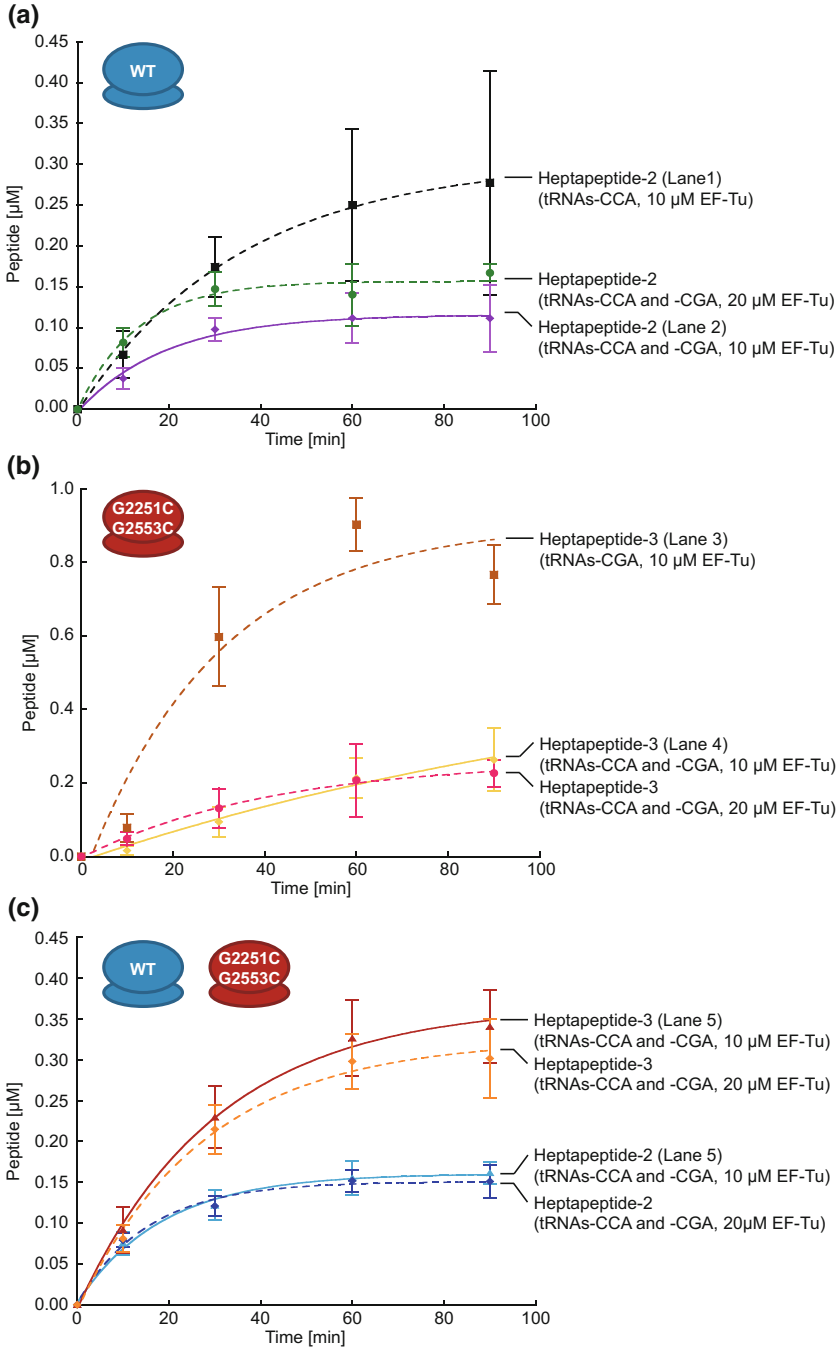
(a)
WT
Peptide [μM]
Time [min]
Heptapeptide-2 (Lane1)
(tRNAs-CCA, 10 μM EF-Tu)
Heptapeptide-2
(tRNAs-CCA and -CGA, 20 μM EF-Tu)
Heptapeptide-2 (Lane 2)
(tRNAs-CCA and -CGA, 10 μM EF-Tu)
(b)
G2251C
G2553C
Peptide [μM]
Time [min]
Heptapeptide-3 (Lane 3)
(tRNAs-CGA, 10 μM EF-Tu)
Heptapeptide-3 (Lane 4)
(tRNAs-CCA and -CGA, 10 μM EF-Tu)
Heptapeptide-3
(tRNAs-CCA and -CGA, 20 μM EF-Tu)
(c)
WT
G2251C
G2553C
Peptide [μM]
Time [min]
Heptapeptide-3 (Lane 5)
(tRNAs-CCA and -CGA, 10 μM EF-Tu)
Heptapeptide-3
(tRNAs-CCA and -CGA, 20 μM EF-Tu)
Heptapeptide-2 (Lane 5)
(tRNAs-CCA and -CGA, 10 μM EF-Tu)
Heptapeptide-2
(tRNAs-CCA and -CGA, 20μM EF-Tu)

◂**Fig. 3.19** Time-course analysis of heptapeptide production with an elevated concentration of EF-Tu. The concentration of EF-Tu was increased to 20 from 10 μM which was the condition in the experiments in Fig. 3.18. **a** Production of heptapeptide-2 when wildype ribosome coexisted with cognate aa-tRNAs-CCA and noncognate aa-tRNA-CGA with 20 μM EF-Tu/Ts were shown as *green dashed line*. **b** Production of heptapeptide-3 when orthogonal ribosome coexisted with its noncognate and cognate aa-tRNAs with 20 μM EF-Tu/Ts were shown as *pink dashed line*. **c** Production of heptapeptide-2 and -3 when both ribosomes with all aa-tRNAs coexisted with 20 μM EF-Tu/Ts were shown as *blue* and *orange dashed lines*. The other lines represent the same result as those shown in Fig. 3.18d. Lane numbers are those described in Fig. 3.18c. The data represents the average of three independent reactions, and the error bars represent the standard deviation of the individual measurements

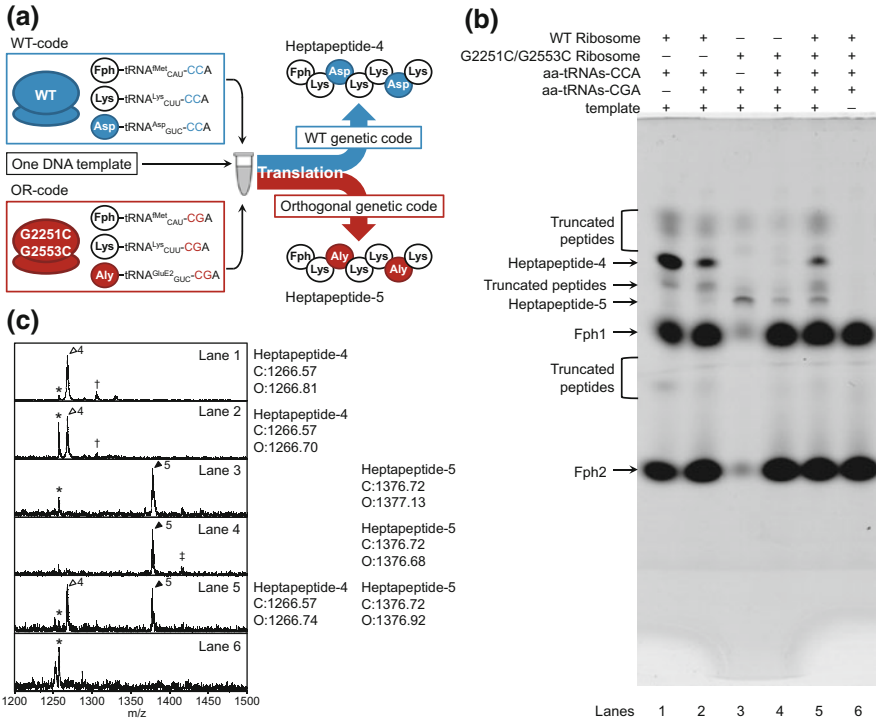

Fig. 3.20 Simultaneous expression of two heptapeptides-4 and -5 from a single mRNA template according to the two artificially programmed genetic codes. **a** Peptide translation from a single mRNA sequence in a single reaction mixture. The pair of wild-type ribosome–tRNAs-CCA and G2251C/G2553C-ribosome–tRNA-CGA generated Fph-Lys-Asp-Lys-Lys-Asp-Lys (heptapeptide-4) and Fph-Lys-Aly-Lys-Lys-Aly-Lys (heptapeptide-5), respectively, according to their respective genetic codes. **b** Tricine-SDS-PAGE analysis of the respective heptapeptides, 4 and 5. Other faint based are truncated peptides generated by peptidyl-tRNA drop-off (Kang and Suga 2011). **c** MALDI-TOF MS of the peptides isolated by gel filtration. Calculated (C) and observed mass (O) values are shown in the right panel of the spectra. † indicates the potassium adduct of heptapeptide-4, ‡ indicates the potassium adduct of heptapeptide-5, *species also present in the "no template" translation product and were likely derived from the translation mixture. The data shown in Fig. 3.20b and c were generated from a sample of the end product of translation reaction

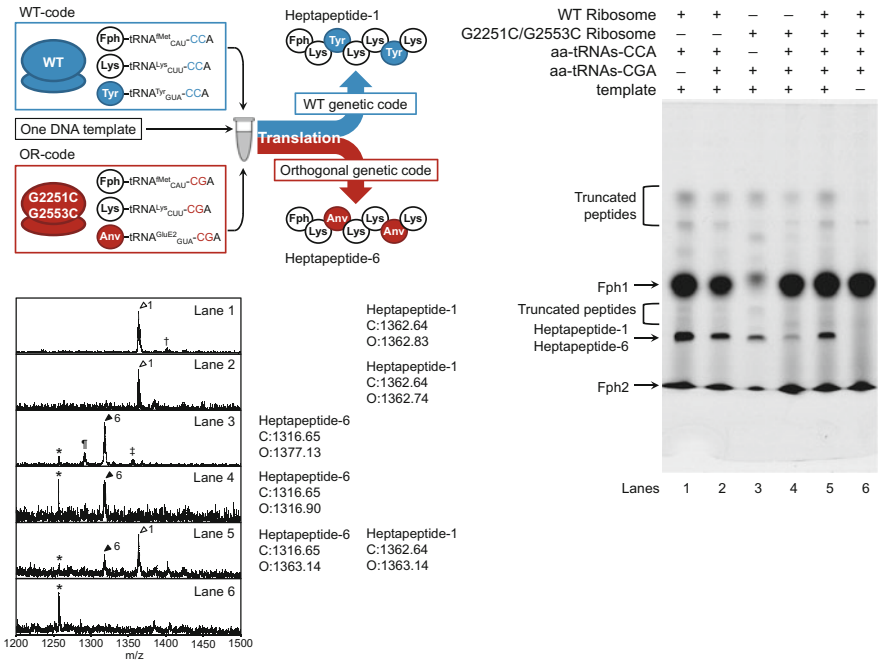

Fig. 3.21 Simultaneous expression of two heptapeptides-1 and -6 from a single mRNA template according to the two artificially programmed genetic codes. **a** Peptide translation from a single mRNA sequence in a single reaction mixture. The pair of wild-type ribosome–tRNAs-CCA and G2251C/G2553C-ribosome–tRNA-CGA generated Fph-Lys-Asp-Lys-Lys-Asp-Lys (heptapeptide-1) and Fph-Lys-Anv-Lys-Lys-Anv-Lys (heptapeptide-6), respectively, according to their respective genetic codes. **b** Tricine-SDS-PAGE analysis. Heptapeptides-1 and -6 could were observed at the same position. Other faint based are truncated peptides generated by peptidyl-tRNA drop-off (Kang and Suga 2011). **c** MALDI-TOF MS of the peptides isolated by gel filtration. Calculated (C) and observed mass (O) values are shown in the right panel of the spectra. † indicates the potassium adduct of heptapeptide-1, ‡ indicates the potassium adduct of heptapeptide-2, ¶ indicates heptapeptide-6 whose azide group was reduced to a primary amino group presumably by thiols present in the FIT system (Sako et al. 2008), *species also present in the "no template" translation product and were likely derived from the translation mixture. The data shown in Fig. 3.21b and c were generated from a sample of the end product of translation reaction

3.3 Conclusion

In this chapter, I developed the method to prepare aa-tRNAs-NNA using compensatory mutated flexizymes. Then, I measured the translation activity of PTC-mutated ribosome–tRNA pair and developed the orthogonal ribosome–tRNAs pair.

First, CCA-3′ end mutated tRNAs were aminoacylated with various amino acids by compensatory mutated flexizymes. In addition to C74N/C75N mutants, A76N

mutant tRNA also can be aminoacylated by prototype of flexizymes "pre-24" (Saito et al. 2001a, b), which indicates that also compensatory mutated flexizymes (eFx, dFx and aFx) can aminoacylate A76N mutant tRNAs. From other groups, an efficient method to prepare homogeneous aa-tRNAs using flexizyme was recently reported (Zhang and Ferre-D'Amare 2014). These results indicate that wild-type and compensatory mutated flexizymes have great potential to charge various amino acids onto any RNA substrates bearing NNN-3′ end.

Next, translation activity of several mutant ribosome–tRNAs pairs were measured. To my knowledge, this is the first report about the whole translation activity of CCA-3′ end mutated tRNAs and compensatory mutated ribosome although peptidyl transfer (Kim and Green 1999) and translocation (Dorner et al. 2006) of those were already reported. Compensatory mutation of 23S rRNA in the PTC restored the whole translation activity, which is consistent with the results of peptidyl transfer (Kim and Green 1999) and translocation (Dorner et al. 2006). However, compensatory mutations did not fully restore the activity of some mutant ribosome–tRNAs pairs. To fully restore the translation activity, more engineering of translation machinery including other positions of rRNAs and translation factors will be required.

Finally, orthogonal mutant ribosome–tRNAs functioning independently to wild-type ribosome–tRNAs according to artificially designed genetic code. Combination of wild-type and orthogonal ribosome–tRNAs pair can produce two different peptides from one mRNA. Unfortunately, the efficiency of translation was decreased when both cognate and non-cognate tRNA were present with ribosomes. To increase the translation efficiency, the more detailed interaction of CCA-3′ end with ribosomes and translation factors should be investigated and more engineering of translation machinery will be required.

The study in this chapter established a novel method for genetic code reprogramming, and demonstrated the importance of interactions between the rRNA and the tRNAs in translation. These results open an entrance to a new opportunity of in vitro synthetic biology involving the engineering of the genetic codes and translation machineries.

3.4 Materials and Methods

Chemical synthesis of L-tyrosine cyanomethyl ester (Tyr-CME), L-aspartic acid 3,5-dinitrobenzyl ester (Asp-DBE), L-lysine 3,5-dinitrobenzyl ester (Lys-DBE), L-acetyllysine 3,5-dinitrobenzyl ester (Aly-DBE), and L-azidonorvaline 3, 5-dinitrobenzyl ester (Anv-DBE)

Tyr-CME, Asp-DBE, Lys-DBE, Aly-DBE and Anv-DBE were synthesized as previously described (Murakami et al. 2006; Sako et al. 2008).

Chemical synthesis of *N*-(5-FAM)-L-phenylalanine-cyanomethyl ester (Fph-CME)

L-phenylalanine-cyanomethyl ester (Phe-CME) was synthesized as previously described (Saito et al. 2001a). Triethylamine (22 μL, 160 μmol) was added to a mixture of Phe-CME (14.4 mg, 60 μmol) and 5-carboxyfluorescein succinimidyl ester (Thermo Fisher Scientific Inc., 19 mg, 40 μmol) in 500 μL of *N*,*N*-dimethylformamide and then the mixture was stirred at room temperature for 13.5 h. After the reaction, ethyl acetate was added, and the solution was treated with 1 M HCl (3 mL × 3) and saturated NaCl (3 mL × 1). The organic layer was dried over Na_2SO_4, and concentrated under reduced pressure. The crude residue was dissolved in methanol and injected into a high-pressure liquid chromatography (HPLC) system equipped with a Cadenza 5CD-18 reverse-phase chromatography column (Code 5CD0Q6). The column was equilibrated with 20% (v/v) acetonitrile in H_2O containing 0.1% (v/v) TFA, and eluted with a 2.2%/min gradient of 99.9% (v/v) acetonitrile in 0.1% (v/v) TFA to 90% (v/v) acetonitrile. The HPLC profile was monitored by measuring the absorbance at 494 nm. The fractions of Fph-CME were lyophilized. The concentration was determined by absorbance at 494 nm in 500 mM Tris-HCl (pH 8.0).

Fph-CME: ^{1}H NMR (300 MHz, DMSO-d_6, δ): 10.16 (br, 2H), 9.36 (d, J = 7.5 Hz, 1H), 8.45 (d, J = 0.6 Hz, 1H), 8.19 (dd, J = 8.1, 1.5 Hz, 1H), 7.39 (d, J = 8.1 Hz, 1H), 7.36–7.20 (m, 5H), 6.68 (d, J = 2.1 Hz, 2H), 6.61–6.52 (m, 4H), 5.05 (s, 1H), 4.87–4.80 (m, 1H), 3.33–3.14 (m, 2H); ^{13}C NMR (125 MHz, DMSO-d_6, δ): 171.0, 168.5, 165.4, 160.0, 155.6, 152.2, 137.6, 135.4, 135.3, 129.7, 129.5, 128.8, 127.1, 127.0, 124.9, 123.9, 116.2, 113.1, 109.3, 102.7, 83.8, 54.5, 50.0, 36.2.

The high-resolution mass spectrum (HRMS) was determined using flow injection (direct electrospray ionization (ESI)-MS) in positive mode (Thermo Exactive). Calculated $[(M + H)^+]$ m/z for $C_{32}H_{23}N_2O_8^+$ = 563.1449, found = 563.1445.

In vitro transcription

The tRNAs, eFxs, and dFxs were prepared using run-off in vitro transcription with T7 RNA polymerase. DNA templates were modified with 2′-*O*-methylation at the second last nucleotide of the 5′-termini to reduce non-templated nucleotide addition by T7 RNA polymerase (Kao et al. 1999). The primers for preparing transcription templates are shown in Table 3.3. All non-methylated primers were purchased from Eurofins Genomics K.K. (Japan) and methylated primers were purchased from Gene Design Inc. (Japan). The sequences of RNAs are shown in Table 3.4.

Expression and purification of maltose binding protein (MBP) -MS2-His_6

The plasmid pMAL-c2g (Amp^R) encoding His_6-tagged MS2 coat protein (a gift from R. Green, Johns Hopkins University) was used to transform *E. coli* BL21-(DE3) in LB medium with 100 μg/mL carbenicillin. A single colony isolated by streaking was used to inoculate a 30 mL overnight culture in LB supplemented with 100 μg/mL carbenicillin, and 10 mL of this culture was used to inoculate one liter

Table 3.3 Primers used in this chapter

Sequence (5′ to 3′)	Used for
GGCGTAATACGACTCACTATAG	dFx, eFx, tRNA, DNA template
GTAATACGACTCACTATAGGATCGAAAGATTTCCGC	dFx-NNU and eFx-NNU
AACGCCATGTACCCTTTCGGGGATGCGGAAATCTTTCGATCC	dFx-NNU
AACGCTAATCCCCTTTCGGGGCCGCGGAAATCTTTCGATCC	eFx-NNU
AC(M)CTAACGCCATGTACCCTTTCGGG	dFx-GGU
AC(M)CTAACGCTAATCCCCTTTCGGG	eFx-GGU
AG(M)CTAACGCCATGTACCCTTTCGGG	dFx-GCU
AG(M)CTAACGCTAATCCCCTTTCGGG	eFx-GCU
AC(M)GTAACGCCATGTACCCTTTCGGG	dFx-CGU
AC(M)GTAACGCTAATCCCCTTTCGGG	eFx-CGU
AG(M)GTAACGCCATGTACCCTTTCGGG	dFx-GGU
AG(M)GTAACGCTAATCCCCTTTCGGG	eFx-GGU
AC(M)TTAACGCCATGTACCCTTTCGGG	dFx-AGU
AC(M)TTAACGCTAATCCCCTTTCGGG	eFx-AGU
GTAATACGACTCACTATACGCGGGGTGGAGCAGCCTGGTAGCTCGTCGG	$tRNA_{CAU}^{fMet}$-NNA
GAACCGACGATCTTCGGGTTATGAGCCCGACGAGCTACCAGGCT	$tRNA_{CAU}^{fMet}$-NNA
TTGCGGGGGCCGGATTTGAACCGACGATCTTCGGG	$tRNA_{CAU}^{fMet}$-NNA
GGCGTAATACGACTCACTATAC	$tRNA_{CAU}^{fMet}$-NNA
TG(M)GTTGCGGGGGCCGGATTTG	$tRNA_{CAU}^{fMet}$-CCA
TG(M)CTTGCGGGGGCCGGATTTG	$tRNA_{CAU}^{fMet}$-GCA
TC(M)GTTGCGGGGGCCGGATTTG	$tRNA_{CAU}^{fMet}$-CGA
TC(M)CTTGCGGGGGCCGGATTTG	$tRNA_{CAU}^{fMet}$-GGA
TA(M)GTTGCGGGGGCCGGATTTG	$tRNA_{CAU}^{fMet}$-CUA
GGCGTAATACGACTCACTATAGTCCCCTTCGTCTAGA	$tRNA_{NNN}^{GluE2}$-NNA

(continued)

Table 3.3 (continued)

Sequence (5′ to 3′)	Used for
CGTCCCCTAGGGGATTCGAACCCCTGTTACCGCC	$tRNA_{NNN}^{GluE2}$-NNA
TATAGTCCCCTTCGTCTAGAGGCCCAGGACACCGCCCTCT	$tRNA_{CUU}^{GluE2}$-NNA
GAACCCCTGTTACCGCCTTAAGAGGGCGGTGTCCTGG	$tRNA_{CUU}^{GluE2}$-NNA
TATAGTCCCCTTCGTCTAGAGGCCCAGGACACCGCCCTGT	$tRNA_{GUA}^{GluE2}$-NNA
GAACCCCTGTTACCGCCTTTACAGGGCGGTGTCCTGG	$tRNA_{GUA}^{GluE2}$-NNA
TATAGTCCCCTTCGTCTAGAGGCCCAGGACACCGCCTTGT	$tRNA_{GUC}^{GluE2}$-NNA
GAACCCCTGTTACCGCCTTGACAAGGCGGTGTCCTGG	$tRNA_{GUC}^{GluE2}$-NNA
TG(M)GCGTCCCCTAGGGGATTC	$tRNA_{NNN}^{GluE2}$-CCA
TG(M)CCGTCCCCTAGGGGATTC	$tRNA_{NNN}^{GluE2}$-GCA
TC(M)GCGTCCCCTAGGGGATTC	$tRNA_{NNN}^{GluE2}$-CGA
TC(M)CCGTCCCCTAGGGGATTC	$tRNA_{NNN}^{GluE2}$-GGA
TA(M)GCGTCCCCTAGGGGATTC	$tRNA_{NNN}^{GluE2}$-CUA
TATAGGGTCGTTAGCTCAGTTGGTAGAGCAGTTGACTCTTAATC	$tRNA_{CUU}^{Lys}$-NNA
GGCGTAATACGACTCACTATAGGGTCGTTAGCTCAGTTG	$tRNA_{CUU}^{Lys}$-NNA
TTCGAACCTGCGACCAATTGATTAAGAGTCAACTGCTCTACC	$tRNA_{CUU}^{Lys}$-NNA
TGGGTCGTGCAGGATTCGAACCTGCGACCAATTGATT	$tRNA_{CUU}^{Lys}$-NNA
TG(M)GTGGGTCGTGCAGGATTCG	$tRNA_{CUU}^{Lys}$-CCA
TC(M)GTGGGTCGTGCAGGATTCG	$tRNA_{CUU}^{Lys}$-CGA
TATAGGAGCGGTAGTTCAGTCGGTTAGAATACCTGCCTGT	$tRNA_{GUC}^{Asp}$-NNA
GGCGTAATACGACTCACTATAGGAGCGGTAGTTCAGTC	$tRNA_{GUC}^{Asp}$-NNA
GAACCCGCGACCCCCTGCGTGACAGGCAGGTATTCTAACCG	$tRNA_{GUC}^{Asp}$-NNA
CGGAACGGACGGGACTCGAACCCGCGACCCCC	$tRNA_{GUC}^{Asp}$-NNA
TG(M)GCGGAACGGACGGGACT	$tRNA_{GUC}^{Asp}$-CCA
AGGTGGGGTTCCCGAGCGGCCAAAGGGAGCAGACTGTAAATCT	$tRNA_{GUA}^{Tyr}$-NNA

(continued)

Table 3.3 (continued)

Sequence (5′ to 3′)	Used for
GGCGTAATACGACTCACTATAGGTGGGGTTCCCGAG	$tRNA_{GUA}^{Tyr}$-NNA
GAACCTTCGAAGTCTGTGACGGCAGATTTACAGTCTGCTCCCT	$tRNA_{GUA}^{Tyr}$-NNA
TGGTGGGGGAAGGATTCGAACCTTCGAAGTCTGTGA	$tRNA_{GUA}^{Tyr}$-NNA
TG(M)GTGGTGGGGGAAGGATTCG	$tRNA_{GUA}^{Tyr}$-CCA
GTAATACGACTCACTATAGGCTCTGTAGTTCAGTCGGTAGAACGGCGGA	$tRNA_{NNN}^{AsnE2}$-NNA
CGGCTCTGACTGGACTCGAACCAGTGACATACGGA	$tRNA_{NNN}^{AsnE2}$-NNA
GAACCAGTGACATACGGATTAAGAGTCCGCCGTTCTACCGACT	$tRNA_{CUU}^{AsnE2}$-NNA
GAACCAGTGACATACGGATTTACAGTCCGCCGTTCTACCGACT	$tRNA_{GUA}^{AsnE2}$-NNA
GAACCAGTGACATACGGATTGACAGTCCGCCGTTCTACCGACT	$tRNA_{GUC}^{AsnE2}$-NNA
TG(M)GCGGCTCTGACTGGACTC	$tRNA_{NNN}^{AsnE2}$-CCA
TG(M)CCGGCTCTGACTGGACTC	$tRNA_{NNN}^{AsnE2}$-GCA
TC(M)GCGGCTCTGACTGGACTC	$tRNA_{NNN}^{AsnE2}$-CGA
TC(M)CCGGCTCTGACTGGACTC	$tRNA_{NNN}^{AsnE2}$-GGA
TA(M)GCGGCTCTGACTGGACTC	$tRNA_{NNN}^{AsnE2}$-CUA
ATACGACTCACTATAGGGCTTTAATAAGGAGAAAAACATG	DNA template
GGCGTAATACGACTCACTATAGGGCTTT	DNA template
GTACTTCTTGTACTTCATGTTTTTCTCCTTATTAAAGCC	DNA template (Heptapeptide-1)
GTACTTGTCGTACTTCATGTTTTTCTCCTTATTAAAGCC	DNA template (Heptapeptide-2, 3)
GTCCTTCTTGTCCTTCATGTTTTTCTCCTTATTAAAGCC	DNA template (Heptapeptide-4, 5)
CGAAGCTCACTTGTACTTCTTGTACTTCATGTTTTTC	DNA template (Heptapeptide-1)
CGAAGCTCAGTCGTACTTGTCGTACTTCATGTTTTTC	DNA template (Heptapeptide-2, 3)
CGAAGCTCACTTGTCCTTCTTGTCCTTCATGTTTTTC	DNA template (Heptapeptide-4, 5)
GGTGGGTAGTTTGACTGCGGCGGTCTCCTCCTAAAGAG	Quick change (G2251C)
CTCTTTAGGAGGAGACCGCCGCAGTCAAACTACCCACC	Quick change (G2251C)

(continued)

Table 3.3 (continued)

Sequence (5′ to 3′)	Used for
GGTGGGTAGTTTGACTGGCGCGGTCTCCTCCTAAAGAG	Quick change (G2252C)
CTCTTTAGGAGGAGACCGCGCCAGTCAAACTACCCACC	Quick change (G2252C)
GGTGGGTAGTTTGACTGCCGCGGTCTCCTCCTAAAGAG	Quick change (G2251C/G2252C)
CTCTTTAGGAGGAGACCGCGGCAGTCAAACTACCCACC	Quick change (G2251C/G2252C)
GGTGGGTAGTTTGACTGAGGCGGTCTCCTCCTAAAGAG	Quick change (G2251A)
CTCTTTAGGAGGAGACCGCCTCAGTCAAACTACCCACC	Quick change (G2251A)
GTCCCAAGGGTATGGCTCTTCGCCATTTAAAGTGGTAC	Quick change (G2553C)
GTACCACTTTAAATGGCGAAGAGCCATACCCTTGGGAC	Quick change (G2553C)
GTCCCAAGGGTATGGCTATTCGCCATTTAAAGTGGTAC	Quick change (G2553A)
GTACCACTTTAAATGGCGAATAGCCATACCCTTGGGAC	Quick change (G2553A)
TACTCTTTAGGAGGAGACCG	Primer extension (2251, 2252)
GCGTACCACTTTAAATGGCG	Primer extension (2553)
CCACCCTTTAATGTTTGATGTTC	Sequencing (2251, 2252)
CAGTCAAGCTGGCTTATGC	Sequencing (2251, 2252)
CATATCGACGGCGGTGTTTG	Sequencing (2553)
GGCAGATAGGGACCGAAC	Sequencing (2553)

Table 3.4 RNAs prepared in this chapter

Name	Sequence (5′ to 3′)
eFx-NNU	*GGAUCGAAAGAUUUCCGCGGCCCCGAAAGGGGAUUAGCGUUANNU*
dFx-NNU	*GGAUCGAAAGAUUUCCGCAUCCCCGAAAGGGUACAUGGCGUUANNU*
$tRNA_{CAU}^{fMet}$-NNA	*CGCGGGGUGGAGCAGCCUGGUAGCUCGUCGGGCUCAUAACCCGAAGAUCGUCGGUUCAAAUCCGGCCCCCGCAANNA*
$tRNA_{CUU}^{EnAsn}$-NNA	*GGCUCUGUAGUUCAGUCGGUAGAACGGCGGACUCUUAAUCCGUAUGUCACUGGUUCGAGUCCAGUCAGAGCCGNNA*
$tRNA_{GUA}^{EnAsn}$-NNA	*GGCUCUGUAGUUCAGUCGGUAGAACGGCGGACUGUAAAUCCGUAUGUCACUGGUUCGAGUCCAGUCAGAGCCGNNA*
$tRNA_{GUC}^{EnAsn}$-NNA	*GGCUCUGUAGUUCAGUCGGUAGAACGGCGGAUUGUCAAUCCGUAUGUCACUGGUUCGAGUCCAGUCAGAGCCGNNA*
$tRNA_{CUU}^{EnGlu}$-NNA	*GUCCCCUUCGUCUAGAGGCCCAGGACACCGCCCUCUUAAGGCGGUAACAGGGGUUCGAAUCCCCUAGGGGACGNNA*
$tRNA_{GUA}^{EnGlu}$-NNA	*GUCCCCUUCGUCUAGAGGCCCAGGACACCGCCCUGUAAAGGCGGUAACAGGGGUUCGAAUCCCCUAGGGGACGNNA*
$tRNA_{GUC}^{EnGlu}$-NNA	*GUCCCCUUCGUCUAGAGGCCCAGGACACCGCCUUGACAAGGCGGUAACAGGGGUUCGAAUCCCCUAGGGGACGNNA*
$tRNA_{CUU}^{Lys}$-NNA	*GGGUCGUUAGCUCAGUUGGUAGAGCAGUUGACUCUUAAUCAAUUGGUCGCAGGUUCGAAUCCUGCACGACCCANNA*
$tRNA_{GUA}^{Tyr}$-NNA	*GGUGGGGUUCCCGAGCGGCCAAAGGGAGCAGACUGUAAAUCUGCCGUCACAGACUUCGAAGGUUCGAAUCCUUCCC CCACCANNA*
$tRNA_{GUC}^{Asp}$-NNA	*GGAGCGGUAGUUCAGUCGGUUAGAAUACCUGCCUGUCACGCAGGGGGUCGCGGGUUCGAGUCCCGUCCGUUC CGNNA*

N means A/U/G/C, italic types indicate ribonucleotides

of the same medium. The culture was grown to an OD_{600} of 0.7 at 37 °C. The expression of MBP-MS2-His_6 was induced using 1 mM isopropyl β-D-1-thiogalactopyranoside, and the cells were cultured for another 4 h at 37 °C. The culture was then centrifuged for 10 min at 4000× *g*, the pelleted cells were resuspended in 30 mL of lysis buffer (50 mM NaH_2PO_4, 300 mM NaCl, 10 mM imidazole, 6 mM β-mercaptoethanol (β-ME), 1 mM phenylmethanesulfonyl fluoride, adjusted to pH 8.0 with NaOH), and were then sonicated. The lysate was clarified twice by centrifugation for 20 min at 15,000× *g* (4 °C) and filtered through a Millex-LH 0.45 μm filter unit (Merck Millipore). MBP-MS2-His_6 was purified using a fast protein liquid chromatography (FPLC) system (AKTA Avant, GE Healthcare) with a His-Trap HP column (GE Healthcare). The column was washed with NiNTA buffer (50 mM NaH_2PO_4, 300 mM NaCl, 10 mM imidazole, 6 mM β-ME, adjusted to pH 8.0 with NaOH) and the protein was eluted with NiNTA buffer containing 250 mM imidazole. Protein-containing fractions were pooled and concentrated using a membrane filter (Amicon Ultra15, 3000 MWCO, Merck Millipore). The concentrated protein was dialyzed against 20 mM Tris-HCl, pH 7.5, 150 mM NaCl, 20% glycerol, and 1 mM dithiothreitol (DTT). The protein concentration was determined by absorbance at 280 nm, assuming an extinction coefficient of 84,800 cm^{-1} M^{-1} (calculated on: http://web.expasy.org/protparam/).

Expression and purification of tagged ribosomes

The plasmid pcI^{857} (Kan^R) encoding a temperature-sensitive mutant of the lambda repressor protein cI (a gift from R. Green, Johns Hopkins University) (Youngman and Green 2005) was used to transform *E. coli* DH5α in LB medium containing 50 μg/mL kanamycin. Any 23S rRNA mutation of interest was introduced into the plasmid p278 MS2 encoding 23S rRNA tagged with the MS2 stem-loop (a gift from R. Green, Johns Hopkins University) by site directed mutagenesis using the Quickchange Lightning Site-Directed Mutagenesis kit (Agilent Technologies). The primers for mutagenesis are shown in Table 3.3. The mutations were confirmed by sequencing. The mutated plasmid p278 MS2 was used to transform DH5α with pcI^{857} in LB medium containing 100 μg/mL ampicillin and 50 μg/mL kanamycin. A colony isolated by streaking was used to inoculate a 50 mL overnight culture grown in LB supplemented with 100 μg/mL ampicillin and 50 μg/mL kanamycin at 30 °C. One liter of this medium was inoculated with 20 mL of an overnight culture and grown to an OD_{600} of 0.7–0.9 at 42 °C. The cultures were centrifuged for 10 min at 4000× *g* and the pelleted cells were resuspended in 5.5 mL ribosome buffer A (20 mM Tris-HCl, pH 7.5, 100 mM NH_4Cl, 10 mM $MgCl_2$, 0.5 mM EDTA, and 6 mM β-ME). Lysozyme (Nacalai Tesque Inc.) was added (final concentration, 0.1 mg/mL) and incubated at 4 °C for 30 min. This solution was disrupted twice using a cell disruption vessel (Parr Instrument Company). The lysate was clarified twice by centrifugation for 15 min at 15,000× *g* (4 °C), layered onto 10 mL of ribosome buffer D (20 mM Tris-HCl, pH 7.5, 500 mM NH_4Cl, 10 mM $MgCl_2$, 0.5 mM EDTA, 1.1 M sucrose) in a 25PC tube (Hitachi), and centrifuged at 104,000× *g* in an S50A rotor (Hitachi) for 18–20 h at 4 °C.

Ribosome buffer A was used to rinse and then dissolve the pellet, which was then stored at −80 °C.

Tagged ribosomes were purified using FPLC (AKTA Avant, GE Healthcare). First, 2 mg MBP-MS2-His_6 was loaded on an MBP Trap HP column (GE Healthcare), and the bound protein was washed with ribosome binding buffer (20 mM Tris-HCl, pH 7.5, 100 mM NH_4Cl, and 10 mM $MgCl_2$). Crude ribosomes were loaded onto the column and washed with 25 mL of ribosome-binding buffer. Tagged ribosomes bound to MBP-MS2-His_6 were eluted with 20 mL of ribosome-elution buffer (20 mM Tris-HCl, pH 7.5, 100 mM NH_4Cl, 10 mM $MgCl_2$, and 10 mM maltose). Purified tagged ribosomes were concentrated to 10–20 μM, and the buffer was exchanged with RE buffer (20 mM HEPES-KOH, pH 7.6, 10 mM $MgCl_2$, 50 mM KCl, 1 mM DTT) using membrane filtration (Amicon Ultra15, 100,000 MWCO, Merck Millipore). The concentration of 70S ribosomes was determined by absorbance at 260 nm using the conversion factor 1 A_{260} = 23 pmol.

Aminoacylation by flexizymes

Aminoacylation reactions of Tyr-CME, Asp-DBE, Lys-DBE, Aly-DBE, and Anv-DBE were performed as previously described (Murakami et al. 2006). The reaction times were changed to 30 min (Tyr-CME), 9 h (Asp-DBE), and 3 h (Lys-DBE, Aly-DBE and Anv-DBE). Aminoacylation of Fph-CME was performed as follows: A mixture of 3 μL of 41.7 μM $tRNA_{CAU}^{fMet}$ and 41.7 μM eFx in 83.3 mM HEPES-KOH (pH 7.5) was heated at 95 °C for 2 min and cooled to room temperature over 5 min. One microliter of 3 M $MgCl_2$ was added, and the mixture was transferred to an ice bath, 1 μL of 5 mM Fph-CME was added, and the mixture was incubated on ice for 16 h. After the reaction, aminoacyl-tRNA (aa-tRNA) was precipitated with ethanol as previously described (Murakami et al. 2006).

Analysis of acylation

Ethanol-precipitated aa-tRNA was dissolved in acid-PAGE loading buffer (150 mM NaOAc, pH 5.2, 10 mM EDTA, and 93% (v/v) formamide) and then loaded on acid-urea 12% polyacrylamide gels (8 M urea, 50 mM NaOAc, pH 5.2). Electrophoresis was performed using 300 V (approximately 10 V cm^{-1}) for 21 h. The gels were stained with ethidium bromide and analyzed using an FLA-5100 fluorescent image analyzer (Fujifilm) or PharosFX molecular imager (BIO-RAD). Aminoacylation efficiency was calculated according to the band intensity of aa-tRNA (A) and free tRNA (T) and is presented as (A)/[(A) + (T)]. Because of the fluorescence of Fph-tRNA, the efficiency for Fph-CME was calculated using the expression $1 - [(T_{aa+})(F_{aa-})]/[(T_{aa-})(F_{aa+})]$ according to the band intensity of flexizyme in the lane without amino acids (F_{aa-}), flexizyme in the lane with amino acids (F_{aa+}), free tRNA in the lane without amino acids (T_{aa-}), and free tRNA in the lane with amino acids (T_{aa+}). Values reported are the average of three independent reactions, and error bars represent the standard deviation.

DNA templates for translation

The DNA templates for translation were prepared using the polymerase chain reaction (PCR), and the amplicons were extracted with phenol-chloroform mixture and precipitated with ethanol. The DNA templates were purified using 12% native-PAGE, and the concentrations were determined by absorbance at 260 nm. The primers for preparing DNA templates for translation are shown in Table 3.3.

In vitro translation using the FIT system

The FIT system comprised a mixture of all desired components for translation (Goto et al. 2011). The tagged-ribosomes and aa-tRNAs were added as necessary in each experiment. The composition of the FIT system was as follows: 50 mM HEPES-KOH (pH 7.6), 12 mM magnesium acetate, 100 mM potassium acetate, 2 mM spermidine, 20 mM creatine phosphate, 2 mM DTT, 2 mM ATP, 2 mM GTP, 1 mM CTP, 1 mM UTP, 0.6 μM MTF, 2.7 μM IF1, 0.4 μM IF2, 1.5 μM IF3, 0.26 μM EF-G, 10 μM EF-Tu, 10 μM EF-Ts, 0.25 μM RF1, 0.25 μM RF2, 0.17 μM RF3, 0.5 μM RRF, 0.1 μM T7 RNA polymerase, 4 μg/mL creatine kinase, 3 μg/mL myokinase, 0.1 μM pyrophosphatase, 0.1 μM nucleotide-diphosphatase kinase, and 400 nM DNA template. The concentration of EF-Tu and EF-Ts only in the experiment shown in Fig. 3.19 was increased to 20 μM. Translation reactions were started by adding aa-tRNAs at 37 °C after a 5 min incubation. Translation reactions were terminated by adding an equal volume of 2×Tricine-SDS-PAGE loading buffer (900 mM Tris-HCl (pH 8.45), 8% (w/v) SDS, 30% (v/v) glycerol).

In the experiment shown in Figs. 3.13 and 3.16, the concentration of ribosomes, Fph-$tRNA_{CAU}^{fMet}$, Lys-$tRNA_{CUU}^{GluE2}$, and Tyr-$tRNA_{GUA}^{GluE2}$ were 2 μM, 5 μM, 20 μM, 10 μM, respectively. The sequence of the DNA template was 5′-GGCGT AATAC GACTC ACTAT AGGGC TTTAA TAAGG AGAAA AACAT GAAGT ACAAG AAGTA CAAGT GAGCT TCG-3′.

In the experiment shown in Figs. 3.18 and 3.19, the concentration of the wild-type ribosomes, G2251C/G2553C ribosomes, Fph-$tRNA_{CAU}^{fMet}$-CCA, Fph-$tRNA_{CAU}^{fMet}$-CGA, Lys-$tRNA_{CUU}^{Lys}$-CCA, Lys-$tRNA_{CUU}^{Lys}$-CGA, Asp-$tRNA_{GUC}^{Asp}$-CCA, Aly-$tRNA_{GUC}^{GluE2}$-CGA, Tyr-$tRNA_{GUA}^{Tyr}$-CCA, and Anv-$tRNA_{GUA}^{GluE2}$-CGA were 0.1, 2, 5, 1.5, 10, 3, 10, 3, 10 and 3 μM, respectively. The sequence of the DNA template was 5′-GGCGT AATAC GACTC ACTAT AGGGC TTTAA TAAGG AGAAA AACAT GAAGT ACGAC AAGTA CGACT GAGCT TCG-3′.

In the experiment shown in Fig. 3.12, the concentration of wild-type ribosomes, Fph-$tRNA_{CAU}^{fMet}$, Lys-$tRNA_{CUU}^{AsnE2}$, and Tyr-$tRNA_{GUA}^{AsnE2}$ were 2, 5, 20, 10 μM, respectively. The sequence of the DNA template was 5′-GGCGT AATAC GACTC ACTAT AGGGC TTTAA TAAGG AGAAA AACAT GAAGT ACAAG AAGTA CAAGT GAGCT TCG-3′.

In the experiment shown in Fig. 3.20, the concentration of the wild-type ribosomes, G2251C/G2553C ribosomes, Fph-$tRNA_{CAU}^{fMet}$-CCA, Fph-$tRNA_{CAU}^{fMet}$-CGA, Lys-$tRNA_{CUU}^{Lys}$-CCA, Lys-$tRNA_{CUU}^{Lys}$-CGA, Asp-$tRNA_{GUC}^{Asp}$-CCA, and Aly-$tRNA_{GUC}^{GluE2}$-CGA were 0.3, 2, 5, 1.5, 20, 6, 10, 3 μM, respectively.

The sequence of the DNA template was 5′-GGCGT AATAC GACTC ACTAT AGGGC TTTAA TAAGG AGAAA AACAT GAAGG ACAAG AAGGA CAAGT GAGCT TCG-3′.

In the experiment shown in Fig. 3.21, the concentration of the wild-type ribosomes, G2251C/G2553C ribosomes, Fph-$tRNA_{CAU}^{fMet}$-CCA, Fph-$tRNA_{CAU}^{fMet}$-CGA, Lys-$tRNA_{CUU}^{Lys}$-CCA, Lys-$tRNA_{CUU}^{Lys}$-CGA, Tyr-$tRNA_{GUA}^{Tyr}$-CCA, and Anv-$tRNA_{GUA}^{AsnE2}$-CGA were 0.3, 2, 5, 1.5, 20, 6, 10, 3 μM, respectively. The sequence of the DNA template was 5′-GGCGT AATAC GACTC ACTAT AGGGC TTTAA TAAGG AGAAA AACAT GAAGT ACAAG AAGTA CAAGT GAGCT TCG-3′.

The aa-tRNAs were prepared by aminoacylation of tRNAs using cognate flexizymes. The concentration of aa-tRNA was calculated from acylation efficiency shown in Fig. 3.9.

MALDI-TOF analysis

After incubation, the in vitro translation mixtures were desalted using a *C*18-tip (Nikkyo Technos) and analyzed using MALDI-TOF mass in linear positive modes. All MALDI-TOF analysis was performed using an Autoflex II (Bruker Daltonics) or ultrafleXtreme (Bruker Daltonics) with external calibration (Peptide Calibration Standard II, Bruker Daltonics).

Tricine-SDS-PAGE analysis of translation products

The quantity of Fph incorporated into peptides was determined using Tricine-SDS-PAGE as previously described (Goto et al. 2011). The concentration of acrylamide in separation gel was 12% for the experiment shown in Figs. 3.12, 3.13and 3.16, 19% for Fig. 3.18 and 20% for Fig. 3.20. The fluorescence of the peptides was determined using the FLA-5100 (Fujifilim) or PharosFX molecular imager (BIO-RAD), and the data were fit to an exponential curve using KaleidaGraph (Synergy Software). The amounts of peptides were quantified according to that of a fluorescent band generated by a known concentration (0–4 μM) of Fph. Values reported are the average of three independent reactions, and error bars represent the standard deviation.

Quantification of the abundance of tagged ribosome by primer extension

Primer extension analysis was performed mainly following the previous report (Youngman and Green 2005). Primer extension using a primer that is complementary to the bases 2254-2273 in 23S rRNA produced a dideoxyguanosine stop at +2 for tagged G2252C, +3 for tagged G2251C, or +6 for untagged wild-type ribosomes, or a dideoxythymidine stop at +3 for tagged G2251A or +7 for untagged wild-type ribosomes. Primer extension using a primer that is complementary to the bases 2556-2575 in 23S rRNA produced a dideoxyguanosine stop at +3 for tagged G2553C or +5 for untagged wild-type ribosomes, or a dideoxythymidine stop at +3 for tagged G2553A or +9 for untagged wild-type ribosomes. Ribosomal RNAs were extracted from purified ribosomes by phenol-chloroform extraction and ethanol precipitation. Primer extension was carried out as follows: A mixture of

7 μL of 57.1 nM rRNA, 171.4 nM [^{32}P] 5′-end labeled primer, 7.14 mM each dATP/dCTP/dTTP/ddGTP or dATP/dGTP/dCTP/ddTTP was heated at 65 °C for 5 min and cooled on ice 1 min. Two microliter of 5× FS buffer (Thermo Fisher Scientific Inc.), 0.5 μL of 0.1 M DTT and 0.5 μL of SuperScript™ III (Thermo Fisher Scientific Inc.) were added, and the mixture were incubated at 55 °C for 1 h. Primer extension products were resolved on a 15% denaturing polyacrylamide gel (8M urea, 1×TBE) and the intensities of the bands were quantified using FLA-5100 (Fujifilim).

Gel-shift analysis of ternary complex of EF-Tu, GTP and aa-tRNA

Binding of EF-Tu to aa-tRNAs was investigated by following previous report (Doi et al. 2007). First, 10 μM EF-Tu was preincubated with 1 mM GTP at 37 °C for 15 min in 5 μL total volume containing 70 mM HEPES-KOH (pH 7.6), 52 mM NH_4OAc, 8 mM $Mg(OAc)_2$, 30 mM KCl, 0.8 mM DTT, 1.6 μM GDP, 6% glycerol, 10 mM phosphoenolpyruvate, and 0.08 U/μL pyruvate kinase. After aminoacylation reaction by flexizyme, the ethanol precipitated mixtures which contain flexizymes, aa-tRNAs and tRNAs were resuspended in 6 mM KOAc at 8.3 μM final concentration of aa-tRNA. The concentrations of aa-tRNAs were calculated from acylaton efficiency shown in Fig. 3.9. This 3 μL aa-tRNA solution and 2 μL of ternary complex buffer, containing 150 mM HEPES-KOH (pH 7.6), 195 mM NH_4OAc, and 30 mM $Mg(OAc)_2$ were added to the preincubated EF-Tu solution. The mixture was incubated at 37 °C for 10 min. Native-PAGE was performed using 8% polyacrylamide gels at 4 °C in a running buffer containing 50 mM Tris-HCl (pH 6.8), 65 mM NH_4OAc, and 10 mM $Mg(OAc)_2$. Gels were stained by SimplyBlue™ SafeStain (Thermo Fisher Scientific Inc.). Intensities of bands were analyzed by Multi Gauge (Fujifilim).

References

Bashan A, Agmon I, Zarivach R, Schluenzen F, Harms J, Berisio R, Bartels H, Franceschi F, Auerbach T, Hansen HA, Kossoy E, Kessler M, Yonath A (2003) Structural basis of the ribosomal machinery for peptide bond formation, translocation, and nascent chain progression. Mol Cell 11(1):91–102. doi:10.1016/S1097-2765(03)00009-1

Cavarelli J, Moras D (1993) Recognition of tRNAs by aminoacyl-tRNA synthetases. FASEB J 7 (1):79–86

Cornish PV, Ermolenko DN, Noller HF, Ha T (2008) Spontaneous intersubunit rotation in single ribosomes. Mol Cell 30(5):578–588. doi:10.1016/j.molcel.2008.05.004

Doi Y, Ohtsuki T, Shimizu Y, Ueda T, Sisido M (2007) Elongation factor Tu mutants expand amino acid tolerance of protein biosynthesis system. J Am Chem Soc 129(46):14458–14462. doi:10.1021/ja075557u

Dorner S, Brunelle J, Sharma D, Green R (2006) The hybrid state of tRNA binding is an authentic translation elongation intermediate. Nat Struct Mol Biol 13(3):234–241. doi:10.1038/nsmb1060

Forster A, Tan Z, Nalam M, Lin H, Qu H, Cornish V, Blacklow S (2003) Programming peptidomimetic syntheses by translating genetic codes designed de novo. Proc Natl Acad Sci USA 100(11):6353–6357. doi:10.1073/pnas.1132122100

Goto Y, Katoh T, Suga H (2011) Flexizymes for genetic code reprogramming. Nat Protoc 6(6):779–790. doi:10.1038/nprot.2011.331

Goto Y, Murakami H, Suga H (2008) Initiating translation with D-amino acids. RNA 14(7): 1390–1398. doi:10.1261/rna.1020708

Green R, Switzer C, Noller HF (1998) Ribosome-catalyzed peptide-bond formation with an A-site substrate covalently linked to 23S ribosomal RNA. Science 280(5361):286–289. doi:10.1126/science.280.5361.286

Kang T, Suga H (2011) Translation of a histone H3 tail as a model system for studying peptidyl-tRNA drop-off. FEBS Lett 585(14):2269–2274. doi:10.1016/j.febslet.2011.05.051

Kao C, Zheng M, Rüdisser S (1999) A simple and efficient method to reduce nontemplated nucleotide addition at the 3′ terminus of RNAs transcribed by T7 RNA polymerase. RNA 5(9):1268–1272. doi:10.1017/S1355838299991033

Kawakami T, Murakami H, Suga H (2008) Messenger RNA-programmed incorporation of multiple N-methyl-amino acids into linear and cyclic peptides. Chem Biol 15(1):32–42. doi:10.1016/j.chembiol.2007.12.008

Kawakami T, Ohta A, Ohuchi M, Ashigai H, Murakami H, Suga H (2009) Diverse backbone-cyclized peptides via codon reprogramming. Nat Chem Biol 5(12):888–890. doi:10.1038/nchembio.259

Kim DF, Green R (1999) Base-pairing between 23S rRNA and tRNA in the ribosomal A site. Mol Cell 4(5):859–864. doi:10.1016/S1097-2765(00)80395-0

Lescoute A, Westhof E (2006) The interaction networks of structured RNAs. Nucleic Acids Res 34(22):6587–6604. doi:10.1093/nar/gkl963

Liu CC, Schultz PG (2010) Adding new chemistries to the genetic code. Annu Rev Biochem 79:413–444. doi:10.1146/annurev.biochem.052308.105824

Liu J, Liu M, Horowitz J (1998) Recognition of the universally conserved 3′-CCA end of tRNA by elongation factor EF-Tu. RNA 4(6):639–646. doi:10.1017/S1355838298980013

Liu M, Horowitz J (1994) Functional transfer RNAs with modifications in the 3′-CCA end: differential effects on aminoacylation and polypeptide synthesis. Proc Natl Acad Sci U S A 91 (22):10389–10393. doi:10.2307/2366033

Machnicka MA, Milanowska K, Osman Oglou O, Purta E, Kurkowska M, Olchowik A, Januszewski W, Kalinowski S, Dunin-Horkawicz S, Rother KM, Helm M, Bujnicki JM, Grosjean H (2013) MODOMICS: a database of RNA modification pathways—2013 update. Nucleic Acids Res 41(Database issue):D262–267. doi:10.1093/nar/gks1007

Magliery TJ, Anderson JC, Schultz PG (2001) Expanding the genetic code: Selection of efficient suppressors of four-base codons and identification of “shifty” four-base codons with a library approach in Escherichia coli. J Mol Biol 307(3):755–769. doi:10.1006/jmbi.2001.4518

Moazed D, Noller HF (1989) Intermediate states in the movement of transfer-RNA in the ribosome. Nature 342(6246):142–148. doi:10.1038/342142a0

Moazed D, Noller HF (1991) Sites of interaction of the CCA end of peptidyl-tRNA with 23S rRNA. Proc Natl Acad Sci USA 88(9):3725–3728. doi:10.1073/pnas.88.9.3725

Mukai T, Kobayashi T, Hino N, Yanagisawa T, Sakamoto K, Yokoyama S (2008) Adding L-lysine derivatives to the genetic code of mammalian cells with engineered pyrrolysyl-tRNA synthetases. Biochem Biophys Res Commun 371(4):818–822. doi:10.1016/j.bbrc.2008.04.164

Murakami H, Ohta A, Ashigai H, Suga H (2006) A highly flexible tRNA acylation method for non-natural polypeptide synthesis. Nat Methods 3(5):357–359. doi:10.1038/nmeth877

Neumann H, Peak-Chew SY, Chin JW (2008) Genetically encoding N(ε)-acetyllysine in recombinant proteins. Nat Chem Biol 4(4):232–234. doi:10.1038/nchembio.73

Neumann H, Wang K, Davis L, Garcia-Alai M, Chin JW (2010) Encoding multiple unnatural amino acids via evolution of a quadruplet-decoding ribosome. Nature 464(7287):441–444. doi:10.1038/nature08817

Nissen P, Hansen J, Ban N, Moore PB, Steitz TA (2000) The structural basis of ribosome activity in peptide bond synthesis. Science 289(5481):920–930. doi:10.1126/science.289.5481.920

Polikanov YS, Steitz TA, Innis CA (2014) A proton wire to couple aminoacyl-tRNA accommodation and peptide-bond formation on the ribosome. Nat Struct Mol Biol 21(9): 787–793. doi:10.1038/Nsmb.2871

Polycarpo CR, Herring S, Berube A, Wood JL, Soll D, Ambrogelly A (2006) Pyrrolysine analogues as substrates for pyrrolysyl-tRNA synthetase. FEBS Lett 580(28–29):6695–6700. doi:10.1016/j.febslet.2006.11.028

Rackham O, Chin JW (2005) A network of orthogonal ribosome • mRNA pairs. Nat Chem Biol 1 (3):159–166. doi:10.1038/Nchembio719

Ruff M, Krishnaswamy S, Boeglin M, Poterszman A, Mitschler A, Podjarny A, Rees B, Thierry JC, Moras D (1991) Class II aminoacyl transfer RNA synthetases: crystal structure of yeast aspartyl-tRNA synthetase complexed with tRNA(Asp). Science 252(5013):1682–1689. doi:10.1126/science.2047877

Saito H, Kourouklis D, Suga H (2001a) An in vitro evolved precursor tRNA with aminoacylation activity. EMBO J 20(7):1797–1806. doi:10.1093/emboj/20.7.1797

Saito H, Watanabe K, Suga H (2001b) Concurrent molecular recognition of the amino acid and tRNA by a ribozyme. RNA 7(12):1867–1878

Sako Y, Morimoto J, Murakami H, Suga H (2008) Ribosomal synthesis of bicyclic peptides via two orthogonal inter-side-chain reactions. J Am Chem Soc 130(23):7232–7234. doi:10.1021/ja800953c

Samaha RR, Green R, Noller HF (1995) A base pair between tRNA and 23S rRNA in the peptidyl transferase centre of the ribosome. Nature 377(6547):309–314. doi:10.1038/377309a0

Schmeing TM, Ramakrishnan V (2009) What recent ribosome structures have revealed about the mechanism of translation. Nature 461(7268):1234–1242. doi:10.1038/Nature08403

Schmeing TM, Voorhees RM, Kelley AC, Gao YG, Murphy FV, Weir JR, Ramakrishnan V (2009) The crystal structure of the ribosome bound to EF-Tu and aminoacyl-tRNA. Science 326(5953):688–694. doi:10.1126/science.1179700

Schulman LH, Pelka H (1977) Structural requirements for aminoacylation of *Escherichia coli* formylmethionine transfer RNA. Biochemistry 16(19):4256–4265. doi:10.1021/bi00638a020

Shimizu Y, Inoue A, Tomari Y, Suzuki T, Yokogawa T, Nishikawa K, Ueda T (2001) Cell-free translation reconstituted with purified components. Nat Biotechnol 19(8):751–755. doi:10.1038/90802

Spiegel PC, Ermolenko DN, Noller HF (2007) Elongation factor G stabilizes the hybrid-state conformation of the 70S ribosome. RNA 13(9):1473–1482. doi:10.1261/Rna.601507

Steitz TA (2008) A structural understanding of the dynamic ribosome machine. Nat Rev Mol Cell Biol 9(3):242–253. doi:10.1038/nrm2352

Terasaka N, Hayashi G, Katoh T, Suga H (2014) An orthogonal ribosome-tRNA pair via engineering of the peptidyl transferase center. Nat Chem Biol 10(7):555–557. doi:10.1038/nchembio.1549

Voorhees R, Weixlbaumer A, Loakes D, Kelley A, Ramakrishnan V (2009) Insights into substrate stabilization from snapshots of the peptidyl transferase center of the intact 70S ribosome. Nat Struct Mol Biol 16(5):528–533. doi:10.1038/nsmb.1577

Wang KH, Neumann H, Peak-Chew SY, Chin JW (2007) Evolved orthogonal ribosomes enhance the efficiency of synthetic genetic code expansion. Nat Biotechnol 25(7):770–777. doi:10.1038/Nbt1314

Wang KH, Sachdeva A, Cox DJ, Wilf NW, Lang K, Wallace S, Mehl RA, Chin JW (2014) Optimized orthogonal translation of unnatural amino acids enables spontaneous protein double-labelling and FRET. Nat Chem 6(5):393–403. doi:10.1038/Nchem.1919

Wang L, Brock A, Herberich B, Schultz PG (2001) Expanding the genetic code of *Escherichia coli*. Science 292(5516):498–500. doi:10.1126/science.1060077

Yamagishi Y, Shoji I, Miyagawa S, Kawakami T, Katoh T, Goto Y, Suga H (2011) Natural product-like macrocyclic N-methyl-peptide inhibitors against a ubiquitin ligase uncovered from a ribosome-expressed de novo library. Chem Biol 18(12):1562–1570. doi:10.1016/j.chembiol.2011.09.013

Yanagisawa T, Ishii R, Fukunaga R, Kobayashi T, Sakamoto K, Yokoyama S (2008) Multistep engineering of pyrrolysyl-tRNA synthetase to genetically encode N(ε)-(o-azidobenzyloxy carbonyl) lysine for site-specific protein modification. Chem Biol 15(11):1187–1197. doi:10.1016/j.chembiol.2008.10.004

Youngman EM, Green R (2005) Affinity purification of in vivo-assembled ribosomes for in vitro biochemical analysis. Methods 36(3):305–312. doi:10.1016/j.ymeth.2005.04.007

Zhang JW, Ferre-D'Amare AR (2014) Direct evaluation of tRNA aminoacylation status by the T-box riboswitch using tRNA-mRNA stacking and steric readout. Mol Cell 55(1):148–155. doi:10.1016/j.molcel.2014.05.017

Zhou XL, Du DH, Tan M, Lei HY, Ruan LL, Eriani G, Wang ED (2011) Role of tRNA amino acid-accepting end in aminoacylation and its quality control. Nucleic Acids Res 39(20): 8857–8868. doi:10.1093/nar/gkr595

Chapter 4
General Conclusion

Abstract In natural, each ARS specifically recognizes each tRNA and amino acid, and tRNAs are specifically aminoacylated with cognate amino acids by cognate ARSs. On the other hand, flexizymes, which are in vitro selected aminoacylation ribozymes, enable to aminoacylate RNAs bearing various 3′-ends with various amino acids including both canonical and noncanonical amino acids. By utilizing these unique characteristics, novel interaction between folic acid and hsa-pre-miR-125a was discovered (Chap. 2), and an orthogonal ribosome–tRNA pair was developed by engineering of peptidyl transferase center (Chap. 3). Aminoacylation at 3′-end of RNA with various amino acids by flexizymes has a great potential to be applied for various RNA studies including analysis of translation mechanisms, engineering of translation, discoveries of novel small ncRNAs.

Keywords Ribozyme · MicroRNA · SELEX · tRNA · Ribosome · Translation

4.1 General Conclusion

In natural, each ARS specifically recognizes each tRNA and amino acid, and tRNAs are specifically aminoacylated with cognate amino acids by cognate ARSs. This rigorously defined correspondence of tRNAs to amino acids defines genetic code, which is essential for accurate translation of mRNAs to proteins in living organism. However, this specific aminoacylation reaction is not favored in the case of application of aminoacylation to other studies or engineering of translation machinery, because it is difficult to arbitrarily aminoacylate RNAs with various amino acids. Flexizymes are in vitro selected aminoacylation ribozymes which have two unique characteristic: (i) using various substrates including both natural amino acids and ncAAs. (ii) recognizing substrate RNA via two consecutive base pairs, which can be substituted with other base pairs (Terasaka et al. 2014). These

N. Terasaka, *Applications of Aminoacylation Ribozymes That Recognize the 3′-end of tRNA*, Springer Theses, DOI 10.1007/978-4-431-56517-8_4

characteristics enable to flexibly aminoacylate RNAs bearing various 3′-ends with various amino acids including both canonical and noncanonical amino acids.

In the study described in Chap. 2, novel interaction between folic acid and hsa-pre-miR-125a was discovered using small RNA transcriptomic SELEX which is in vitro selection integrated with flexizymes. This is the first example of interaction between metabolite and microRNA precursors, which suggests that more RNA aptamer elements exist in microRNA precursors. The same procedure will be usable to discover other small RNAs interacting with small molecules. MicroRNAs have been extensively studied as therapeutic targets and some small molecule inhibitors have been developed targeting microRNA precursors (Bose et al. 2012; Velagapudi et al. 2014). Because miR-125a-5p is antioncogene, folic acid has a potential as a small molecule drug which binds to miR-125a precursors and regulates the processing of miR-125a. In addition, folic acid derivatives will be also drug candidates targeting miR-125a precursors. Recently, macrocyclic peptides armed with a mechanism-based warhead inhibiting human deacetylase SIRT2 was developed (Morimoto et al. 2012). If folic acid moiety could be incorporated into peptide as warhead, it is possible to develop peptide drug targeting miR-125a precursors. As described above, the discovery of new interaction between miRNAs and metabolite has not only scientific importance but also essential information to develop drugs targeting miRNAs.

Flexizymes specifically aminoacylated tRNAs in many small RNAs. This result demonstrated that aminoacylation by flexizymes is usable technology to easily label and deplete endogenous tRNAs with much abundance, and to discover new small ncRNAs whose length is similar to tRNAs. In addition, this technology can be used for tRNAs of any species even if the sequences were unknown because flexizymes only recognizes CCA-3′ end which is universally conserved in all organisms.

On the other hand, this methodology can be applied not only for depleting but also for recovering specific RNAs. Recently several small ncRNAs bearing CCA-3′ end such as mascRNA (Wilusz et al. 2008), MEN β tRNA-like small RNA (Sunwoo et al. 2009), and Y RNA (Chen et al. 2014) are discovered, which are produced by cleavage by RNaseP and CCA addition by CCA-adding enzyme. It has been suggested that CCA addition is related to stability of RNAs (Wilusz et al. 2011). Labeling CCA-3′ end of RNAs by flexizymes can be applied to discover such RNAs bearing CCA-3′ end.

In the study described in Chap. 3, compensatory-mutated flexizymes aminoacylated tRNAs bearing mutation at the 3′-end. In addition to C74N/C75N mutants, A76N mutant tRNA also can be aminoacylated by prototype of flexizymes “pre-24” (Saito et al. 2001a, b), which suggests also that compensatory mutated flexizymes (eFx, dFx, and aFx) can aminoacylate A76N mutant tRNAs. These results indicate that wild-type and compensatory mutated flexizymes have great potential to charge various amino acids onto any tRNAs bearing NNN-3′ end. Therefore, A76 of tRNA is also candidate to be mutated for engineering of peptidyl transferase center to

develop more orthogonal translation machinery. However, further engineering of ribosome and translation factors will be necessary because A76 residue is important for formation of aa-tRNA•EF-Tu•GTP ternary complex (Liu et al. 1998) and translocation of peptidyl-tRNA from A-site to P-site (Virumae et al. 2002).

In the study in Chap. 3, only in vitro translation activity and orthogonality was demonstrated. If this orthogonal translation machinery will work in vivo, it will be possible that engineered proteins containing ncAAs are expressed without affecting the endogenous translation machinery. In order to achieve this, there are many problems to be solved. First is the low efficiency of translation by orthogonal ribosome and tRNA pair. In this study, short seven polypeptide was expressed but it is necessary to increase translation efficiency in order to produce full-length protein. Second is the misincorporation of aa-tRNAs into noncognate ribosomes. In the case of FIT system, the amount of translation components including ARS, factors, amino acids, tRNAs, and ribosomes can be optimized. However, it is very difficult to express the appropriate amount of translation components in vivo to avoid the misincorporation. Further engineering of translation components as described above will be necessary to solve these problems. Finally, it is necessary that orthogonal ribosome–tRNA pair translates the specific mRNA encoding target protein in order not to affect the endogenous translation of other proteins. To achieve this, we need to construct orthogonal ribosome–tRNA–mRNA system. Orthogonal ribosome–mRNA pair was already reported, but anti-SD sequence of 16S rRNA was engineered in the study (Neumann et al. 2010; Rackham and Chin 2005; Wang et al. 2007). Therefore, an orthogonal 50S–30S pair is necessary to construct orthogonal ribosome–tRNA–mRNA system. To avoid constructing an orthogonal 50S–30S pair, it is promising that PTC and anti-SD mutations are introduced to a ribosome with tethered subunits (Orelle et al. 2015; Fried et al. 2015). As described above, although there are many problems to express the orthogonal translation machinery in vivo, these will be solved in future.

From the results in both Chaps. 2 and 3, flexizymes can aminoacylate any RNAs bearing not only CCA-3′ end but also other 3′-end sequences with various amino acids bearing. In addition, 3′-end of flexizymes will be further engineered, flexizymes will be able to recognize longer 3′-end sequences. Therefore, flexizymes have great potential to deplete or enrich RNAs bearing specific 3′-end sequences.

Until now, flexizymes have been mainly applied for preparing aa-tRNA bearing ncAAs used for genetic code reprogramming to produce nonstandard peptides (Terasaka and Suga 2014). However, as discussed above, aminoacylation at 3′-end of RNA with various amino acids by flexizymes has a great potential to be applied for RNA studies including analysis of translation mechanisms, engineering of translation, discoveries of novel small ncRNAs. The discovery of interaction between folic acid and hsa-pre-miR-125a proposes new regulation mechanism of miRNA biogenesis and the development of orthogonal translation system opens an entrance to a new opportunity of in vitro synthetic biology.

References

Bose D, Jayaraj G, Suryawanshi H, Agarwala P, Pore SK, Banerjee R, Maiti S (2012) The tuberculosis drug streptomycin as a potential cancer therapeutic: inhibition of miR-21 function by directly targeting its precursor. Angew Chem Int Ed Engl 51(4):1019–1023. doi:10.1002/anie.201106455

Chen XG, Sim S, Wurtmann EJ, Feke A, Wolin SL (2014) Bacterial noncoding Y RNAs are widespread and mimic tRNAs. RNA 20(11):1715–1724. doi:10.1261/rna.047241.114

Fried SD, Schmied WH, Uttamapinant C, Chin JW (2015) Ribosome subunit stapling for orthogonal translation in *E. coli*. Angew Chem Int Edit 54(43):12791–12794. doi:10.1002/anie.201506311

Liu J, Liu M, Horowitz J (1998) Recognition of the universally conserved 3′-CCA end of tRNA by elongation factor EF-Tu. RNA 4(6):639–646. doi:10.1017/S1355838298980013

Morimoto J, Hayashi Y, Suga H (2012) Discovery of macrocyclic peptides armed with a mechanism-based warhead: isoform-selective inhibition of human deacetylase SIRT2. Angew Chem Int Ed Engl 51(14):3423–3427. doi:10.1002/ange.201108118

Neumann H, Wang K, Davis L, Garcia-Alai M, Chin JW (2010) Encoding multiple unnatural amino acids via evolution of a quadruplet-decoding ribosome. Nature 464(7287):441–444. doi:10.1038/nature08817

Orelle C, Carlson ED, Szal T, Florin T, Jewett MC, Mankin AS (2015) Protein synthesis by ribosomes with tethered subunits. Nature 524(7563):119–289. doi:10.1038/nature14862

Rackham O, Chin JW (2005) A network of orthogonal ribosome • mRNA pairs. Nat Chem Biol 1 (3):159–166. doi:10.1038/Nchembio719

Saito H, Kourouklis D, Suga H (2001a) An in vitro evolved precursor tRNA with aminoacylation activity. EMBO J 20(7):1797–1806. doi:10.1093/emboj/20.7.1797

Saito H, Watanabe K, Suga H (2001b) Concurrent molecular recognition of the amino acid and tRNA by a ribozyme. RNA 7(12):1867–1878

Sunwoo H, Dinger ME, Wilusz JE, Amaral PP, Mattick JS, Spector DL (2009) MEN ε/β nuclear-retained noncoding RNAs are up-regulated upon muscle differentiation and are essential components of paraspeckles. Genome Res 19(3):347–359. doi:10.1101/gr.087775.108

Terasaka N, Suga H (2014) Flexizymes-facilitated genetic code reprogramming leading to the discovery of drug-like peptides. Chem Lett 43(1):11–19. doi:10.1246/Cl.130910

Terasaka N, Hayashi G, Katoh T, Suga H (2014) An orthogonal ribosome–tRNA pair via engineering of the peptidyl transferase center. Nat Chem Biol 10(7):555–557. doi:10.1038/nchembio.1549

Velagapudi SP, Gallo SM, Disney MD (2014) Sequence-based design of bioactive small molecules that target precursor microRNAs. Nat Chem Biol 10(4):291–297. doi:10.1038/Nchembio.1452

Virumae K, Saarma U, Horowitz J, Remme J (2002) Functional importance of the 3′-terminal adenosine of tRNA in ribosomal translation. J Biol Chem 277(27):24128–24134. doi:10.1074/jbc.M200393200

Wang KH, Neumann H, Peak-Chew SY, Chin JW (2007) Evolved orthogonal ribosomes enhance the efficiency of synthetic genetic code expansion. Nat Biotechnol 25(7):770–777. doi:10.1038/Nbt1314

Wilusz JE, Freier SM, Spector DL (2008) 3′ end processing of a long nuclear-retained noncoding RNA yields a tRNA-like cytoplasmic RNA. Cell 135(5):919–932. doi:10.1016/j.cell.2008.10.012

Wilusz JE, Whipple JM, Phizicky EM, Sharp PA (2011) tRNAs marked with CCACCA are targeted for degradation. Science 334(6057):817–821. doi:10.1126/science.1213671

Curriculum Vitae

Personal Information

Name:	Naohiro Terasaka
Sex:	Male
Date of birth:	February 3, 1988
Nationality:	Japanese
Affiliation:	Laboratory of Organic Chemistry, ETH Zürich
Address Correspondence:	HCI F328, Vladimir-Prelogweg 3, 8093, Zürich
Tel:	+41 44 633 4329
Fax:	+41 44 632 1486
E-mail:	tnaohiro@org.chem.ethz.ch

Educations

2012–2015:	Ph.D., "Applications of aminoacylation ribozymes that recognize the 3′-end of tRNA via two consecutive base pairs", Department of Chemistry, Graduate School of Science, The University of Tokyo, Japan
2010–2012	Master of engineering, "In vitro selection of human small non-coding RNA binding to the metabolites", Department of Chemistry & Biotechnology, Graduate School of Engineering, The University of Tokyo, Japan
2006–2010	Bachelor of engineering, "Functional analysis of the archaeal tRNA modification enzyme, TiaS" Department of Chemistry & Biotechnology, School of Engineering, The University of Tokyo, Japan

Awards

2015–present	Long-Term Fellowship of Human Frontier Science Program (HFSP)
2015	Research Incentive Award from Graduate School of Science, The University of Tokyo

N. Terasaka, *Applications of Aminoacylation Ribozymes That Recognize the 3′-end of tRNA*, Springer Theses, DOI 10.1007/978-4-431-56517-8

2012–2015: Research Fellow of the Japan Society of the Promotion of Science (JSPS)
2014 Sidney Altman Endowment Travel Award (The 25th tRNA conference)
2013 Best presenter award (The 15th annual meeting of the RNA Society of Japan)
2013 Travel Grant for Attending the 63rd Lindau Nobel Laureate Meeting from JSPS

Publications

1. Terasaka N., Futai K., Katoh T. & Suga H. A human micro RNA precursor binding to folic acid discovered by small RNA transcriptomic SELEX. *RNA*, **22**, 1918–1928 (2016)
2. Futai K., Terasaka N., Katoh T. & Suga H. tRid, an enabling method to isolate previously inaccessible small RNA fractions. *Methods*, **106**, 105–111 (2016)
3. Terasaka N., Iwane Y., Geiermann AS., Goto Y. & Suga H. Recent developments of engineered translational machineries for the incorporation of non-canonical amino acids into polypeptides. *Int. J. Mol. Sci.*, **16**, 6513–6531 (2015)
4. Terasaka N., Hayashi G., Katoh H. & Suga H. An engineered ribosome-tRNAs pair functions orthogonally to the wild-type under an artificially programmed genetic code. *Nat. Chem. Biol.*, **10**, 555–557. (2014)
   "Selected as Greatest hits in *Nature Chemical biology* over the past decade."
5. Terasaka N. & Suga H. Flexizymes-facilitated genetic code reprogramming leading to the discovery of drug-like peptides. *Chem. Lett.*, **43**, 11–19 (2014).
6. Osawa T., Inanaga H., Kimura S., Terasaka N., Suzuki T. & Numata T. Crystallization and preliminary X-ray diffraction analysis of an archaeal tRNA-modification enzyme, TiaS, complexed with $tRNA^{Ile2}$ and ATP. *Acta Crystallogr. Sect. F Struct. Biol. Cryst. Commun.* **67**, 1414–1416 (2011).
7. Osawa T., Kimura S., Terasaka N., Inanaga H., Suzuki T. & Numata T. Structural basis of tRNA agmatinylation essential for AUA codon decoding. *Nat. Struct. Mol. Biol.*, **18**, 1275–1280 (2011).
8. Terasaka N., Kimura S., Osawa T., Numata T. & Suzuki T. Biogenesis of 2-agmatinylcytidine catalyzed by the dual protein and RNA kinase TiaS. *Nat. Struct. Mol. Biol.*, **18**, 1268–1274 (2011).
9. Suga H., Hayashi G. & Terasaka N. The RNA origin of transfer RNA aminoacylation and beyond. *Phil. Trans. R. Soc. B*, **366**, 2959–2964 (2011).

International Conference Presentations

1. Ishida S., Terasaka N., Katoh T. & Suga H. Ribozymes with tRNA recognition and aminoacylation properties. 26th tRNA conference, Jeju, KOREA, 2016.09.04–08 (Oral)

2. Terasaka N. & Hilvert D. Microfluidic cell sorter-aided directed evolution of box C/D snoRNP to site-specifically introduce N6-methyladenosine. 16th HFSP meeting, Biopolis, SINGAPORE, 2016.07.10–13 (Poster)
3. Terasaka N. & Hilvert D. Microfluidic compartmentalized directed evolution of box C/D snoRNP to methylate RNA bases. RNA 2016, Kyoto, JAPAN, 2016.06.28–07.02 (Poster)
4. Terasaka N., Ishida S., Katoh T. & Suga H. Ribozymes that catalyze tRNA aminoacylation. Pacifichem 2015, Hawaii, United States, 2015.12.15–20 (Oral)
5. Ishida S., Terasaka N., Katoh T. & Suga H., A T-box eibozyme with tRNA aminoacylation activity. 10th International Symposium on Aminoacyl-tRNA Synthetases, Barcelona, SPAIN, 2015. 10. 18–22 (Oral)
6. Terasaka N., Hayashi G., Katoh H. & Suga H. An orthogonal ribosome-tRNA pair via engineering of the peptidyl transferase center. The 3rd Japan-Swiss Chemical Biology Symposium, Bern, SWITZERLAND, 2014. 10. 02–03 (Poster)
7. Terasaka N., Hayashi G., Katoh H. & Suga H., An orthogonal ribosome-tRNAs pair by the engineering of peptidyl transferase center. 25th tRNA conference, Kyllini, GREECE, 2014. 9. 21–25 (Oral)
8. Terasaka N., Hayashi G., Katoh H. & Suga H., Mutant ribosome•tRNA pair towards orthogonal genetic code. 9th International Symposium on Aminoacyl-tRNA Synthetases, Hakone, JAPAN, 2013 10. 6–11 (Oral)
9. Terasaka N., Futai K., Katoh T. & Suga H. Discovery of human small non-coding RNAs binding to small molecules by SELEX-NT. RiboClub Annual Meeting 2013, Quebec, CANADA, 2013. 9. 23–25 (Poster)
10. Terasaka N. & Suga H. The translational activity of a CCA-mutated tRNA-ribosome mutant pair. Annual Symposium on Academic English for Chemistry, Tokyo, JAPAN, 2013. 2. 28, 2013 (Oral)
11. Terasaka N., Hayashi G., Katoh H. & Suga H. Translational activity of CCA-mutated tRNA-ribosome mutant pair. XXIV tRNA conference, Olmue, CHILE, 2012. 12. 2–6 (Poster)